2022

DNA Methylation and DNA Methyltransferases in the Clonal Raider Ant, Ooceraea biroi

Ivasyk Iryna

DNA Methylation and DNA Methyltransferases in the Clonal Raider Ant, *Ooceraea biroi*

A Thesis Presented to the Faculty of
The Rockefeller University
in Partial Fulfillment of the Requirements for
the degree of Doctor of Philosophy

by
Iryna Ivasyk
June 2022

DNA Methylation and DNA Methyltransferases in the Clonal Raider Ant, *Ooceraea biroi*

Iryna Ivasyk, Ph.D.
The Rockefeller University 2022

DNA methylation and DNA methyltransferase enzymes (DNMTs) are ubiquitous and predate the origin of eukaryotes. In animals, DNA methylation primarily is carried out by DNMT1, which targets hemi – methylated DNA and maintains methylation patterns through cycles of cell replication, and DNMT3, the *de novo* methyltransferase. These genes are essential to mammalian development, and mutations lead to embryonic (DNMT1 and DNMT3b) or post – natal (DNMT3a) lethality. Studies of DNA methylation and DNMTs in invertebrates have been limited to non – traditional model organisms because *Caenorhabditis elegans* and *Drosophila melanogaster* lack the DNMT enzymes, and their DNA has no detectable methylation. In other invertebrates, global DNA methylation levels are generally much lower than those of mammals and largely concentrated in exons of protein coding genes. In social insects, some studies have argued that DNA methylation regulates social behavior or caste differentiation, but others have challenges this idea and it remains controversial.

To further understand the DNMT enzymes, we used the clonal raider ant, *Ooceraea biroi*, a tractable model organism with robust DNA methylation. We utilized CRISPR/Cas9 to mutate the DNMT genes (DNMT1 and DNMT3) and generate four unique mutants (two targeting different regions of DNMT1, one targeting DNMT3 and a DNMT1/DNMT3 double mutant). In the DNMT1 catalytic domain mutant we observed a drastic drop in global levels of DNA methylation as well as reproductive sterility and increased mortality. We did not observe any reproductive or DNA methylation phenotypes in the other DNMT1 mutant or the DNMT3 mutant. Furthermore, in both

of these mutants, we observed faithful transcription of the frameshift mutations in aligned mRNA reads, but did not observe any differential gene expression compared to wildtypes. Recently, studies have come to light regarding CRISPR/Cas9 mutagenesis inducing mechanisms of genomic plasticity, such as alternative splicing or translation reinitiating, which ultimately can rescue gene function. It is possible that we did not detect any phenotypes in these DNMT1 and DNMT3 mutants due to such a mechanism, leading to normal gene function despite successful mutagenesis.

The sterility we observed as a result of DNMT1 catalytic domain mutagenesis is consistent with growing work demonstrating that DNMT1 plays an essential, possibly methylation – independent, role during oogenesis in insects. To further evaluate this phenomenon, we characterized DNMT1 mRNA and protein in the ant ovary using fluorescence *in situ* hybridization and immunohistochemistry. We found DNMT1 present in somatic cells within the ovary, in addition to being maternally provisioned into oocytes early in development. Furthermore, we observed developing oocytes in the ovaries of DNMT1 catalytic domain mutants, indicating that this gene is not essential for the initiation or early stages of oogenesis.

Our findings demonstrate that unlike in mammals, normal development after DNMT1 inhibition is possible in insects. However, DNMT1 is essential for longevity and progression of insect oogenesis. Further work to understand the precise mechanism of DNMT1 involvement in oogenesis, and potentially meiosis, may shed light on its evolutionary role and why it has been conserved across so many forms of life.

ACKNOWLEDGMENTS

First and foremost, I owe many thanks to my advisor, Daniel Kronauer for his dedication to guiding me and helping shape me into the scientist that I am today. Thank you for creating a lab environment which taught me to think critically as a scientist, carefully plan experiments, and persevere relentlessly. I may have started at the lab as the first MD/PhD student, but hope to finish as the first ant scientist pursuing medical education.

I want to thank my committee, Erich Jarvis, Li Zhao and Jochen Buck for always critically assessing my work, as well as their continued guidance, support and encouragement. I would like to also extend my gratitude to Sarah Kocher, for participating as an external examiner on my thesis committee. I want to thank my collaborators, Hosung Jang and Bob Schmitz at the University of Georgia, who conducted and analyzed all of the Whole Genome Bisulfite Sequencing experiments, shared their methods and helped prepare our manuscript. All data in this dissertation regarding methylation analysis, as well as the Whole Genome Bisulfide Sequencing methods section, is their work.

I owe great thanks to Cris Rosario, Marta Delgado, Stephanie Fernandez, Kristen Cullen, Emily Harms and Sid Strickland for their support at the Rockefeller University Dean's office during the course of my graduate training. I would also like to thank Olaf Andersen, Katharine Hsu, Ruth Gotian, Catharine Boothroyd, Renee Horton, Hanna Silvast and Ben Levitt for their tireless work at the Tri – Institutional MD/PhD program. Additionally, I owe many thanks to Mark Pecker, for his guidance in my professional development, and dedication to improving medical education in Ukraine.

I offer my enormous gratitude to Leonora Olivos – Cisneros for her commitment to this project, both intellectually and physically. Thank you for offering your wisdom, helping me with new techniques and, above all, for spending countless hours with me injecting eggs. Likewise, Stephany Valdes Rodriguez also played an essential role in bringing this project to life including setting up and maintaining the egg laying units and stock colonies, helping with egg injections and with genotyping of mutants. Finally, the injection team, and my injection training, would be incomplete without the help of Marie Droual and Amelia Ritger. Thank you to everyone who made manual collection, alignment and individual injection of ~ 25,600 ant eggs for this project possible.

I have many other former and current Kronauer lab members to thank, without whom this work would not have been possible. Buck Trible helped answer all of my questions about the CRISPR/Cas9 protocol in *Ooceraea biroi*, in addition to providing other valuable advice on this project. Lindsey Lopes helped me prepare and image the brains. Additionally, I owe thanks to Vikram Chandra, Taylor Hart, Alex Paul, Kip Lacy, Dennis Melendez, Orli Snir, Dominic Frank, Asaf Gal, Patrick Piekarski and Sean McKenzie for their support and exciting intellectual discussions about my work and the field. I must also acknowledge the hard work of the *Ooceraea biroi* ants, who produced ~ 25,600 eggs, and tirelessly fed, cleaned and nourished my mutants to adulthood.

Outside of the Kronauer lab, I would like to acknowledge the Ant Course, the Nouragues research field station in French Guiana, as well as the course instructors including Brian Fisher, Christian Peeters and Phil Ward, from whom I learned a vast amount of myrmecology.

At Rockefeller, I especially need to thank Rebecca Timson, for her eagerness to try new experiments, sharing her knowledge and experience with molecular and cell biology, and continually offering support. Additionally, I am lucky to have found many incredible friends at Rockefeller University, Weill Cornell Medical College, the Tri- Institutional MD/PhD program, including my classmates, with whom I started the program in 2015. I also would like to thank my friends outside of Tri – I, all of whom now know more about ants than they ever imagined they would.

I am grateful for my family, including my parents, Marianna and Ihor, along with my grandparents for the sacrifices that they made in order for me to gain a higher education. Thank you for pushing me to succeed, teaching me to persevere and encouraging my curiosity. And a thank you to my younger brothers for their support. Finally, with enormous gratitude, I must acknowledge my wonderful partner, Kai, who stood by my side, listened to infinite practice talks and experimental ideas, and most importantly always reminded me to believe in myself and not lose sight of the bigger picture.

TABLE OF CONTENTS

ACKNOWLEDGMENTS ..... **iii**
TABLE OF CONTENTS ..... **vi**
LIST OF FIGURES ..... **viii**
LIST OF TABLES ..... **x**
LIST OF ABBREVIATIONS ..... **xi**
CHAPTER 1. INTRODUCTION **1**
1.1 DNA (CYTOSINE – 5) METHYLATION 1
1.2 DNA METHYLATION IN INSECTS 2
1.3 DNA METHYLTRANSFERASES (DNMTs) 3
1.3.1 DNMT1 4
1.3.2 DNMT3 8
1.4 DNMTs AND DNA METHYLATION IN *O. BIROI* 9
CHAPTER 2. CRISPR/CAS9 AND THE DNMT1 GENE IN *O. BIROI* **10**
2.1 *O. BIROI* LIFE CYCLE AND CRISPR/CAS9 MUTAGENESIS 10
2.2 *O. BIROI* DNMT1 GENE STRUCTURE AND MUTATION TARGET SELECTION 15
CHAPTER 3. DNMT1 GENE EARLY EXON MUTAGENESIS **20**
3.1 REAGENT VALIDATION AND MUTANT GENERATION 21
3.2 MUTANT VALIDATION AND PHENOTYPING 25
3.3 RNA SEQUENCING AND TRANSCRIPTION 30
3.4 DISCUSSION AND FUTURE DIRECTIONS 35
CHAPTER 4. DNMT1 CATALYTIC DOMAIN MUTAGENESIS LEADS TO DNMT1 INHIBITION **38**
4.1 REAGENT VALIDATION AND MUTANT GENERATION 39
4.2 MUTANT VALIDATION AND PHENOTYPING 43
4.3 DISCUSSION AND FUTURE DIRECTIONS 53
CHAPTER 5. DNMT1 mRNA AND PROTEIN LOCALIZATION PATTERNS IN *O. BIROI* **57**
5.1 *O. BIROI* OVARY ANATOMY 57
5.2 DNMT1 mRNA AND PROTEIN IN THE *O. BIROI* OVARY 60
5.3 DNMT1 BRAIN IMMUNOHISTOCHEMISTRY 69
5.4 DNMT1 PROTEIN IN DNMT1g1 AND DNMT1g2 MUTANTS USING IMMUNOHISTOCHEMISTRY 71
5.5 DISCUSSION AND FUTURE DIRECTIONS 80
CHAPTER 6. DNMT3 ..... **83**
6.1 *O. BIROI* DNMT3 GENE STRUCTURE 83
6.2 CRISPR/CAS9 DNMT3 MUTAGENESIS 84
6.3 DNMT3 MUTANT RNA SEQUENCING 90
6.4 DISCUSSION AND FUTURE DIRECTIONS 94
CHAPTER 7. DNMT1g1 AND DNMT3 DOUBLE MUTANT **96**
7.1 DNMT1g1/DNMT3 DOUBLE MUTANT GENERATION 96
7.2 FUTURE DIRECTIONS 100

CHAPTER 8. MATERIALS AND METHODS 103
8.1 SELECTION OF GENE TARGETS AND AMPLIFICATION 103
8.2 gRNA DESIGN 105
8.3 CRISPR/CAS9 REAGENTS *IN VITRO* VALIDATION 106
8.4 EGG INJECTIONS AND REARING 106
8.5 CRISPR/CAS9 *IN VIVO* REAGENT TESTING AND MUTAGENESIS 107
8.6 DNMT1g1 AND DNMT3 REPRODUCTION AND SURVIVAL 108
8.7 DNMT1g2 REPRODUCTION, SURVIVAL AND MORPHOMETRICS 108
8.7.1 DNMT1g2 REPRODUCTION AND SURVIVAL EXPERIMENT 109
8.7.2 DNMT1g2 MORPHOMETRICS AND SAMPLE COLLECTION FOR METHYLATION AND IMMUNOHISTOCHEMISTRY ANALYSIS 109
8.8 RNA SEQUENCING 110
8.8.1 RNA EXTRACTION, LIBRARY PREPARATION AND SEQUENCING 110
8.8.2 DATA PROCESSING AND ANALYSIS 110
8.9 WHOLE GENOME BISULFITE SEQUENCING 111
8.9.1 LIBRARY CONSTRUCTION 111
8.9.2 METHYLOME MAPPING 111
8.10 FLUORESCENCE *IN SITU* HYBRIDIZATION 112
8.11 IMMUNOHISTOCHEMISTRY 112
REFERENCES 114

LIST OF FIGURES

Figure 1.1. Review of Current Research in DNMT1. 7

Figure 2.1. CRISPR/Cas9 Mutagenesis in *O. biroi*. 14
Figure 2.2. *O. biroi* DNMT1 Gene Structure. 16
Figure 2.3. DNMT1 Splice Variants and DNMT1g1/DNMT1g2 Guide RNA Binding Sequences. 18

Figure 3.1. DNMT1g1 Guide RNA *in vitro* Verification. 22
Figure 3.2. DNMT1g1 Mutant Genotypes Observed in The First Generation (G1) Adults. 25
Figure 3.3. Genome – Wide DNA Methylation in DNMT1g1 Mutants. 27
Figure 3.4. DNMT1g1 Mutant Reproductive and Survival. 29
Figure 3.5. DNMT1g1 Mutation in mRNA Reads Aligned to the DNMT1 Second Exon. 31
Figure 3.6. Splicing in the DNMT1 Gene in DNMT1g1 Mutants. 33
Figure 3.7. Analysis of Differential Gene Expression Resulting from DNMT1g1 Mutagenesis. 35

Figure 4.1. DNMT1g2 Guide RNA *in vitro* Verification. 40
Figure 4.2. DNMT1g2 Mutant Genotypes Observed in G0 Adults. 43
Figure 4.3. DNMT1g2 Mutant Female Gross Morphology. 44
Figure 4.4. DNMT1g2 Mutant Male Gross Morphology. 45
Figure 4.5. Genome – Wide DNA Methylation in DNMT1g2 Mutants. 47
Figure 4.6. Diagram of Female *O. biroi* Morphological Measurements. 48
Figure 4.7. DNMT1g2 Mutant Morphological Feature Measurements. …. 50
Figure 4.8. DNMT1g2 Reproduction and Survival. 53

Figure 5.1. *O. biroi* Ovary Anatomy. 59
Figure 5.2. DNMT1 mRNA Fluorescence *in situ* Hybridization in Ovaries. 61
Figure 5.3. DNMT1 Protein Immunohistochemistry in Ovaries. 63
Figure 5.4. DNMT1 Protein Immunohistochemistry in Oocytes Pre – Oviposition. 65
Figure 5.5. Protein Immunohistochemistry Detecting Mitochondria in *O. biroi* Ovaries. 67
Figure 5.6. Mitochondria and DNMT1 in *O. biroi* Oocytes Pre – Oviposition. 68
Figure 5.7. DNMT1 Protein Immunohistochemistry in the Brain. 70
Figure 5.8. DNMT1 Protein Immunohistochemistry in DNMT1g1 Mutant Ovaries. 72
Figure 5.9. DNMT1 Protein Immunohistochemistry in DNMT1g1 Mutant Oocytes. 74
Figure 5.10. DNMT1 Protein Immunohistochemistry in DNMT1g2 Mutant Ovaries. …. 76
Figure 5.11. Ovariole Number and Oocyte Size in DNMT1g2 Mutants. 78
Figure 5.12. Brain Morphology in DNMT1g2 Mutants. 79

Figure 6.1. *O. biroi* DNMT3 Gene Diagram. 84
Figure 6.2. DNMT3 Guide RNA *in vitro* Verification. 85
Figure 6.3. DNMT3 Mutant Genotypes. 87
Figure 6.4. Genome – Wide DNA Methylation in DNMT3 Mutants. 88
Figure 6.5. DNMT3 Reproduction and Survival. 89
Figure 6.6. DNMT3 Mutation in mRNA Reads Aligned to the DNMT3 First Exon. 91
Figure 6.7. DNMT3 RNA Splicing in DNMT3 Mutants 92
Figure 6.8. Analysis of Differential Gene Expression Resulting from DNMT3 Mutagenesis. 93

Figure 7.1. Comparing *O. biroi* Egg Hatch Rates Across Different CRISPR/Cas9 Experiments. 98
Figure 7.2. Sanger Sequences for DNMT1 and DNMT3 Genes Recovered from a Mutagenized G1 Egg. 99

LIST OF TABLES

Table 8.1. Primers Targeting DNMT1g1, DNMT1g2 and DNMT3. 104
Table 8.2 gRNAs Targeting DNMT1g1, DNMT1g2 and DNMT3 for CRISPR/Cas9 Mutagenesis. 105

LIST OF ABBREVIATIONS

AA – Amino Acid

BAH – Bromo – Adjacent Homology Domain

CRISPR – Clustered Regularly Interspersed Palindromic Repeats

Cas9 – CRISPR Associated Protein 9

DNMT – DNA Methyltransferase

DNMT1g1 – DNMT1 Guide 1 Mutant (2nd Exon)

DNMT1g2 – DNMT1 Guide 2 Mutant (11th Exon, Catalytic Domain)

ER – Essential Residue

ESCs – Embryonic Stem Cells

gRNA – Guide RNA

G0 – 0^{th} generation animal (mutagenized as an egg)

G1 – 1^{st} generation animal, offspring of mutagenized G0

Gn – offspring of G0 mutagenized animal of unknown generation

PAM – Protospacer Adjacent Motif

RFTS – Replication Focus Targeting Sequence

WGBS – Whole Genome Bisulfite Sequencing

WT - Wildtype

CHAPTER 1. INTRODUCTION

1.1 DNA (CYTOSINE – 5) METHYLATION

DNA (cytosine – 5) methylation, the addition of a methyl group to the 5th carbon of cytosine to form C5 – methylcytosine, is catalyzed by DNA methyltransferase enzymes (DNMTs). This epigenetic modification can be found across prokaryotic and eukaryotic organisms including fungi, plants and animals (Chen and Li, 2004). Most cytosine methylation is found in a CpG genetic context and CpG methylation patterns are replicated from parent onto daughter DNA strands during replication, allowing for methylation patterns to be inherited across generations (Chen and Li, 2004).

In prokaryotes, DNA methylation is part of the restriction – modification system and is involved in various processes, including gene regulation and host defense (Seong et al., 2021). Meanwhile, in eukaryotes, the role of this epigenetic modification has diverged across different organisms, and it is associated with processes such as transposon silencing and genomic imprinting, including X chromosome inactivation in mammals (Chen and Li, 2004; Feng et al., 2010). DNA methylation of protein coding genes, particularly within exons, is believed to be an ancestral form of methylation, and is highly conserved across plant and animal species (Feng et al., 2010). Some studies have argued that gene body methylation may be involved in genome stability or regulation of alternative splicing (Lev Maor et al., 2015; Li-Byarlay et al., 2013; Lorincz et al., 2004; Maunakea et al., 2013).

One limitation in studying DNA methylation and the DNA methyltransferase enzymes has stemmed from the fact that traditional model organisms, namely *Drosophila melanogaster* and *Caenorhabditis elegans* lack detectable levels of DNA methylation and have evolutionarily lost the DNMT enzymes (Chen and Li, 2004; Colot and Rossignol, 1999; Simpson et al., 1986; Urieli-Shoval et al., 1982). As a result, the majority of research on these enzymes has been conducted in mammals, where 70% – 80% of all CpG sites are methylated across somatic tissues (Li and Zhang, 2014). Mammalian DNMT genes include DNMT1, DNMT2 and two DNMT3 genes – DNMT3a and DNMT3b (Li and Zhang, 2014). These genes are essential, and mutagenesis of DNMT1 or DNMT3b results in embryonic lethality (Li et al., 1992; Li and Zhang, 2014; Okano et al., 1999; Unterberger et al., 2006).

1.2 DNA METHYLATION IN INSECTS

DNA methylation levels in insects are far less pronounced than in mammalian genomes, highly variable, ranging from 0% in Diptera to ~10 – 14% in some *Blattella* species, and largely concentrated in coding regions, particularly within the exons of genes (Bewick et al., 2016). Among insects that methylate their DNA, Hymenoptera species have some of the lowest rates of genome wide methylation (Bewick et al., 2016).

Overexpression of mouse DNMTs in *Drosophila melanogaster*, a species without native DNA methylation or DNMTs, resulted in ~ 1 – 4% genome wide CpG methylation (Lyko et al., 1999; Mund et al., 2004). Although these DNMTs were of mammalian origin, the observed methylation pattern was more similar to that of insects, implying that the differences in methylation observed

between species may be context dependent, and differences in DNA methylation is determined by the genomic context rather than being a result of evolutionary divergence in the DNMT genes.

Since the discovery of DNMTs in *Apis mellifera* (Wang et al., 2006), DNA methylation has been proposed as the underlying epigenetic mechanism regulating caste differentiation (Alvarado et al., 2015; Bonasio et al., 2012; Elango et al., 2009; Kucharski et al., 2008), social behavior (Herb et al., 2018, 2012) and learning in social insects (Biergans et al., 2017, 2016), including ants. However, results have not always been consistent, and these hypotheses have remained controversial (Cardoso-Junior et al., 2021; Herb et al., 2012; Libbrecht et al., 2016; Patalano et al., 2015).

Furthermore, since the majority of DNA methylation in insects is concentrated in gene bodies, this form of methylation has been proposed to directly regulate gene expression (Elango et al., 2009; Foret et al., 2012). However, evidence for this link has not been consistent across species and others have disputed this idea (Cardoso-Junior et al., 2021; Libbrecht et al., 2016; Patalano et al., 2015). Finally, some studies have argued for an association between DNA methylation and alternative splicing (Foret et al., 2012; Herb et al., 2012; Lev Maor et al., 2015; Li-Byarlay et al., 2013).

1.3 DNA METHYLTRANSFERASES (DNMTs)

In animals, DNA methylation is primarily carried out by two enzymes, DNMT1 and DNMT3. DNMT1 prefers hemi – methylated DNA as a substrate, and functions to maintain methylation patterns through replication cycles (Bashtrykov et al., 2012; Fatemi et al., 2001; Gowher and

Jeltsch, 2001). DNMT3, which primarily targets unmethylated DNA, is categorized as the "*de novo"* methyltransferase, although it may have the ability to methylate hemi – methylated DNA as well (Chen and Li, 2004; Gowher and Jeltsch, 2001). In experiments where mammalian DNMTs are expressed in *Drosophila melanogaster*, de novo methylation activity was observed after transgenic expression of the DNMT3 genes but not DNMT1 (Lyko et al., 1999; Mund et al., 2004).

1.3.1 DNMT1

The DNMT1 protein demonstrates a high preference for hemi – methylated CpG sites, and plays a central role in copying CpG methylation patterns from parent onto daughter strands during replication, thereby acting as a maintenance methyltransferase (Chen and Li, 2004). In Hymenoptera, there has been a duplication of the DNMT1 gene, resulting in DNMT1a and DNMT1b among Apoidea (bees) (Bewick et al., 2016). However, after an evolutionary loss of DNMT1b in Formicidae, ants carry only a single copy of DNMT1, DNMT1a (Bewick et al., 2016).

Furthermore, studies in various organisms, from mammals to insects, have shown that DNMT1 plays an essential role in oogenesis and spermatogenesis. Yet, questions remain regarding the underlying mechanism, and whether it is conserved across eukaryotes. Interestingly, some studies in insects and *Xenopus laevis* (the African Clawed Frog) have demonstrated that this function of DNMT1 may be methylation independent (Amukamara et al., 2020; Bewick et al., 2019; Dunican et al., 2008; Schulz et al., 2018; Washington et al., 2020). The results of these studies are summarized in Figure 1.1 and discussed below.

In mice, DNMT1 knockout leads to replication arrest in embryonic stem cells (ESCs) and embryonic lethality (Brown and Robertson, 2007; Li et al., 1992; Li and Zhang, 2014; Unterberger et al., 2006). In this species, a splice variant of DNMT1 which lacks the first 118 N – terminal amino acids, DNMT1o, has been associated with oogenesis (Chen and Li, 2004; Ratnam et al., 2002; Smith and Meissner, 2013). While DNMT1 is expressed in virtually all tissues, including post – mitotic neurons, DNMT1o appears limited to ovaries and is the predominant form of DNMT1 in embryos until the 4 – cell stage (Ratnam et al., 2002). Maternal DNMT1o knockout leads to placental abnormalities which appear more severe in female embryos (McGraw et al., 2013, p. 1). Finally, this gene is important during pairing of homologous chromosomes early in meiotic prophase (Takada et al., 2021), and DNMT1 inhibition during spermatogenesis is associated with germline stem cell apoptosis (Takashima et al., 2009).

Likewise, in insects, DNMT1 has been associated with development and gametogenesis across multiple species. Studies in *Nasonia* (wasp) and *Blattella germanica* (cockroach) have shown that maternally provisioned DNMT1 is essential for various aspects of embryonic development including the maternal to zygotic transition (Arsala et al., 2021), gastrulation (Zwier et al., 2012), and blastoderm formation (Ventós-Alfonso et al., 2020). Furthermore, knockdown of DNMT1 during larval and pupal development led to reproductive defects in both male and female milkweed bugs, *Oncopeltus fasciatus* (Amukamara et al., 2020; Bewick et al., 2019; Washington et al., 2020) and in the cotton mealybug, *Phenacoccus solenopsis* (Omar et al., 2020). Decreased fecundity and longevity was also observed with knockdown of DNMT associated protein 1 (DMAP1), a key activator of DNMT1, in the ladybeetle, *Harmonia axyridis* (Gegner et al., 2020).

Interestingly, sterility as a result of DNMT1 knockdown has also been observed in *Tribolium castaneum*, the red flour beetle, a species carrying the conserved DNMT1 gene, despite having no detectable levels of methylation (Schulz et al., 2018). Together, this work suggests that maternally provisioned DNMT1 is essential for both oogenesis and early embryogenesis, where it may serve a methylation independent role. Indeed, in *Xenopus laevis* (African Clawed Frog) embryos, one study found that DNMT1 plays an essential role in suppressing premature gene activation, and demonstrated that this mechanism is independent of DNA methylation (Dunican et al., 2008).

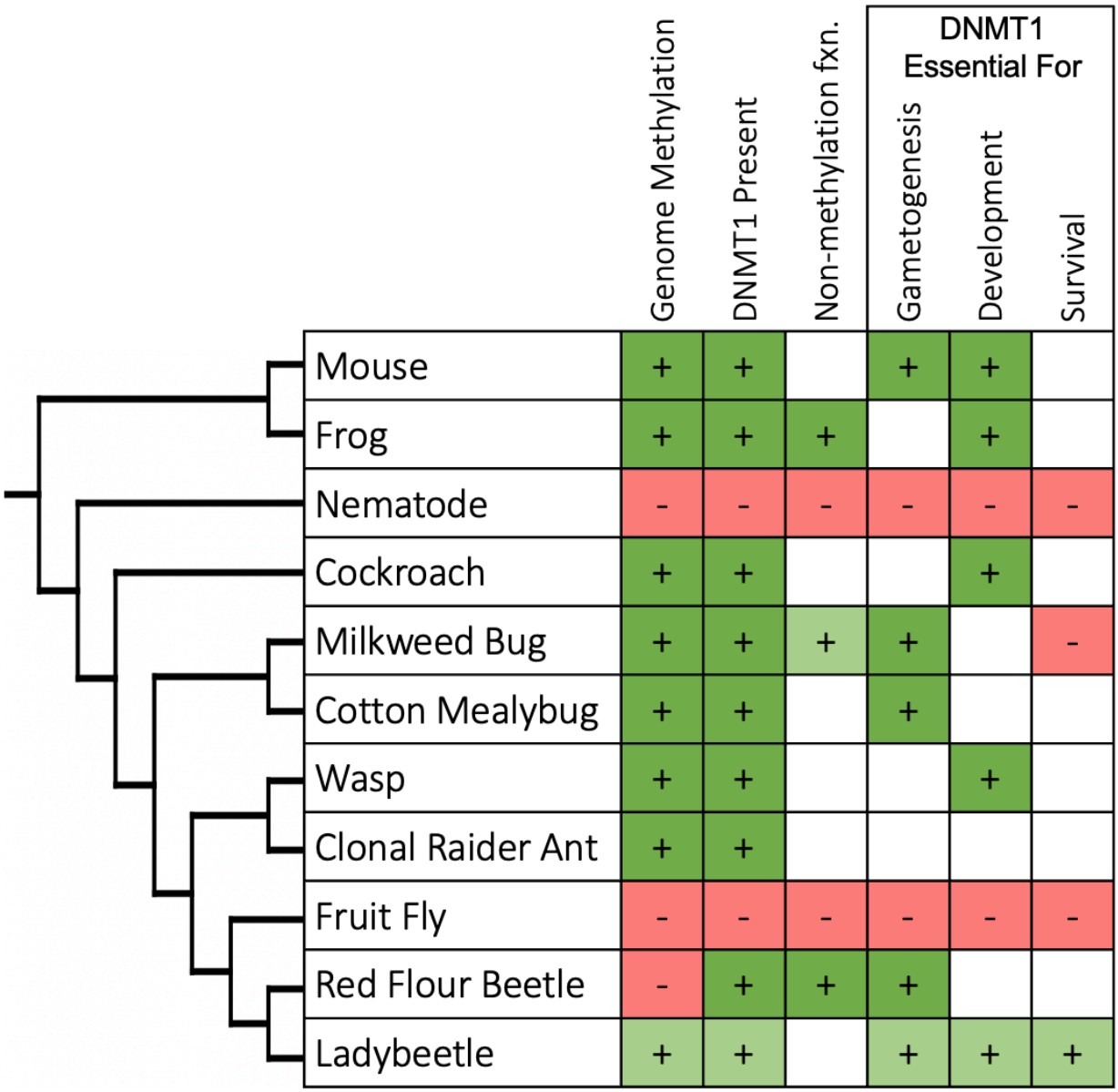

Figure 1.1. Review of Current Research in DNMT1.

DNA Methylation and known DNMT1 function across animal species along with phylogeny shown. Notably, the DNMT1 gene has been lost in *Caenorhabditis elegans* (Nematode) (Simpson et al., 1986) and *Drosophila melanogaster* (Fruit Fly) (Urieli-Shoval et al., 1982). The phylogeny demonstrates that these are evolutionarily independent losses of the ancestral DNMT1 gene. Evidence for a methylation – independent function of DNMT1 is found in *Xenopus laevis* (Frog)

(Dunican et al., 2008), *Oncopeltus fasciatus* (Milkweed Bug) (Amukamara et al., 2020; Bewick et al., 2019; Washington et al., 2020) and *Tribolium castaneum* (Red Flour Beetle) (Schulz et al., 2018), which notably has no evidence of genome wide methylation despite carrying a copy of the DNMT1 gene which is essential for gametogenesis. Finally, studies in *Blattella germanica* (Cockroach) (Ventós-Alfonso et al., 2020), *Nasonia* (Wasp) (Arsala et al., 2021), *Harmonia axyridis* (Ladybeetle) (Gegner et al., 2020) and *Phenacoccus solenopsis* (Cotton Mealybug) (Omar et al., 2020) have also shown an association between DNMT1 and development. Red color represents evidence of no relationship, dark green represents strong evidence, light green represents weaker evidence.

1.3.2 DNMT3

While DNMT1 has a strong preference for hemi – methylated DNA over unmethylated DNA as a substrate, DNMT3 has no such preference, and is known as the "*de novo*" methyltransferase (Gowher and Jeltsch, 2001; Hsieh, 1999). In mice, the DNMT3 genes are highly expressed during development (Okano et al., 1999), and mutations in DNMT3b are lethal, leading to arrest in development at the E9.5 stage (Okano et al., 1999). Furthermore, exogenous expression of mouse DNMT3b in *Drosophila melanogaster* leads to increased developmental mortality (Lyko et al., 1999). In this species, mouse DNMT3 genes, DNMT3a and DNMT3b, exhibit robust *de novo* CpG methylation activity, in addition to non – CpG methylation (Mund et al., 2004).

In social insects, DNMT3 expression appears to be highest in the embryo, and decreases through stages of larval development (Kay et al., 2018). In honeybees, inhibition of DNMT3 by RNAi leads to a ~ 21% methylation decrease (Li-Byarlay et al., 2013), and may be associated with caste

differentiation by leading to more "queen – like" development (Kucharski et al., 2008). Additionally, this inhibition results in alternative splicing including exon skipping and intron retention (Li-Byarlay et al., 2013). Finally, studies using pharmacological manipulations of DNMT3 in honeybees have proposed that it may be involved in olfaction and learning (Biergans et al., 2017, 2016).

1.4 DNMTs AND DNA METHYLATION IN *O. BIROI*

The clonal raider ant, *Ooceraea biroi* is a queenless species which reproduces asexually through parthenogenesis (Kronauer et al., 2012; Ravary and Jaisson, 2002). In this species, previous work revealed robust DNA methylation (2.1% of cytosines methylated), which is largely concentrated within genes (~82.5%), and often increased in constitutively active genes (Libbrecht et al., 2016). The life cycle of an *O. biroi* colony is composed of two distinct phases, a reproductive phase during which the colony is stationary and a brood care phase, which is characterized by increased activity and foraging behavior (Ravary et al., 2006; Ravary and Jaisson, 2002; Teseo et al., 2013; Ulrich et al., 2016). Furthermore, this reproductive cycle, and the division of labor that emerges during the brood care phase, are not driven by DNA methylation changes (Libbrecht et al., 2016).

This robust DNA methylation, along with a previously established CRISPR/Cas9 protocol in this species present a unique opportunity to study the function of DNMT1 and DNMT3 genes in insects. Specifically, using CRISPR/Cas9, we aimed to inactivate each of these genes, and evaluate the impact of such mutations on genome wide methylation, development, adult morphology and reproduction.

CHAPTER 2. CRISPR/CAS9 AND THE DNMT1 GENE IN *O. BIROI*

To further understand the role of DNMT1 in social insects, we used a previously established protocol for CRISPR/Cas9 mutagenesis in *O. biroi* (Trible et al., 2017) to generate DNMT1 mutants. We first identified conserved protein domains, essential residues and possible splice variants in the *O. biroi* DNMT1 gene. We then selected two unique target sites, which are ubiquitous among all splice variants, for mutagenesis. One of these targets was in the second exon of the gene, with the idea that a frameshift mutation here will have the highest impact in disrupting the reading frame, and subsequently protein function. Results from these experiments are discussed in Chapter 3. We additionally selected a second target site in the catalytic domain of DNMT1, the results of which are discussed further in Chapter 4.

2.1 *O. BIROI* LIFE CYCLE AND CRISPR/CAS9 MUTAGENESIS

The CRISPR/Cas9 mutagenesis protocol for *O. biroi* was previously developed for a study of odorant receptor coreceptor (ORCO), where CRISPR/Cas9 was used to introduce a single double stranded break into the ORCO gene, which generated a small insertion or deletion and resulted in a knockout – like phenotype. This protocol requires for special considerations to be taken into account in order to generate and rear *O. biroi* mutants that may not be necessary for other model organisms. Specifically, *O. biroi* larvae are unable to develop to adulthood in isolation and must be fostered into a colony of adults upon hatching. Furthermore, colonies are only receptive to young larvae at specific stages of their reproductive cycle, which must be carefully synchronized to successfully accomplish this “fostering”. If a colony is not in a reproductive state which is receptive to brood, or becomes stressed, all fostered larvae may be cannibalized by the adults.

The *O. biroi* reproductive cycle is composed of two alternating phases, which are marked by changes in colony activity (Ravary et al., 2006; Ravary and Jaisson, 2002). During the brood care phase, which can last between 2 – 4 weeks, larvae are present in the colony, the adults are highly active and ants are observed foraging outside the nest. During this phase, the presence of larvae in the colony suppresses reproduction in the adult workers and no eggs are laid. This reproductive synchrony is additionally enforced by "reproductive policing" where any ants with active ovaries in the colony are identified and removed by the workers (Teseo et al., 2013). The brood care phase ends when larvae pupate, the colony activity decreases and ants will rarely be found outside of the nest. A few days after the onset of this reproductive phase, eggs can be observed in the colony. After ~3 weeks, the pupae complete metamorphosis and callows (young adult workers) eclose. Shortly before callow emergence, the next cohort of larvae hatches from the eggs, and the colony enters a new brood care phase.

Unlike many other social insects, there are no distinct reproductive castes in *O. biroi*, and all workers are capable of reproduction through parthenogenesis during the reproductive phase of their cycle (Kronauer et al., 2013, 2012; Ravary et al., 2006; Tsuji and Yamauchi, 1995). *O. biroi* colonies are composed of all female workers and, in this species, males are produced very rarely and perish shortly after eclosion. It is not yet known if the female workers are capable of sexual reproduction. In this species, meiosis begins in the ovary, and completes post – partum. Prophase I can be observed shortly after oviposition, and upon completion of reductional division, the zygote is formed by central fusion of the meiotic products (Oxley et al., 2014).

Although the unique reproductive properties in this species present additional barriers in generating and rearing mutants, their clonal nature also allows for a single mutation, when

introduced shortly after oviposition, to penetrate all cell lineages including the germline and be propagated for many generations. Furthermore, colonies or mutants can be raised from a single individual without the need for genetic crosses.

The time point after oviposition at which the CRISPR/Cas9 reagents need to be injected to successfully accomplish this was previously identified at 5 hours post – partum (Trible et al., 2017). After testing our reagents, we manually collected, aligned and injected eggs, originating from the *O. biroi* "B" genetic line, at < 5 hours old with a CRISPR mix containing the selected guide RNA (gRNA) and Cas9 enzyme. Eggs are reared on slides and regularly cleaned and checked. Additionally, we recorded which ones reached the "transition" checkpoint, where the color of the eggs will change from opaque to clear, and distinct structures begin to appear. Eggs which do not transition, are arrested to development and will not hatch.

After hatching, the larvae are harvested and placed into a "rearing" colony of chaperones, originating from the *O. biroi* "A" genetic line, whose reproductive cycle had been synchronized to accept larvae. Notably, high egg mortality (~98%) is observed in attempts of CRISPR/Cas9 mutagenesis, therefore large numbers of eggs (~2,000 – 5,000) must be injected to successfully generate and rear mutants to adulthood. The reason for this high mortality is unknown but it may be related to off target mutagenesis or DNA stability in this species. After these larvae pupate and the callows eclose, they are considered G0 adults. These G0 adults had been mutagenized as eggs and could potentially be mosaic (Figure 2.1). However, we rarely see evidence of mosaicism when sequencing in these animals.

Upon eclosion, the G0 animals are removed from their rearing colony and pooled with all G0s across all "rearing" units to create a G0 egg "laying" unit. All eggs from this G0 egg laying unit are removed 1 – 2 times weekly, until the ants stop laying eggs at 6 – 7 months of age. These eggs are fostered in batches of 20 – 60 eggs with 20 chaperone ants and reared to adulthood, resulting in G1 adults (Figure 2.1). This process continues until enough adults are generated to create pure genetic lines. For genotyping, adults of G1 – G*n* are individually painted and placed into colonies. A single leg is removed for DNA extraction and PCR amplification, and the resulting genotypes can be associated with the correct ant using the unique paint identifier. An enzyme digest of the mitochondrial CO1 gene is used to distinguish line "B" ants originating from G0s and the line "A" chaperones. Sanger sequencing traces of line "B" ants are manually scored to identify mutant individuals.

The average generation time from egg to egg in this species is ~ 9 weeks with most variability in the brood care phase, during which larval development takes place, rather than the reproductive phase, which encompasses metamorphosis. On average, ~ 30% of eggs which are laid make it to adulthood. *O. biroi* females will generally begin laying eggs ~1 – 2 weeks after eclosion and, if the colony is artificially maintained in the reproductive phase of the cycle, by regular removal of all eggs, can continue to lay eggs for ~ 6 months. Despite this, a single ant will ultimately give rise to < 10 offspring that reach adulthood. This is largely due to low egg laying rate and high developmental mortality.

Further work is needed to understand if these numbers are representative of the natural reproductive fecundity of *O. biroi* workers within a colony outside of the lab. These animals may behave differently in a more heterogeneous colony, which is able to undergo the natural

reproductive cycle. Additionally, although there are no distinct reproductive castes in this species, *O. biroi* workers exhibit a range of reproductive traits, including the number of ovarioles, which may vary from two to six. It is not yet known how this variability in ovariole number tracks with reproductive output in this species. It is plausible that workers with fewer ovarioles give rise to fewer offspring in their lifetime. However, further studies are necessary to evaluate this relationship.

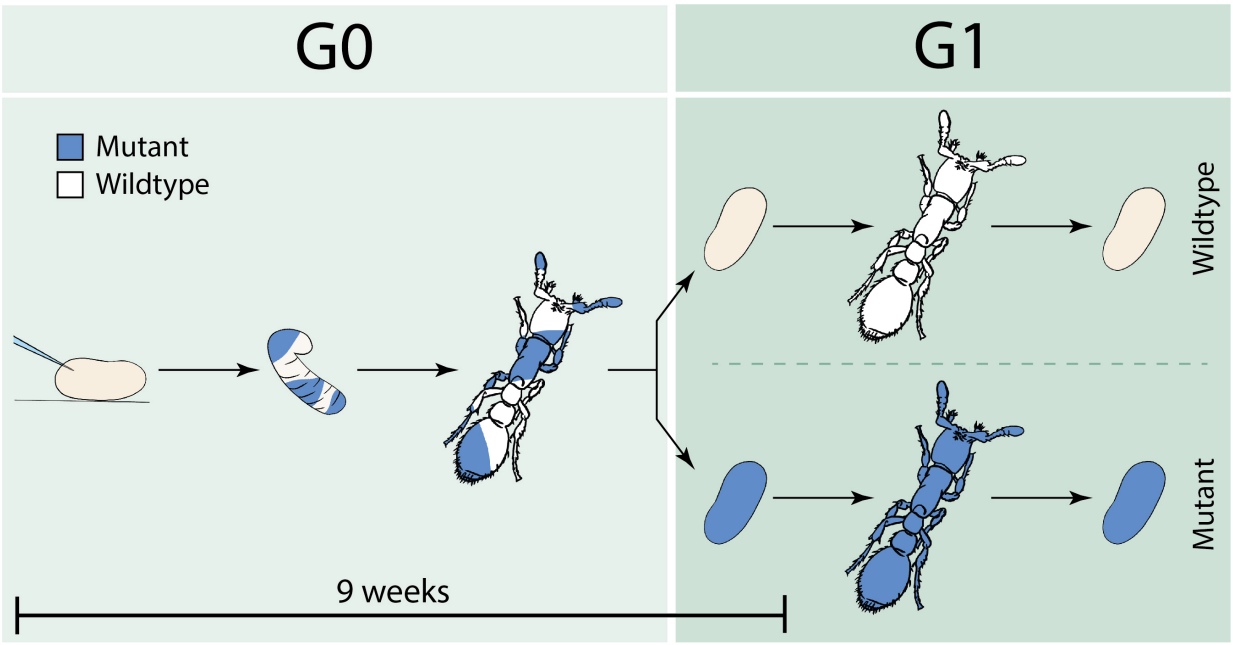

Figure 2.1. CRISPR/Cas9 Mutagenesis in *O. biroi*.

Diagram demonstrating the CRISPR/Cas9 protocol. G0 eggs are injected with a mix of Cas9 and gRNAs and reared to larvae in special incubation boxes. The larvae are then transferred to rearing units and raised to adulthood by chaperone ants until eclosion. It is possible that these G0 adults are mosaics and only carry the induced mutation(s) in some cell lineages. The eclosing G0 callows are then separated, set as egg laying units, and G1 eggs are collected. The G1 eggs are reared by

chaperone ants to adulthood and can give rise to mutant or wildtype offspring (heterozygous wildtype/mutant; not shown). The generation time from egg to egg is ~9 weeks.

2.2 *O. BIROI* DNMT1 GENE STRUCTURE AND MUTATION TARGET SELECTION

The DNMT1 gene is composed of multiple evolutionarily conserved domains, including the replication focus targeting sequence (RFTS), CXXC domain, the bromo – adjacent homology domain (BAH) and the DNA – cytosine methylase catalytic domain (Chen and Li, 2004). The catalytic domain is found at the N – terminus of the DNMT1 protein, and is responsible for enzymatically attaching a methyl group to the 5th carbon of a cytosine residue (Svedružić, 2011). The catalytic domain likely requires allosteric activation by the remainder of the protein, as it is enzymatically inactive in isolation (Fatemi et al., 2001). The RFTS and BAH domains are essential for targeting DNMT1 to replication foci during the synthesis phase of cellular replication (Rountree et al., 2000; Yarychkivska et al., 2018).

The *O. biroi* DNMT1 gene (NCBI GenBank, Gene ID: 105286975) is found on Chromosome 14, and is composed of 16 exons. At ~ 1,450 amino acids (aa), the *O. biroi* DNMT1 protein is slightly smaller than the ~ 1,620 aa mammalian DNMT1 (Zhang et al., 2015). We identified the location of the conserved DNMT1 domains including the RFTS, BAH and the catalytic domain, which appeared heavily conserved (Figure 2.2). Additionally, previous work in mice demonstrated that a single residue within the catalytic domain of DNMT1, Cys1229, is essential for its methyltransferase function (essential residue, ER) (Damelin and Bestor, 2007). We identified this conserved amino acid in the catalytic domain of the *O. biroi* DNMT1 protein (Figure 2.2) and used

this information in selecting one of the mutagenesis target locations as described in more detail in Chapter 4.

Furthermore, various other mutations in the human DNMT1 protein, near the RFTS, have been linked to hereditary genetic diseases (Norvil et al., 2019), including autosomal dominant cerebellar ataxia, deafness and narcolepsy (ADCA – DN) (Winkelmann et al., 2012) and hereditary sensory and autonomic neuropathy (HSAN) type IE (Klein et al., 2011; Yuan et al., 2013). We have also annotated the locations of the loci associated with these mutations within the *O. biroi* DNMT1 gene (Figure 2.2).

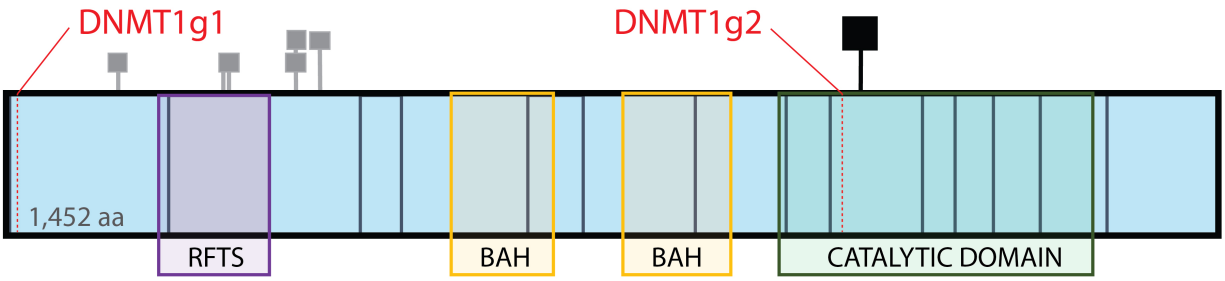

Figure 2.2. *O. biroi* DNMT1 Gene Structure.

Structure of conserved domains in the DNMT1 gene including Replication Focus Targeting Sequence (RFTS), Bromo – Adjacent Homology Domain (BAH) and the Catalytic DNA Methyltransferase Domain (Catalytic Domain). Black square signifies conserved cytosine residue essential for methyltransferase function in mammals. Grey squares indicate conserved amino acid changes due to mutations associated with genetic diseases in humans. Mutagenesis target sites indicated at the second (DNMT1g1) and eleventh (DNMT1g2) exons and discussed in more detail in Chapters 3 and 4, respectively.

In *O. biroi*, two splice variants of the DNMT1 mRNA, XM_011352333.3 and XM_011352329.2 (NCBI GenBank ID), have been observed. Evaluation of all possible splice variants is an essential first step to selecting a mutagenesis target in order to ensure that a frameshift mutation would be transcribed for all splice variants and lead to a nonsense protein in all instances. Therefore, mutagenesis targets for DNMT1 were selected such that the guide RNA binding sequence would be present on all transcript variants (Figure 2.3). The DNMT1g1 and DNMT1g2 guide RNAs can be observed overlapping both variants in the second and eleventh exons, respectively (Figure 2.3). Results of using CRISPR/Cas9 to mutagenize the *O. biroi* DNMT1 gene at each of these locations are further discussed in Chapters 3 and 4, respectively.

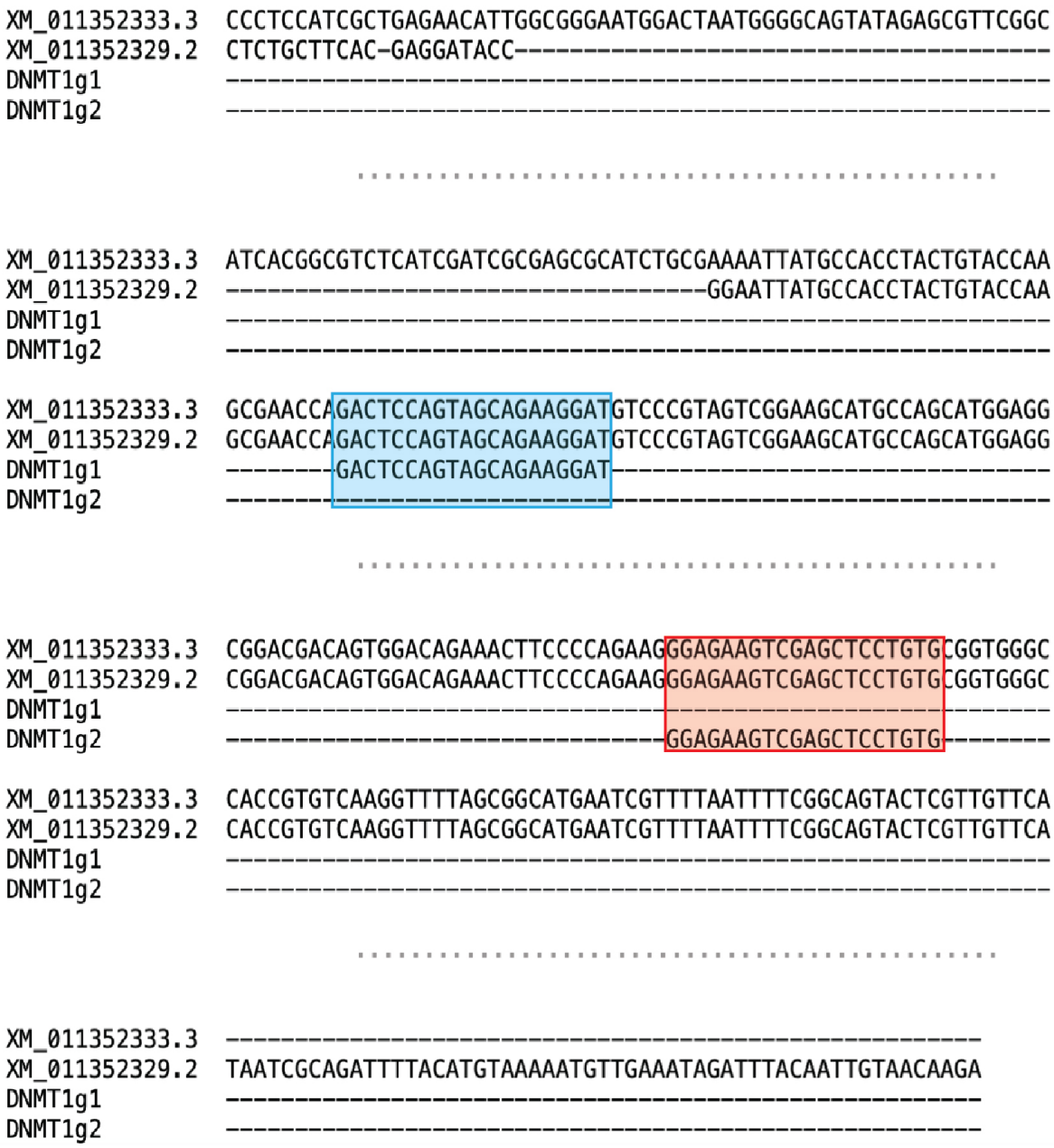

Figure 2.3. DNMT1 Splice Variants and DNMT1g1/DNMT1g2 Guide RNA Binding Sequences.

Aligned mRNA splice variants of DNMT1 (NCBI: XM_011352333.3 and XM_011352329.2) with gRNA targets for DNMT1g1 (blue) and DNMT1g2 (red) mutants shown in the second and eleventh exon, respectively. Although alternative splicing occurs of the first and last exons of the

gene, the gRNAs align with both detected splice variants. The gRNAs displayed for each gene represent the ones which were selected from *in vitro* and *in vivo* testing of four guides per target region (Chapters 3 and 4). Dots (...) indicate suppressed mRNA sequence which is not shown but can be accessed on GenBank with the NCBI IDs.

CHAPTER 3. DNMT1 GENE EARLY EXON MUTAGENESIS

To further understand the function of DNMT1 in social insects, we aimed to inactivate this gene in *O. biroi*. To accomplish this, we used CRISPR/Cas9 (Jinek et al., 2012) with the goal of creating a double stranded break in the second exon of DNMT1 (Figure 2.2). Repair of this double stranded break by the error prone non – homologous end joining mechanism (Ran et al., 2013) often results in small insertions or deletions. Such frameshift mutations in an "early" exon can lead to gene inactivation through mRNA transcript degradation via nonsense mediated decay, or translation to a nonsense protein due to reading frame disruption (Popp and Maquat, 2016; Ran et al., 2015; Rubio et al., 2016; Trible et al., 2017).

We were able to successfully generate double stranded breaks *in vivo* and *in vitro* within the second exon of the DNMT1 gene by using a previously established CRISPR/Cas9 protocol in this species (Trible et al., 2017). Furthermore, we were able to penetrate the germline and generate multiple unique genetic lines of frameshift mutants with mutations in both alleles of the DNMT1 gene (Section 3.1). We did not see any phenotypic effects as a result of these mutations including changes in methylation levels or in survival or fecundity (Sections 3.1, 3.2). This is despite the fact that these mutations were faithfully transcribed, and observed in aligned mRNA reads, without introducing any major alternative splicing (Section 3.3). Questions remain about whether DNMT1 gene inactivation was achieved in these mutants, and the potential mechanism of gene rescue despite successful mutagenesis.

3.1 REAGENT VALIDATION AND MUTANT GENERATION

After identifying the target region for mutagenesis within the second exon of the DNMT1 gene, we used Synthego's gRNA design tool to design four unique synthetic sgRNAs. To amplify the DNA segment of interest, we designed and tested three sets of primers (forward and reverse) of which one was selected (see Chapter 8 – Materials and Methods). We then amplified the genomic region of interest and tested all gRNAs for their ability to associate with the Cas9 enzyme and generate double stranded breaks *in vitro*. We were able to observe double stranded breaks on gel electrophoresis as smaller, digested DNA fragments when compared to the DNMT1 PCR product for all gRNAs tested (Figure 3.1). As expected, the sizes of DNA fragments generated in the digestion differ between the tested guide RNAs (Figure 3.1). This is because each one targets a different sequence in the second exon of the DNMT1 gene, and as a result, digests the amplified PCR product into unique segments.

Additionally, in some instances (DNMT1g1 1 here), we observed bands which were substantially larger than the original DNMT1 PCR product. While this could be indication of contamination, we regularly observe such bands of increased molecular weight in this digest assay, and attribute this increase in weight to PCR product that is still bound to the Cas9/gRNA complex. We have anecdotally observed a decrease in such bands if an additional heating step is added, which denatures the Cas9 enzyme at the end of the DNA digestion.

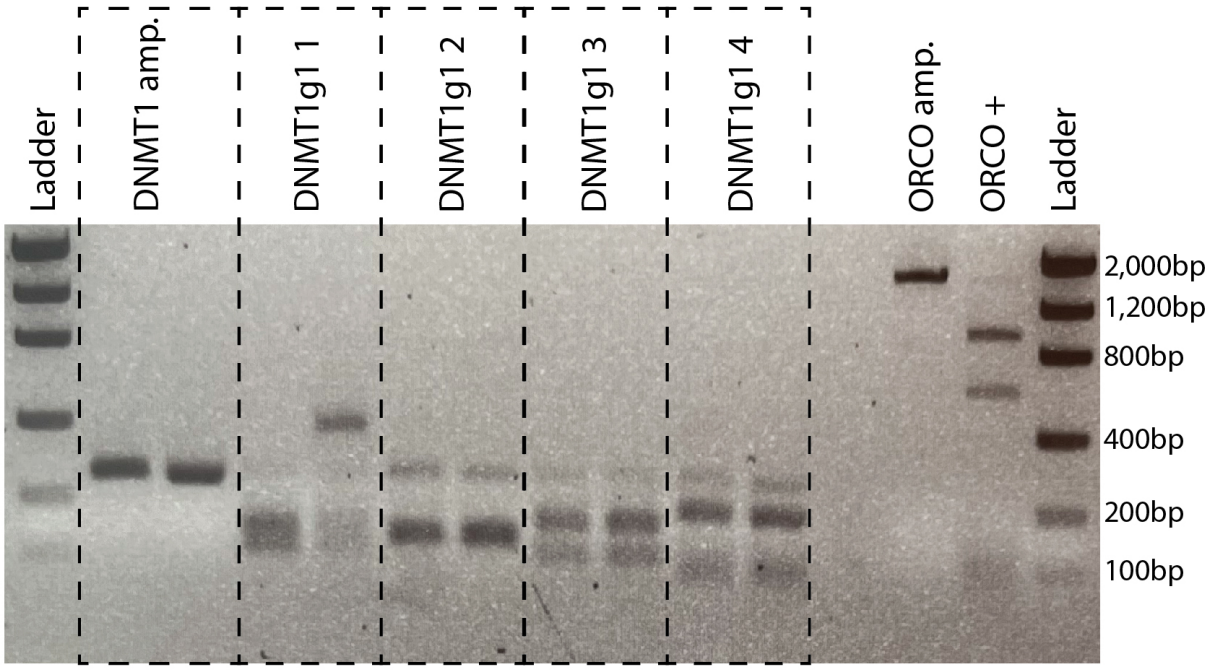

Figure 3.1. DNMT1g1 Guide RNA *in vitro* Verification.

The region of the DNMT1 gene containing the target cut site for DNMT1g1 is shown on gel electrophoresis after amplification, purification and dilution to 100 ng/ul (DNMT1 amp.). Degraded PCR product shown after incubation with Cas9 enzyme and four different gRNAs (DNMT1g1 1 – 4) demonstrating cutting activity of all four potential gRNAs. Two replicates are shown for each reaction. Control Odorant Receptor Coreceptor (ORCO) amplified DNA (OCRO amp.) digestion using previously verified gRNA (Trible et al., 2017) shown on right (ORCO+) under the same conditions. Band of increased molecular weight observed in one replicate for DNMT1g1 gRNA1. Molecular weight ladder on both sides and annotated as shown.

From the *in vitro* digest experiment, all guides appeared to associate with Cas9 and produce double stranded breaks successfully. DNMT1g1 guide number 4 was selected for further *in vitro* testing. After injection of 2,222 eggs, 60 larvae hatched (hatch rate = 2.7%) of which 45 were sequenced.

The high mortality rate observed in the injected eggs is likely due either to physical damage from injection of fluids, or molecular damage from the Cas9/gRNA mix. High mortality in the context of CRISPR/Cas9 mutagenesis is expected and has previously been observed when targeting multiple other genes in *O. biroi* (Trible et al., 2017). Of the sequenced larvae, 8 were mutant, of which 7 mutants contained in – frame mutations and 1 contained only frameshift mutations. An in – frame mutation would not lead to reading frame disruption and instead may only result in the loss of a single amino acid without inactivating the gene. As a result, an alternate guide, guide number 3 was selected for further *in vivo* testing and ultimately generation of the DNMT1g1 mutant.

To test DNMT1 guide number 3 *in vivo*, we injected a mix of Cas9 enzyme and DNMT1g1 guide RNA 3 into 617 young eggs (< 5 hours) of which 10 transitioned and 5 ultimately hatched (hatch rate = 8.1%). Additionally, to control for rearing environment, 117 control eggs were not injected but reared in parallel, of which 57 hatched (hatch rate 48.7%), again, demonstrating a high mortality in eggs injected with Cas9/gRNA mix. Out of the injected eggs, we observed mutagenesis in 70% of immature eggs (n = 20), 60% of transitioned eggs (n = 5) and 20% of larvae (n = 5). This decrease in mutagenesis rate across later developmental stages could be attributed to early death of highly mutagenized eggs. One explanation for this phenomenon is that in these instances, there was more efficient delivery of the Cas9 and guide RNA to the nucleus. This would lead to increased rates of double stranded breaks including potential off – target activity, increasing both mutagenesis rates and mortality as observed.

Importantly, we did not observe the same high rate of in – frame mutations as with DNMT1 guide number 4, and the presence of frameshifted mutagenized larvae indicated that type of mutagenesis

in the second exon of the DNMT1 gene does not lead to embryonic lethality. This result indicated that generating a DNMT1 mutant may be possible in *O. biroi*, even though all previous attempts at mutating DNMT1 have resulted in developmental arrest (Brown and Robertson, 2007; Li et al., 1992; Li and Zhang, 2014; Unterberger et al., 2006). The next step in assessing the effect of this mutation on DNMT1 function was to generate and propagate colonies of mutant adults. Across five experiments, we injected 5,152 line B eggs of which 140 transitioned and 76 hatched (hatch rate = 1.5%). Of the larvae, we were able to foster 65 with line A *O. biroi* chaperones to be reared to adulthood. Additionally, we sequenced 8 larvae, of which 2 were mutant (mutagenesis rate = 25%). Similar to the pilot experiment, mutagenesis was substantially lower in larvae than in eggs arrested during early development (67%) and those which transitioned (30%).

These fostered G0 larvae were reared to adulthood, and all eclosing G0 callows were collected and pooled. When the G0 adult colony began laying eggs, all G1 eggs were collected, DNA extracted and the amplified DNMT1 mutation target locus was Sanger sequenced to evaluate whether the mutation had penetrated the germline. Once a mutant egg was found, we began to foster all G1 eggs with line A *O. biroi* chaperones to propagate these mutants for multiple generations. Ultimately, we successfully generated two unique mutant lines with frameshift mutations in both alleles (Figure 3.2).

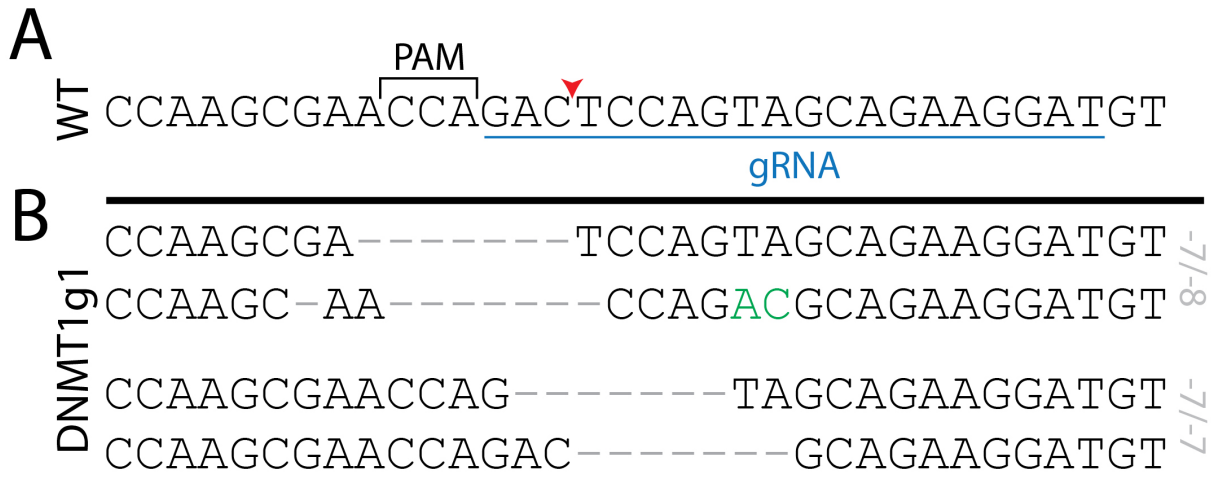

Figure 3.2. DNMT1g1 Mutant Genotypes Observed in The First Generation (G1) Adults. (A) Wildtype sequence at the second exon of the *O. biroi* DNMT1 gene. Guide RNA (gRNA) target shown for DNMT1g1 gRNA3 in blue, next to the protospacer adjacent motif in black (PAM) with predicted Cas9 cut site shown as red arrowhead. DNA shown on the positive strand in the 5' to 3' direction. (B) Two unique genotypes observed using Sanger sequencing for DNMT1g1 mutants with frameshift mutations in both alleles (-7bp / -7bp and -7bp / -8bp). Of note, exact nucleotide resolution between strands is the best estimate based on Sanger sequencing traces and may not be the precise sequence.

3.2 MUTANT VALIDATION AND PHENOTYPING

To gain insight into the impact of the DNMT1g1 mutation, we looked at changes in genome wide methylation to evaluate changes in DNMT1 function in DNMT1g1 mutants. We expected that the frameshift mutation in the second exon of DNMT1 would be transcribed into all RNA splice variants, and disrupt the mRNA reading frame, resulting in a nonsense protein product, thereby inactivating DNMT1, and creating a knockout – like phenotype. Because DNMT1 is responsible

for maintaining methylation in cells across cycles of replication, successful inactivation of this gene in the embryo should result in drastic decreases in genome wide methylation levels across all adult tissues (Li et al., 2015).

We used low coverage Whole Genome Bisulfite Sequencing (WGBS) to evaluate global methylation levels in mutant and wildtype ants. For this experiment, a colony of callows of mixed generations (G1 – G*n*) was isolated and aged to 1 month. All ants were genotyped using the DNA extracted from a single leg, and the remaining ant tissue frozen. Four wildtype and mutant ants were selected, and DNA was extracted from the remainder of the body for methylation analysis. Surprisingly, we did not observe any differences in methylation levels when comparing either genotype of DNMT1g1 mutants to wildtype ants ($p = 0.4092$, Figure 3.3). This finding indicates either that the mutation did not have the expected impact on DNMT1 function, or that the DNMT1 gene is not essential for maintenance of methylation in this species.

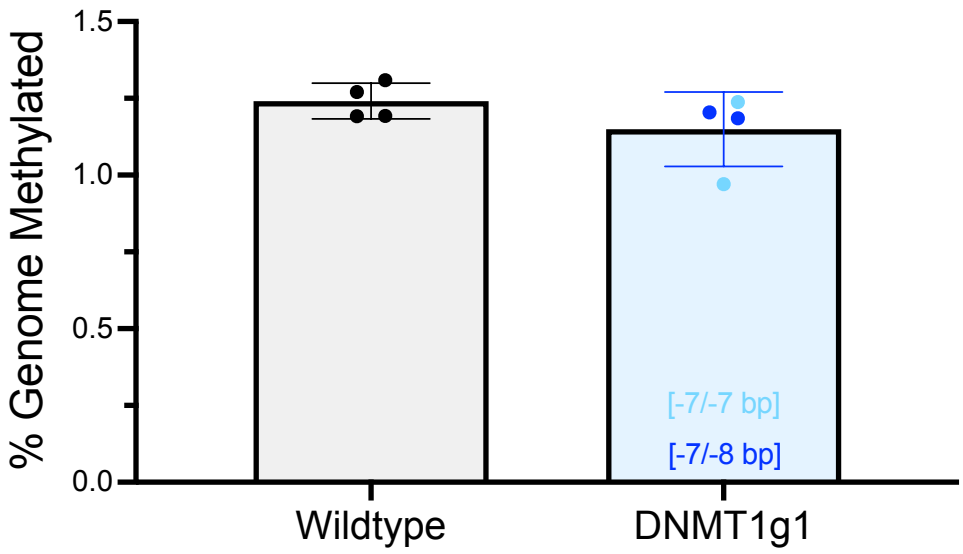

Figure 3.3. Genome – Wide DNA Methylation in DNMT1g1 Mutants.

Genome – wide methylation analysis using low coverage Whole Genome Bisulfite Sequencing. Data shown is corrected for bisulfite non – conversion estimates. Each datapoint represents DNA extracted from a single ant. For the mutant samples, two replicates of each genotype (-7bp/-7bp and -7bp/-8bp) were evaluated. In this sequencing experiment, four wildtype animals, four DNMT1g1 mutants and six DNMT3 mutants (see below) were evaluated, therefore all analysis requires multiple comparison testing instead of a simple t – test. No significant difference in genome wide methylation levels was observed with $p = 0.4092$ (Dunnett's multiple comparison test).

Additionally, we evaluated the impact of the DNMT1g1 mutation on survival and reproductive fecundity. For analysis of survival, G1 adults were individually painted and placed into small colonies of 16 ants. Throughout the experiment, all carcasses were removed regularly and frozen for genotyping until no ants remained in the colony. Because ants often dismember deceased nest mates, not all carcasses could be collected for each colony, but those that were successfully

retrieved and genotyped serve as a representative sample. The mutants lived to a median of 264 days, meanwhile the wildtype controls had a median survival of 258 days with a maximum longevity observed just short of 1 year at 347 days (Figure 3.4). No statistically significant difference was found in ant survival between wildtype and DNMT1g1 mutant ants (Log rank test, $p = 0.6624$).

For analysis of reproduction, eggs were collected from three colonies of painted G1 ants and sequenced. The frequency of mutant genotypes was then compared between the first 25 eggs successfully genotyped from each colony (75 total eggs) to the frequency of mutant genotypes in the G1 adults (genotypes for 32 out of 48 animals recovered successfully) among these colonies. Of the 75 eggs, 20% were mutant (of either genotype, -7bp / -7bp or -8bp / -8bp) and 80% were wildtype (of either line A or B). Among the 32 sequenced adults, 15.6% were mutant (of either genotype) and 84.4% were wildtype (of either genetic line). No statistically significant difference was observed when comparing the frequency of mutants in the adult G1 population to the G2 eggs laid by these adults (Fisher's exact test, $p = 0.7876$), implying that the DNMT1g1 frameshift mutations did not lead to any observable changes in fecundity in these animals (Figure 3.4).

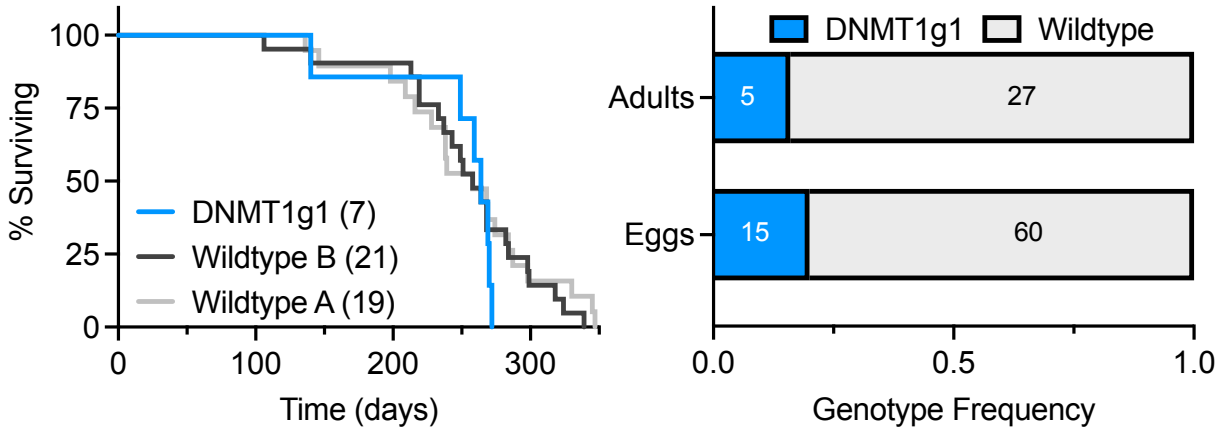

Figure 3.4. DNMT1g1 Mutant Reproductive and Survival.

(Left) Survival data for generation 1 (G1) DNMT1g1 mutants (of -7bp/-8bp or -7bp/-7bp genotype, Line B) compared to wildtype survival as well as wildtype survival of another genetic line (Line A). The median survival was 264 days for mutants, 258 days for wildtype controls (B) and 258 days for line A wildtype controls. No significant difference was observed between the three groups, with p = 0.6624 (Log – rank test). (Right) Sequencing of the first 25 G2 eggs collected from G1 colonies containing both wildtypes (either line A or line B) and DNMT1g1 mutants. No significant difference is observed when comparing the frequency of mutant G1 adults to the frequency of G2 eggs laid by these mutant and wildtype animals, with p = 0.7876 (Fisher's exact test).

Overall, we did not observe any obvious phenotypes in the DNMT1g1 mutants including changes in survival, reproduction and, most surprisingly, genome – wide methylation levels. We were able to successfully generate multiple unique mutant lines and propagate them for multiple generations. One possible explanation for these findings would be if DNMT1 did not play an essential function in development, reproduction or survival. This would not be implausible as some insects such as

D. melanogaster have lost DNMTs altogether and do not methylate their DNA (Urieli-Shoval et al., 1982). However, previous studies have demonstrated that DNMT1 knockdown in insects leads to decreased genome wide methylation levels (Amukamara et al., 2020; Bewick et al., 2019; Ventós-Alfonso et al., 2020). Together, these findings imply that while we successfully introduced frameshift mutations into the second exon of DNMT1, these mutations likely did not lead to the intended consequence of disrupting the mRNA reading frame and inactivating the DNMT1 protein, which appears to have retained its methylation function.

3.3 RNA SEQUENCING AND TRANSCRIPTION

Despite the introduction of frameshift mutations into the second exon of the DNMT1 gene, we did not observe any changes in the global DNA methylation levels, implying that DNMT1 function had not been affected. Indeed, recent studies have found that frameshift mutations using CRISPR/Cas9 in early exons do not always result in gene inactivation, and may even induce exon skipping or alternative splicing (Mou et al., 2017; Smits et al., 2019; Zhang et al., 2020).

We used RNA sequencing to further investigate this phenomenon in the context of DNMT1 second exon mutagenesis. Specifically, we wanted to understand the implication of these frameshift mutations on gene transcription, including that of DNMT1. We sequenced mRNA of three DNMT1g1 mutants (-8bp / -7bp genotype) and three wildtype nestmates (of the same genetic line). We first verified that the genomic DNMT1g1 mutations that we had observed using Sanger sequencing of amplified DNA were transcribed to mRNA successfully. We evaluated this by manually examining aligned mRNA reads to the second exon of the DNMT1 gene. For this genotype, we observed both the expected frameshift mutations (-8bp and -7bp) in mRNA at the

predicted mutagenesis location and did not see any anomalies at this location in the wildtype animals (Figure 3.5). This provided concrete evidence that these frameshift mutations are successfully transcribed into mRNA.

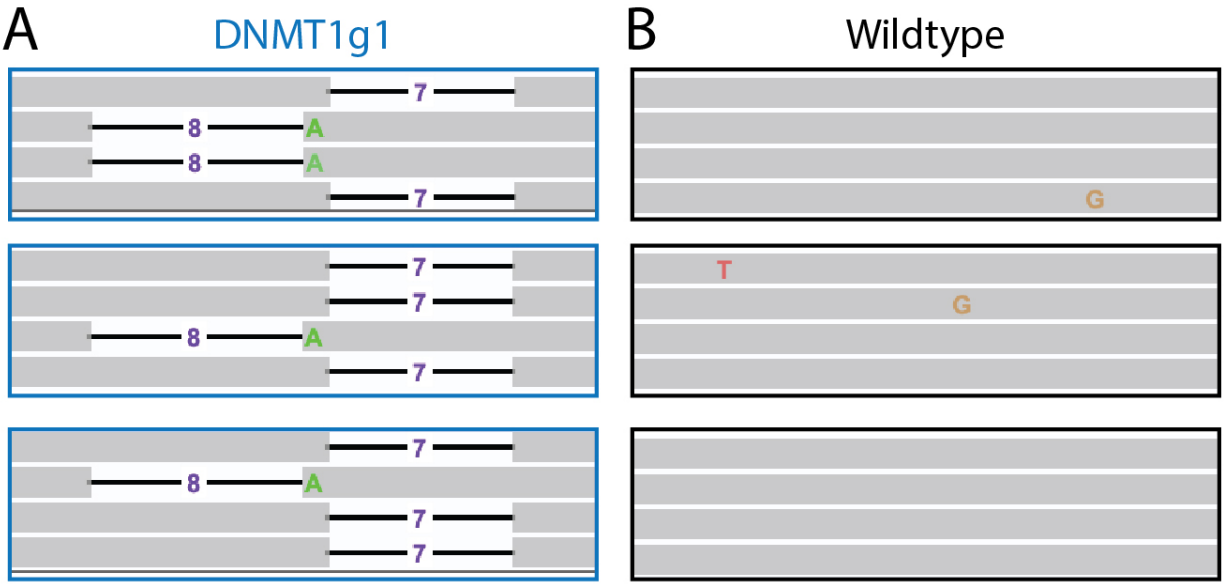

Figure 3.5. DNMT1g1 Mutation in mRNA Reads Aligned to the DNMT1 Second Exon. mRNA sequences aligned to the DNMT1g1 mutation target region. Each box encompasses mRNA sequences from a single replicate. Frameshift mutations observed in three DNMT1g1 mutants (A) of a single genotype (-7bp / -8bp) but not in mRNA sequences of wildtype animals (B) at the same locus. The mutation in the genome of these animals is transcribed and correctly spliced into the second exon for DNMT1.

After observing faithful transcription of the DNMT1g1 frameshift mutations, we explored if alternative splicing or exon skipping could explain the lack of DNMT1 gene inhibition in these animals. All reads aligned to the DNMT1 gene were plotted as sashimi plots, allowing for

visualization of splice junctions. As expected, we were able to observe both native splice variants of DNMT1 (XM_011352333.3 and XM_011352329.2) in the wildtype animals, with XM_011352333.3 appearing to be the major isoform and only a small fraction of the reads aligning to the alternative first exon of XM_011352329.2 (Figure 3.6). This minor isoform, XM_011352329.2, was only observed in two of the three wildtype replicates (Figure 3.6). In the mutants, only the major, XM_011352333.3, isoform was observed, but it is possible that both splice variants would have been observed with increased coverage. While a few splicing anomalies were present in the first DNMT1g1 replicate, no major alternative splicing events were observed consistently across mutant replicates (Figure 3.6). This result implies that there must be an alternate explanation for the lack of observable phenotypes including changes in methylation, as the frameshift mutations are faithfully transcribed and not spliced out of the mRNA.

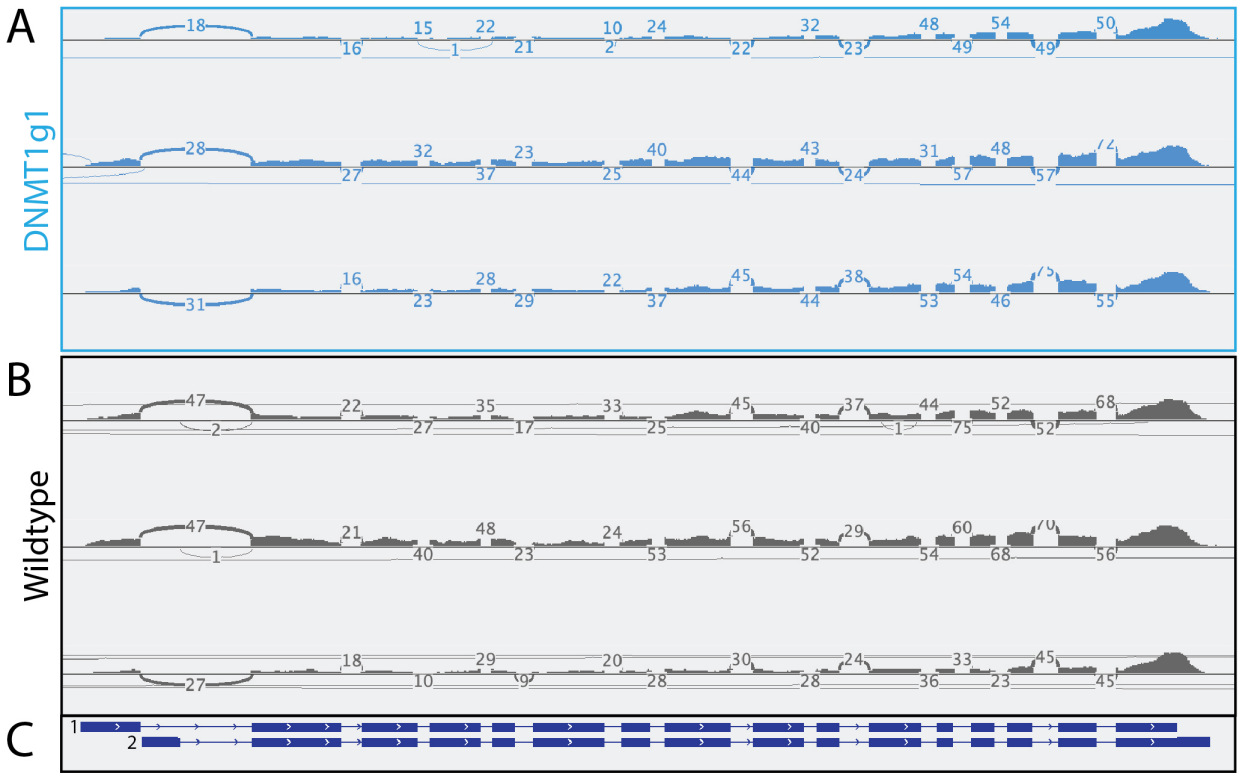

Figure 3.6. Splicing in the DNMT1 Gene in DNMT1g1 Mutants.

(A – B) Three mutants (A, blue) of a single genotype (-7bp/-8bp) and wildtype (B, grey) replicates shown on sashimi plots with read depth represented as graph height, and the number of reads spanning each splice junction indicated. (C) Two splice variants of DNMT1 (XM_011352333.3 (1) and XM_011352329.2 (2)) shown. XM_011352333.3 appears to be the major splice variant across all replicates. XM_011352329.2 detected only in two of the three wildtype replicates. No major novel splice variants observed across mutant replicates. In the first DNMT2g1 mutant, a single read is seen skipping exon 4 and two reads indicate possible alternative splicing of exon 7. Neither of these anomalies were observed in either of the remaining two mutant replicates.

Finally, we used the RNA sequencing data to evaluate differential gene expression between DNMT1g1 mutant and wildtype animals. We found that a majority of genes, including DNMT1 (LOC 10528975), did not appear to be differentially expressed (Figure 3.7). Out of 13,123 genes with aligned mRNA reads, only 4 (0.03%) were differentially expressed at an adjusted p – value cutoff of 0.01 and none at 0.005. None of these genes appeared associated with DNA methylation or methyltransferases and included flocculation protein FLO11 (LOC105284632, padj. = 0.0069), general odorant – binding protein 72 (LOC105287745, padj. = 0.0069), an uncharacterized protein (LOC105279809, padj. = 0.0070), and alpha – tocopherol transfer protein – like (LOC105284890, padj. = 0.007). It is possible that these four "differentially expressed" genes are false positives. Finally, the lack of decrease in DNMT1 expression in DNMT1g1 mutants provided evidence that the early frameshift mutation in this instance likely did not lead to nonsense mediated decay of the mRNA transcript (Figure 3.7).

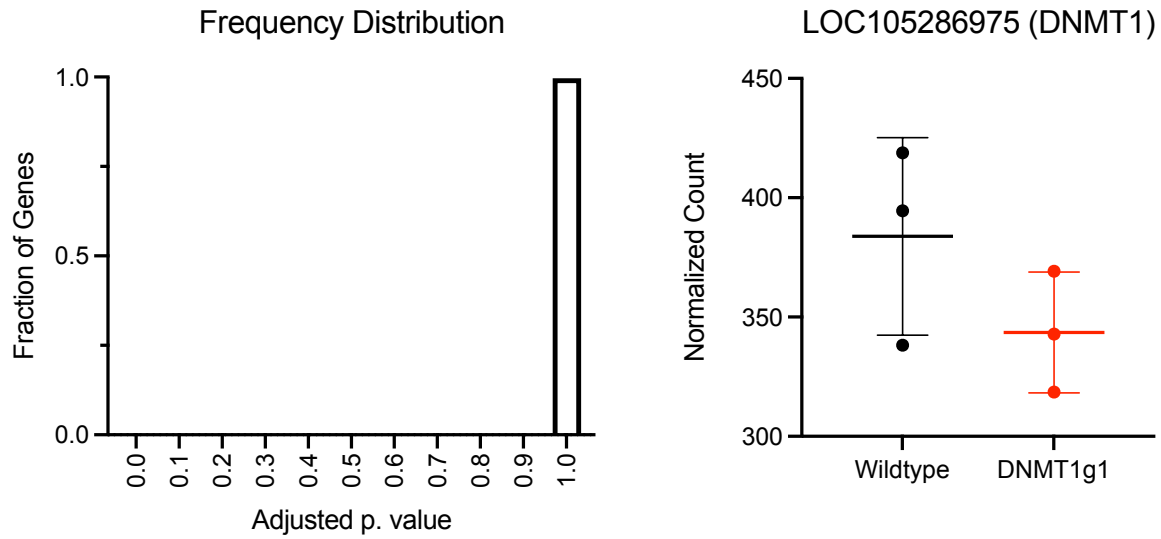

Figure 3.7. Analysis of Differential Gene Expression Resulting from DNMT1g1 Mutagenesis. (Left) Frequency distribution of adjusted p – values resulting from differential gene expression analysis between wildtype and DNMT1g1 mutant animals of the -7bp / -8bp genotype. No significant difference is seen in the vast majority of all genes between the genotypes. (Right) Normalized counts of reads for wildtype compared to DNMT1g1 transcripts aligning to LOC105286975 (*O. biroi* DNMT1 gene locus). No significant difference is observed (adjusted p. value = 0.9997).

3.4 DISCUSSION AND FUTURE DIRECTIONS

Since its discovery, CRISPR/Cas9 has been widely used as a tool for gene deletion and gene inactivation (Jinek et al., 2012; Ran et al., 2013). Introduction of a single double stranded break, early in the coding region of the gene, can lead to small insertions and deletions at the cut site, due to the error prone non-homology end joining repair mechanism (Ran et al., 2013). This will often

generate a frameshift mutation resulting in gene inactivation by RNA degradation via nonsense mediated decay (Popp and Maquat, 2016; Rubio et al., 2016) or reading frame disruption and translation disruption due to an early stop codon. However, recent studies have demonstrated that successful frameshifting of a gene does not always result in gene inactivation (Mou et al., 2017; Smits et al., 2019; Sui et al., 2018; Zhang et al., 2020). Interestingly, small insertions and deletions generated by CRISPR/Cas9 have been shown to induce splicing, which can ultimately rescue gene function (Mou et al., 2017; Zhang et al., 2020). In one study, researchers demonstrated that an early termination codon as a result of the frameshift mutation can, itself, induce nonsense mediated splicing and rescue gene function (Sui et al., 2018).

In these experiments, we were able to successfully generate multiple DNMT1 mutants, by introducing frameshift mutations into the second exon, penetrate the germline and propagate these mutations across multiple generations. We did not observe a decrease in methylation levels as expected, or any abnormalities in development, reproduction or survival. Upon RNA sequencing, we were able to confirm faithful transcription of the genomic frameshift mutations into mRNA and did not observe any major alternative splicing or exon skipping. Ultimately, the means of gene "rescue" in this instance remain unknown.

There are many possible explanations for remaining DNMT1 function despite these findings. For instance, it is possible that a minor splice variant exists in the mutants, which is able to rescue the reading frame, but was not detected in the RNA sequencing due to limitations in read coverage. Other explanations for this phenomenon could include mechanisms such as an alternate translation start site, translation reinitiating or ribosomal skipping during translation. Future work to understand the mechanism of gene rescue would require assessment of the resulting DNMT1

protein. For instance, methods such as Western blot could be used to detect changes in protein size and Mass Spectrometry could be used to evaluate possible missing peptides. These experiments would shed light on exactly which components of the DNMT1 protein are retained in the DNMT1g1 mutants. If these experiments demonstrate that DNMT1g1 mutants contain an incomplete DNMT1 protein, additional studies may lead to novel insight into the structure and function of this protein in insects. Moreover, understanding the mechanisms of biological plasticity available for gene rescue after mutagenesis may lead to discoveries with valuable biomedical applications.

Finally, this study provides a valuable example of the importance of phenotype validation in the context of CRISPR/Cas9 mutagenesis. As this technique becomes more popular and widely used, researchers should be aware of its drawbacks and unexpected results, despite successful mutagenesis. It is crucial that all mutants generated using CRISPR/Cas9, particularly by means of introducing frameshift mutations, are validated using an assay of protein detection (including methods such as immunohistochemistry), or protein function (in this instance WGBS). Without validation that the mutation induced the expected effect on the target gene, any phenotypes observed cannot be conclusively attributed to the expected protein inhibition.

CHAPTER 4. DNMT1 CATALYTIC DOMAIN MUTAGENESIS LEADS TO DNMT1 INHIBITION

After additional evaluation of the *O. biroi* DNMT1 gene, we selected a new mutagenesis target in the catalytic domain at exon 11 (Figure 2.2). Importantly, all DNMTs including DNMT1 and DNMT3 carry a conserved cysteine residue in their catalytic domain, which in DNMT1, is essential for methyltransferase activity but not DNA binding (Hsieh, 1999; Pósfai et al., 1989). Point mutations at this residue in DNMT1 have resulted in loss of genome wide DNA methylation and a knockout – like phenotype in mouse embryonic stem cells (Damelin and Bestor, 2007).

We aligned the *O. biroi* DNMT1 protein to the mammalian DNMT1 and identified this cysteine residue within the *O. biroi* DNMT1 protein as Cys1020 (isoform 1, NCBI Reference Sequence: XP_011350631.1) or Cys1014 (isoform 2, NCBI Reference Sequence: XP_011350635.1). We designed gRNAs to target just upstream of this residue in order to ensure that any exon skipping or alternative splicing that may ensue would also lead to a loss of this residue and render the protein inactive. After careful selection and testing of our reagents, we were able to successfully generate frameshift mutations at this target site in eggs and rear the animals to adulthood (see below). However, although female and male mutants were able to undergo normal development, we were not able to propagate these animals beyond the G0 generation, because the mutation resulted in female sterility and early mortality. Furthermore, we observed a drastic decrease in genome wide DNA methylation levels. Finally, the mutation did not lead to more "queen – like" traits, and instead gave rise to sterile, and possibly smaller, more "worker – like" ants.

4.1 REAGENT VALIDATION AND MUTANT GENERATION

Using similar methods to those described in Chapter 3, Section 1 for *in vitro* testing of DNMT1g1 reagents, we designed and tested four unique synthetic guide RNAs for DNMT1g2. We also developed and tested new DNMT1 primers to amplify the DNMT1g2 target site (see Chapter 8 – Materials and Methods). All guide RNAs exhibited enzymatic activity, in conjunction with Cas9, when incubated with amplified PCR product of the DNMT1 catalytic domain target site (Figure 4.1). As previously noted in Chapter 3 (Figure 3.1), we again observed DNA of higher molecular weight in multiple samples when compared to the control amplified PCR product (DNMT1 amp.). It is possible that this is due to contamination, or again, likely evidence of incomplete DNA digestion with the Cas9 / gRNA complex still bound (Figure 4.1).

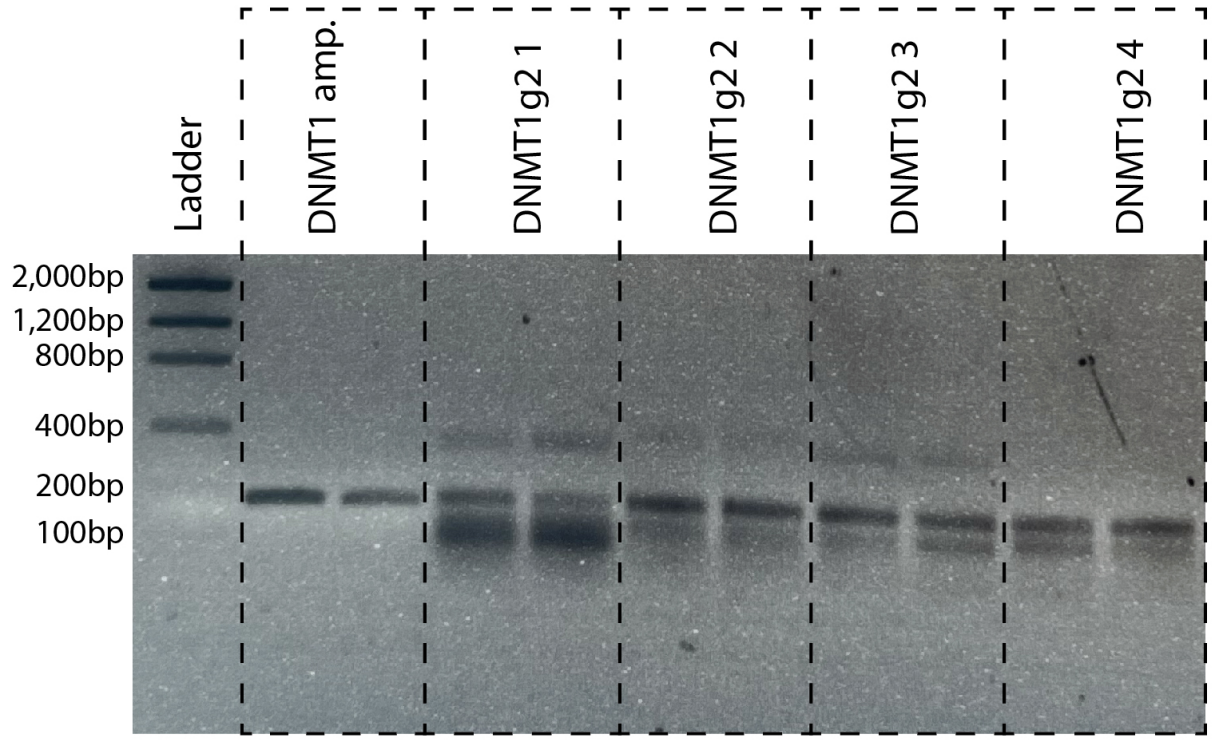

Figure 4.1. DNMT1g2 Guide RNA *in vitro* Verification.

The genomic coding region for a segment of the DNMT1 catalytic domain, which includes the target sites for all four DNMT1g2 guides, amplified by PCR and purified (DNMT1 amp.). This purified PCR product was then diluted to 100 ng/ul and incubated with Cas9 enzyme and each tested guide RNA (1 – 4), respectively. Results shown on gel electrophoresis. Intact DNA fragment without fragmentation seen in the control sample (DNMT1 amp., left), which was incubated with Cas9 without gRNA. Fragmentation of DNA observed on incubation with Cas9 and any of the four potential gRNAs. Remaining DNMT1 amplicon seen in all digested samples, implying partial digestion. Molecular weight ladder shown and annotated on left.

After validating activity of all synthetic guide RNAs *in vitro*, we selected gRNA 3 for *in vivo* testing and generation of mutants. For this experiment, 812 eggs were injected with the CRISPR

reagents (100ng/ul Cas 9 and 100 ng/ul DNMT1g2 gRNA3), of which 14 transitioned and 8 larvae hatched (hatch rate 0.985%). As with previous experiments, high mortality was observed among injected eggs when compared to 188 control eggs reared in parallel of which 127 hatched (hatch rate 67.6%). Unlike guides tested for DNMT1g1, the DNMT1g2 gRNA3 was highly effective, with mutagenesis observed in all recovered Sanger sequences of arrested eggs (n = 12), transitioned eggs (n = 2) and larvae (n = 7). Importantly, observation of mutagenized larvae, particularly larvae with no wildtype DNMT1 sequences, demonstrated that disruption of the DNMT1 gene near the essential cysteine residue, in the catalytic domain, does not lead to embryonic lethality.

After we validated the CRISPR/Cas9 reagents, as well as embryonic viability after mutagenesis, we attempted to generate and rear G0 DNMT1g2 adults across two separate experiments. In the first experiment, 3,227 line B eggs were injected, of which 167 transitioned and 109 larvae hatched (hatch rate 3.4%). Meanwhile, 287 out of 617 control eggs, which were not injected, hatched (hatch rate 46.5%). Of the hatched larvae, 92 were fostered across four rearing units with line A chaperones. Of these rearing units, one was excluded form analysis because all six G0 animals, which reached adulthood, carried wildtype alleles. The remaining three units, which produced mutants, generated 18 G0 adults, of which four were mutant and 14 were wildtype. Finally, uninjected eggs were reared to adulthood, in parallel, to be used as matched controls. Animals from this experiment were used for morphometric studies (Section 4.2), evaluation of genome wide methylation (Section 4.2), and immunohistochemistry (Chapter 5).

In the second experiment, high egg mortality was again observed when 2,416 line B eggs were injected of which 72 transitioned and 45 hatched (hatch rate 1.9%). Meanwhile, 230 out of the 378

control eggs hatched (hatch rate 60.8%). Of the hatched G0 larvae, 39 were fostered into rearing units with line A chaperones, and ultimately 9 female G0s and 1 male G0 eclosed. Of these 9 females, one died within 24 hours of eclosion and was excluded from analysis. Mortality immediately after eclosion is often observed in wildtype colonies and may be an indication of developmental abnormality independent of mutagenesis. The remaining 8 G0 females were used to evaluate survival and reproduction phenotypes.

Across these two experiments, we were able to generate multiple unique alleles, which included both insertions and deletions, at the target mutation locus (Figure 4.2). Because we are unable to propagate these mutants beyond the G0 generation (see below), all phenotyping experiments were carried out on the G0 animals. Because of the possibility of mosaicism in the G0 generation (Figure 2.1), only a subset of alleles generated are shown and individual alleles cannot be resolved with certainty for each animal, unlike those of G1 DNMT1g1 adults discussed in Chapter 3. Although mosaicism is possible in the G0 adults (Figure 2.1), we did not find evidence of mosaicism in this experiment; for each wildtype and mutant animal only wildtype or mutant alleles were observed using Sanger sequencing respectively.

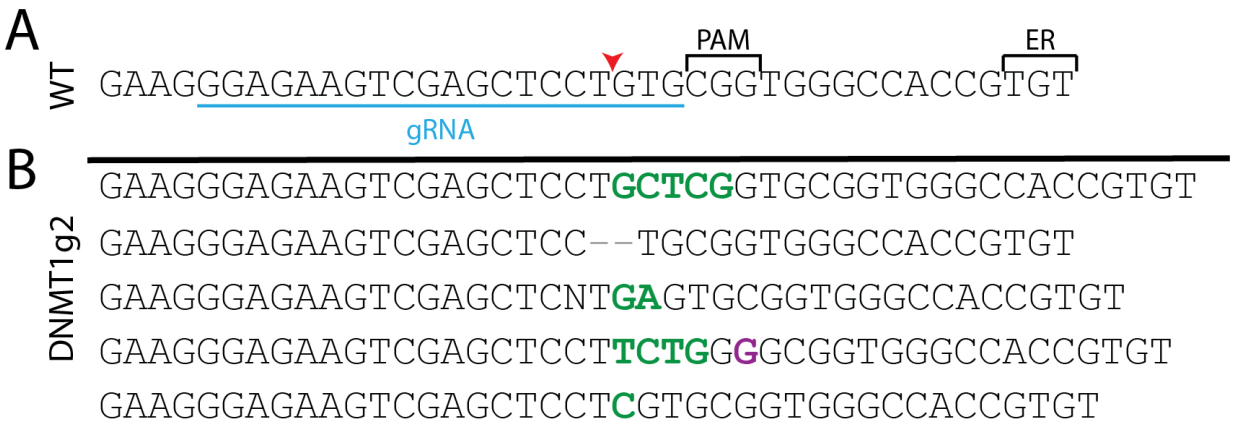

Figure 4.2. DNMT1g2 Mutant Genotypes Observed in G0 Adults.

(A) Wildtype allele at the DNMT1g2 mutagenesis target site, with guide RNA sequence (blue), PAM sequence, expected cut site (red arrowhead) and codon for essential cysteine residue (ER) noted. (B) A subset of recovered DNMT1g2 mutant alleles from Sanger sequencing of G0 animals. All sequences were scored and aligned manually. Insertions denoted in green and deletions indicated with grey dashes, base changes shown in purple, unresolved bases noted ("N"). Because it is possible for these animals to be mosaic, exact allele genotypes cannot be conclusively resolved per animal, and therefore, only a subset of alleles generated is shown.

4.2 MUTANT VALIDATION AND PHENOTYPING

All G0 animals from the first experiment were female and underwent normal development, including metamorphosis, and developed grossly normal features. Mutant animals were not visually distinguishable from wildtype (Figure 4.3) and could only be separated using DNA amplification and Sanger sequencing.

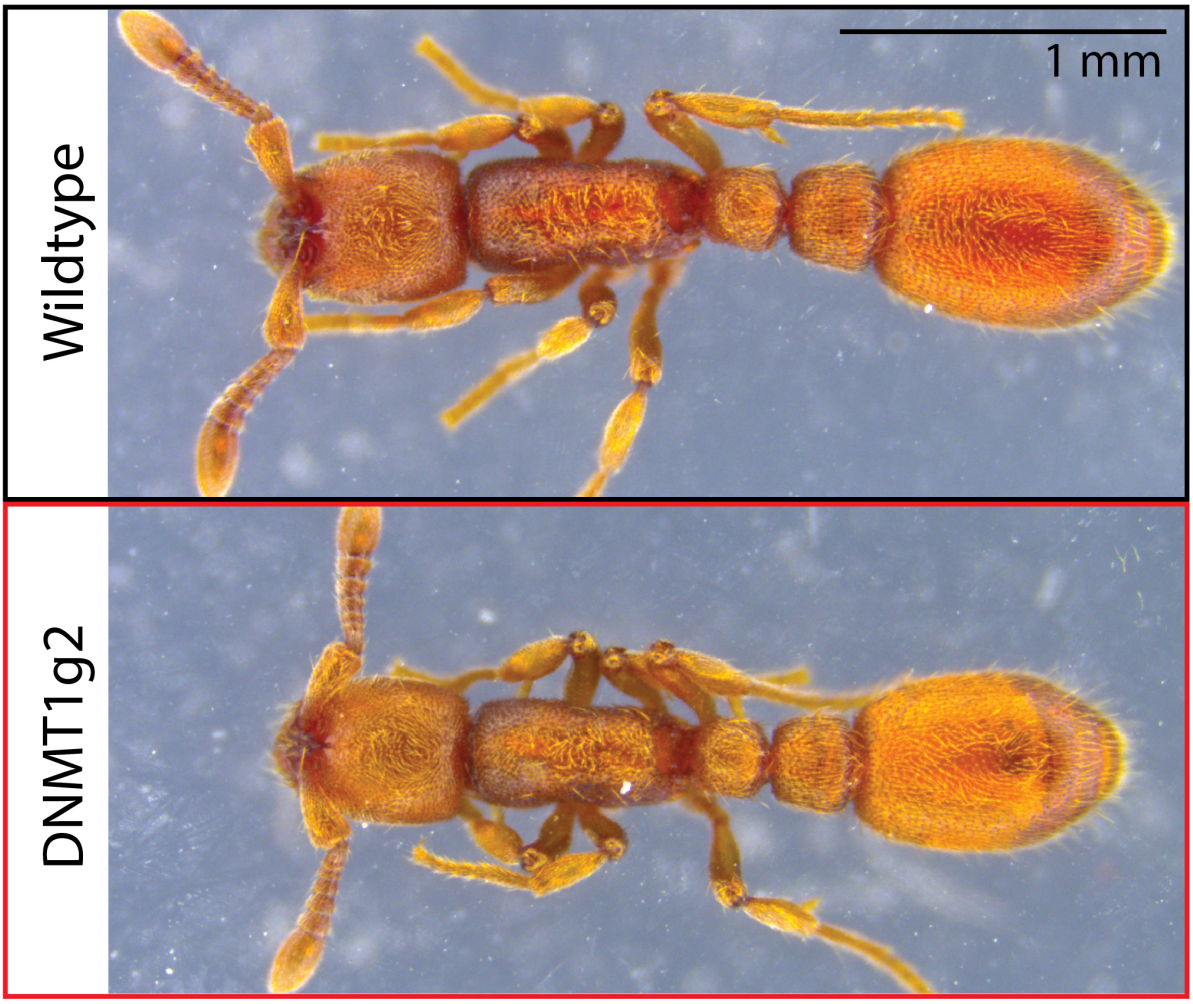

Figure 4.3. DNMT1g2 Mutant Female Gross Morphology.

Gross morphology of *O. biroi* wildtype animals (top) compared to a G0 DNMT1g1 mutant (bottom). DNMT1g2 mutant females develop grossly normal morphology and are able to undergo largely normal developmental program from egg to adulthood including metamorphosis.

While wildtype *O. biroi* colonies are entirely made of female workers, short lived males can be observed at a low frequency. Although they are usually haploid, diploid males have been observed occasionally. In our second experiment, one of the G0 animals was male, and appeared to develop

grossly normal features (Figure 4.4). Upon repeated genotyping, with Sanger sequencing, only a single allele with a five base pair insertion (+ “CGAGC”) was recovered. It is possible that only one allele was amplified by PCR in a heterozygous animal, if, for instance, there is a large size disparity between allele sizes, or if both alleles carry the same mutation. However, because haploidy is common among males, and the same single allele was recovered from multiple independent rounds of Sanger sequencing, this male was likely a haploid mutant. In this animal, it should be noted that the wings did not fully eclose, however, this may be independent from DNMT1 mutagenesis.

Figure 4.4. DNMT1g2 Mutant Male Gross Morphology.

DNMT1g2 mutant G0 male with a 5 base pair insertion in the DNMT1 catalytic domain (“+CGAGC”) is able to successfully complete normal development.

To evaluate the impact of the DNMT1g2 mutation on DNMT1 gene function, we measured methylation levels using whole genome bisulfite sequencing (WGBS). We extracted DNA from

the remaining tissue of four mutant and four wildtype DNMT1g2 G0 animals, after the ovaries and head had been removed. Global DNA methylation and any changes in this tissue are assumed to be representative of all tissues in the G0 animal, including the removed brain and ovary tissue, because work in other insects demonstrated that there are no tissue specific differences in global DNA methylation levels (Amukamara et al., 2020).

The bisulfite conversion rate was ~ 99.4% for all samples, with no significant differences in bisulfite non – conversion across genotypes. When correcting for cytosine bisulfite non – conversion, 1.02% of the genome was methylated in the wildtype ant tissue (95% CI, 0.90%, 1.24%) compared to 0.26% in the DNMT1g2 G0 mutant tissue (95% CI, 0.21%, 0.31%), demonstrating a fourfold decrease in global methylation in the mutants (Figure 4.5). This result provided direct evidence of DNMT1 inactivation as a result of the DNMT1g2 mutation. Furthermore, this is consistent with other insect studies, where decreased methylation levels are observed as a consequence of DNMT1 depletion by RNA interference (Amukamara et al., 2020; Bewick et al., 2019; Ventós-Alfonso et al., 2020). The remaining detected global methylation in the mutants can be attributed to a number of potential factors including undetected mosaicism, maternal provisions of wildtype DNMT1 protein, and methylation carried out by DNMT3 or another uncharacterized protein.

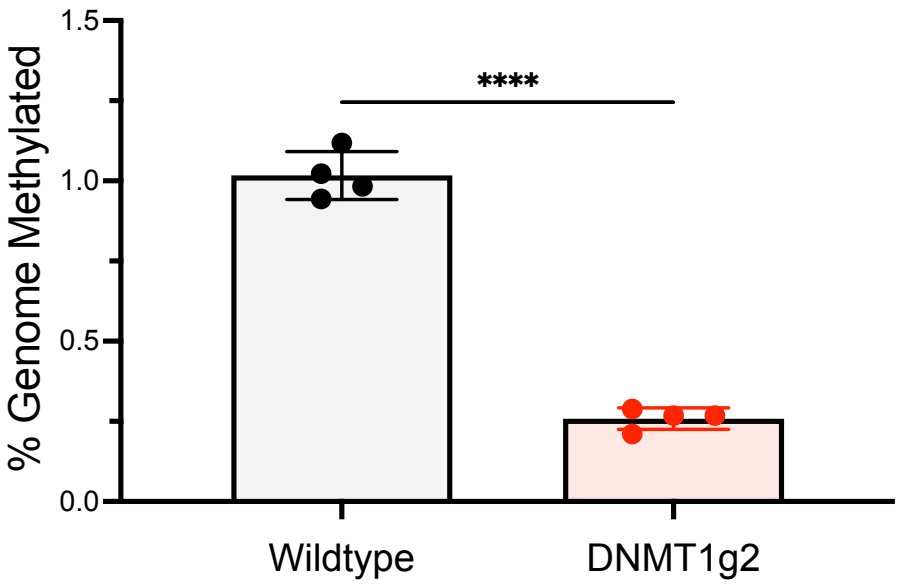

Figure 4.5. Genome – Wide DNA Methylation in DNMT1g2 Mutants.

Genome – wide methylation analysis using low coverage Whole Genome Bisulfite Sequencing. Data shown is corrected for bisulfite non – conversion estimates. Each data point represents DNA extracted from the body of a single ant after the head and ovaries had been removed. Drastic decrease in methylation observed in DNMT1g2 mutants compared to wildtype animals (Unpaired t – test, $p < 0.0001$).

After validating the impact of the DNMT1g2 mutation on DNMT1 function, as observed by decreased methylation, we wanted to characterize the impact of DNMT1 inhibition on caste and morphology. In social insects, more reproductive, or "queen – like" individuals, tend to be larger in body size (Trible and Kronauer, 2021). Furthermore, previous studies in social insects, including ants, have argued that DNMTs and DNA methylation suppress "queen – like" development, and that decreased levels of methylation are associated with larger, more "queen – like" individuals (Alvarado et al., 2015; Kucharski et al., 2008). To evaluate the possibility of such morphological

changes, G0 ants were restrained, photographed under a microscope, and different body segments were measured. Recorded measurements included head length and width, thorax length and width, petiole length, post petiole length and gaster length (Figure 4.6).

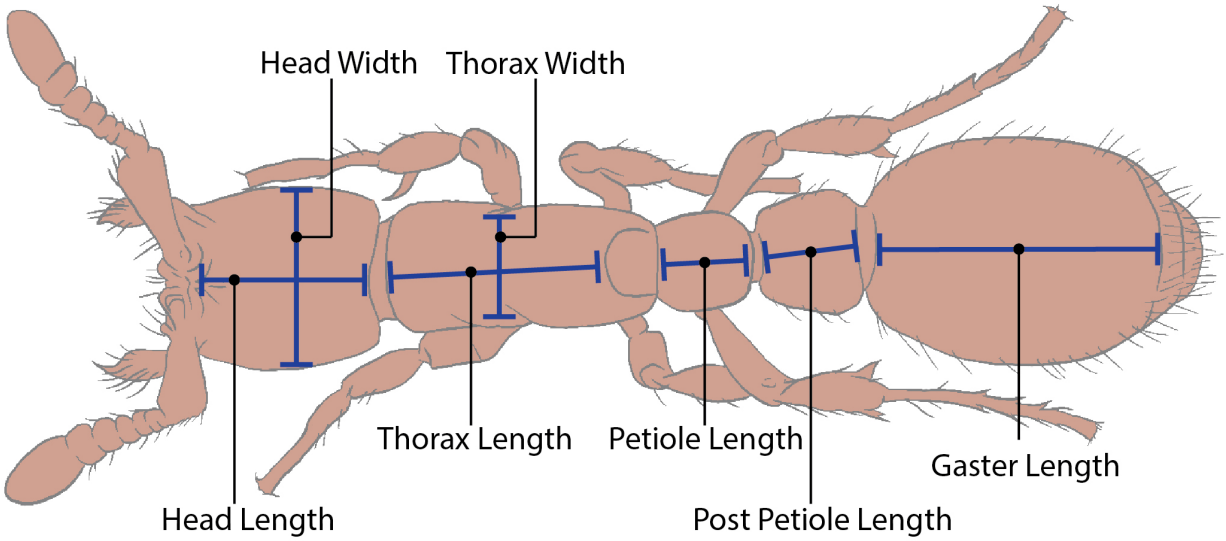

Figure 4.6. Diagram of Female *O. biroi* Morphological Measurements.

Diagram showing morphometric traits which were measured and compared between wildtype and mutant DNMT1g2 G0 animals. Importantly, all segments were measured in a consistent manner, independent of slight variation in positioning of the ant. Together, "Head Length", "Thorax Length", "Petiole Length", "Post Petiole Length" and "Gaster Length" provide a proxy measurement for total body size which can be measured consistently across ants.

All measurements were compared for three groups – G0 mutant (Inj. (Mut.)) and wildtype (Inj. (WT)) nestmates, as well as a control group of ants (Control). This second control group stemmed from eggs which were collected simultaneously as the G0 eggs, but were not injected with CRISPR/Cas9 reagents, and reared in parallel. To account for minor variation in ant orientation, a

sum of the cuticle lengths was used as a proxy for total body size (Figure 4.6). Overall, the G0 mutants appeared slightly smaller when compared to either G0 wildtypes (Tukey's multiple comparisons test, $p = 0.050$) or the uninjected control group (Tukey's multiple comparisons test, $p = 0.019$) (Figure 4.7). Specifically, a significant difference was observed in post petiole length (one – way ANOVA, $p = 0.0460$) and gaster length (one – way ANOVA, $p = 0.0022$) between the three groups. No other measured features differed at a statistically significant level (Figure 4.7).

While differences in morphology were observed, and DNMT1g2 mutants may appear slightly smaller than their wildtype nestmates, further studies would be necessary to provide concrete proof of an association between this mutation and "worker – like" body size. However, when taken together with the observed decreased methylation levels in these mutants (Figure 4.5), this result provides compelling evidence against the idea that DNA methylation suppresses "queen – like" traits, including body size, in social insects (Alvarado et al., 2015; Maleszka, 2008).

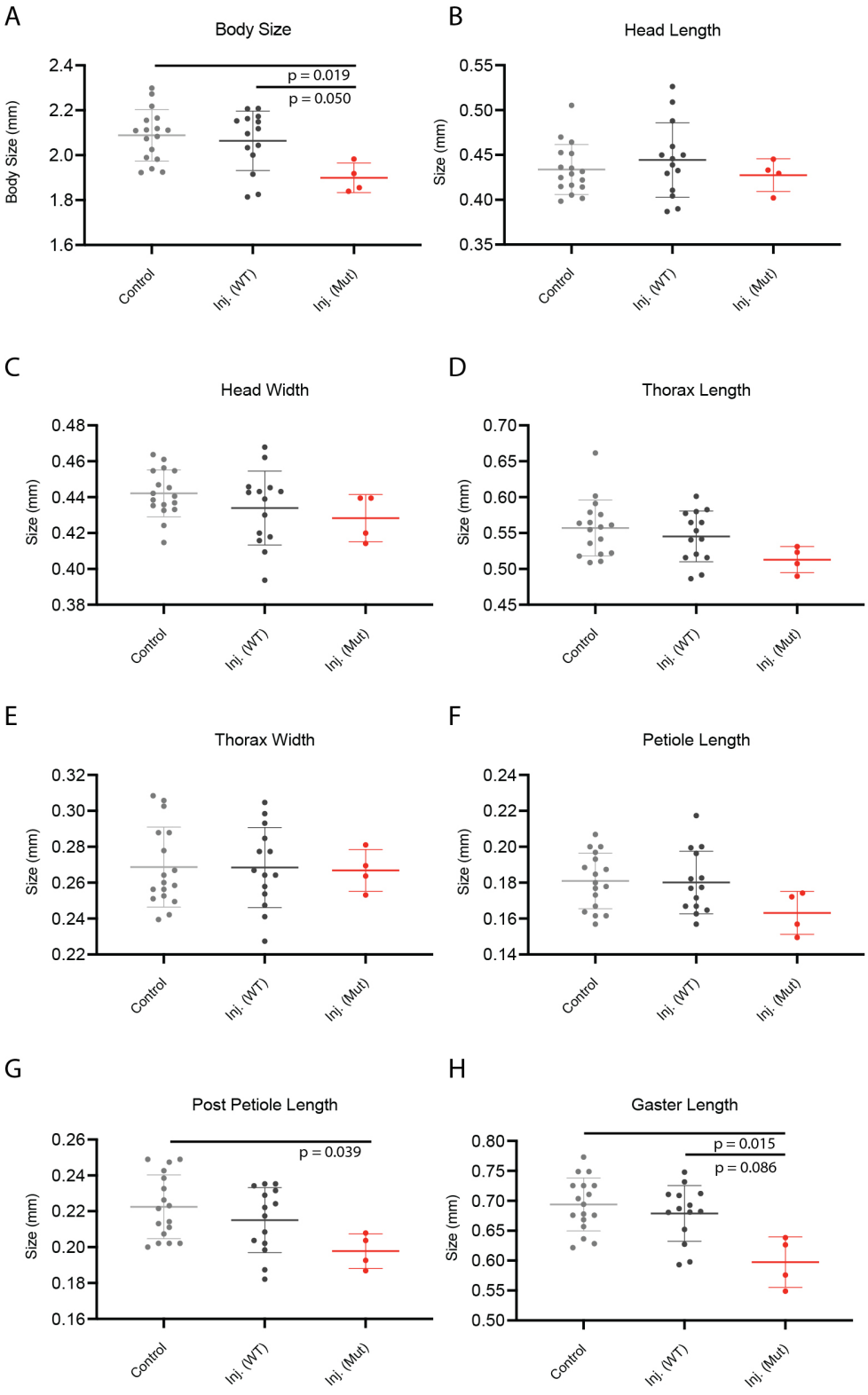

Figure 4.7. DNMT1g2 Mutant Morphological Feature Measurements.

Morphology measurements compared across two groups of samples – eggs which were injected (Inj.) with Cas9 and gRNA targeting DNMT1g2 or not injected and reared in parallel (Control). Injected eggs were reared to adulthood, and adults genotyped to evaluate which animals carried mutations at the target site in the DNMT1 catalytic domain (Mut.), and which did not (WT). (A) Body Size, as measured by the summation of head length, thorax length, petiole length, post petiole length and gaster length (Figure 4.6). Mutants appear slightly smaller compared to wildtype animals (one – way ANOVA, $p = 0.0248$). (B – F) No significant difference is observed in Head Width (one – way ANOVA, $p = 0.2178$), Head Length (one – way ANOVA, $p = 0.5659$), Thorax Width (one – way ANOVA, $p = 0.9883$), Thorax Length (one – way ANOVA, $p = 0.1018$), or Petiole Length (one – way ANOVA, $p = 0.1390$). (G) Significant difference observed in Post – Petiole Length (one – way ANOVA, $p = 0.0460$) between the three groups. (H) Significant difference observed in Gaster Length (one – way ANOVA, $p = 0.0022$) between the three groups. Multiple comparisons (Tukey's multiple comparisons test) p – values indicated where significant differences are observed on each graph. Lines indicate mean and standard deviation.

Finally, we aimed to evaluate the impact of DNMT1 inhibition observed in these DNMT1g2 mutants on fecundity and survival. For these experiments, eight G0 ants were placed in a colony with painted line A chaperones. Carcasses of any perished G0 ants were removed and frozen, at regular intervals. After 61 days, only two G0s remained in the colony, and were sacrificed. Six of the eight original G0s could be successfully genotyped, of which four were mutant. There was a drastic increase in mortality among the G0 mutants when compared to their G0 wildtype nestmates (log – rank test, $p = 0.049$) (Figure 4.8).

All eggs were removed from the colony and genotyped, to reveal 19 eggs stemming from the G0s (line B), which were successfully genotyped, and revealed to all be wildtype. This differed significantly from the frequency of mutants observed in the colony (four out of six genotyped) (Fisher exact test, $p = 0.0012$) (Figure 4.8). These data provide compelling evidence that DNMT1 inactivation as a result of the DNMT1g2 mutation leads to sterility.

These results are consistent with previous studies in insects, which have shown DNMT1 to play an important, potentially methylation independent, role in oogenesis and spermatogenesis (Amukamara et al., 2020; Bewick et al., 2019; Schulz et al., 2018; Ventós-Alfonso et al., 2020; Washington et al., 2020). However, the mechanism of this function of DNMT1, and its relationship to DNA methylation, remains unknown. Furthermore, it is possible that the increased mortality observed in these mutants may not be a direct consequence of decreased DNA methylation. Rather, this could be an indirect result of the observed abnormalities in oogenesis and reproductive system function.

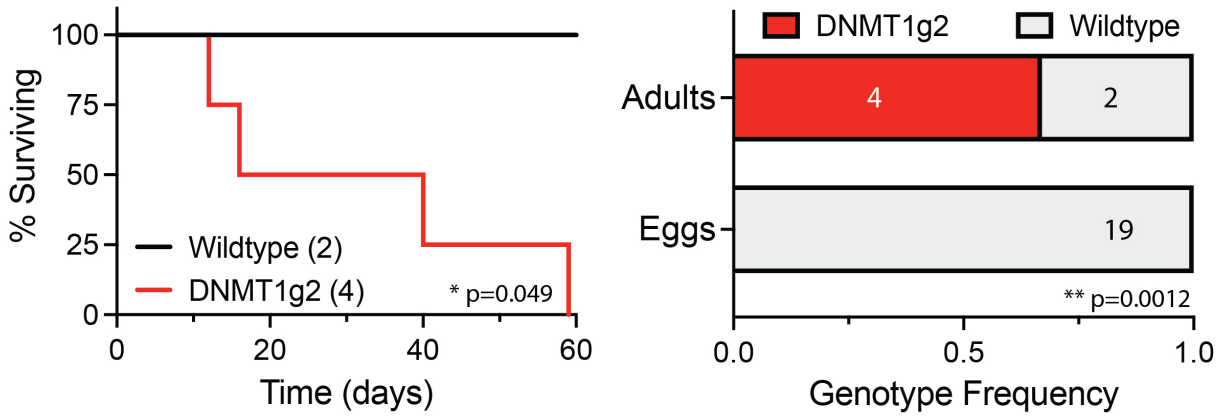

Figure 4.8. DNMT1g2 Reproduction and Survival.

(Left) Survival of DNMT1g2 G0 mutants compared to wildtype animals. Of the six animals for which genotypes could be recovered, all mutants died in the first two months, meanwhile at 61 days, the two wildtypes within the colony remained alive, demonstrating a drastic survival deficit as a result of mutation in the DNMT1 catalytic domain (Log – rank test, $p = 0.0494$). (Right) Out of the six G0 animals retrieved, four were mutant and two were wildtype, but all 19 sequenced eggs were wildtype, indicating a decrease in fertility or complete reproductive sterility as a result of mutagenesis in the DNMT1 catalytic domain (Fisher exact test, $p = 0.0012$).

4.3 DISCUSSION AND FUTURE DIRECTIONS

We successfully generated and reared DNMT1 catalytic domain mutants. The DNMT1g2 mutation led to DNMT1 inhibition, which we were able to observe as a drastic decrease in genome wide CpG methylation levels. Despite this inhibition and drastic in DNA methylation, both male and female G0 mutants were able to largely develop normally, including undergoing metamorphosis. The only developmental abnormality observed was the incomplete eclosion of the G0 mutant male's wings. However, this phenotype may not be associated with DNMT1 mutagenesis, because

it has previously been observed in wildtype males within stock colonies. Yet, it should be noted that abnormal male wing development, in the context of DNMT1 impairment, is not unprecedented, and has previously been observed in *Phenacoccus solenopsis*, the cotton mealybug (Omar et al., 2020). Therefore, further investigation is warranted to understand if this phenotype is associated with DNMT1 inhibition in *O. biroi*.

In these DNMT1 mutants, normal development is a notable finding, as all previous attempts at DNMT1 mutagenesis have resulted in embryonic lethality (Brown and Robertson, 2007; Damelin and Bestor, 2007; Li et al., 1993, 1992). However, all of these previous experiments were conducted in mammals, where DNMTs and DNA methylation may play a different role, including in genomic imprinting and X chromosome inactivation. Additionally, DNMTs may not be essential to insect development as some insect species, such as *D. melanogaste*r, have lost DNMTs altogether, and do not need to methylate their DNA (Urieli-Shoval et al., 1982).

Most methylation in insects that methylate their DNA, including *O. biroi,* appears to be concentrated in the gene bodies, and is pronounced at constitutively expressed, housekeeping, genes (Libbrecht et al., 2016). As a result, if DNA methylation were a major transcriptional regulator, global disruptions in methylation would have led to dysregulation of housekeeping genes. Dysregulation of these genes can be expected to trigger replication checkpoints or lead to embryonic lethality. The fact that normal development was observed, despite vast decreases in methylation, argues against the proposition that DNA methylation plays a direct role in transcriptional regulation, consistent with recent work in the field, which has further disputed this relationship (Bewick et al., 2019; Cardoso-Junior et al., 2021; Patalano et al., 2015).

Nonetheless, future work to understand DNMT1 in this species would benefit from RNA sequencing to evaluate the impacts of DNMT1 inhibition on gene transcription. Because these animals have abnormal reproduction and longevity, it should be expected that differential gene expression will be observed. However, the genes which are differentially expressed (DEGs) in DNMT1g2 mutants will likely be a combination of those responsible for the observed phenotypes and those whose expression may change as a result of these phenotypes. Among all differentially expressed genes, these two groups of DEGs may be difficult to disentangle. However, RNA sequencing may give us concrete evidence regarding the direct relationship between gene body DNA methylation and transcription. In principle, if DNA methylation were to suppress gene expression, all genes where methylation is decreased in the mutants should also be upregulated in expression. However, it is likely that this relationship does not exist or is indirect. For instance, only changes in methylation of certain transcription factors may directly regulate their expression, which in turn could regulate the expression of many other genes.

Despite normal development, the animals carrying the DNMT1g2 catalytic domain mutation in DNMT1 were sterile. This is consistent with other research in insects, where inhibition of DNMT1 during development by RNA interference leads to sterility in adults, demonstrating the importance of DNMT1 in oogenesis and spermatogenesis (Amukamara et al., 2020; Arsala et al., 2021; Bewick et al., 2019; Schulz et al., 2018; Ventós-Alfonso et al., 2020; Washington et al., 2020). Further studies of the ovarian structure are an essential first step in further evaluating this phenotype (discussed in Chapter 5), as in some of these studies, DNMT1 inhibition led to abnormal ovarian somatic tissue (Amukamara et al., 2020). Furthermore, questions remain about whether the role of DNMT1 in the ovaries and oocytes is methylation independent. This is because sterility

is observed after inhibition of DNMT1 in *Tribolium castaneum*, a species which carries a copy of the DNMT1 gene, but has no discernable levels of DNA methylation (Schulz et al., 2018).

Additionally, it is not clear whether the mortality observed is a direct consequence of decreased DNA methylation or a byproduct of the reproductive sterility. In social insects, less reproductive individuals tend to have a drastically decreased life span (Keller, 1998). However, it is also important to note that this mutation may not mimic physiological sterility of worker ants, and while mortality may result from this sterility, the underlying mechanism may be different. Furthermore, it is possible that neither the sterility nor mortality observed are a direct consequence of DNMT1 inhibition. This would be the case if, for instance, inhibition of DNMT1 and/or DNA methylation leads to endocrine dysfunction, which could ultimately result in both phenotypes.

Interestingly, we did not observe an association between decreased methylation levels and larger, more "queen – like" individuals (Bonasio et al., 2012; Maleszka, 2008). The DNMT1g2 mutants had decreased genome wide methylation levels, and simultaneously, appeared smaller and were sterile. Our results argue against the idea that DNA methylation is an inhibitory mechanism to "queen – like" development in social insects. However, because *O. biroi* is a queenless species, it is possible that reproductive caste regulation in this species is not representative of caste regulation in social insects. Nonetheless, further studies on DNMT1 inhibition by means of mutagenesis or RNAi in social insects with distinct reproductive castes are warranted to investigate this relationship.

CHAPTER 5. DNMT1 mRNA AND PROTEIN LOCALIZATION PATTERNS IN *O. BIROI*

To understand the basis of the phenotypes observed in DNMT1 catalytic domain mutants, we aimed to characterize the DNMT1 protein and localize DNMT1 gene expression. In previous studies on ants, DNMT1 expression seemed particularly high in ovaries (Arsala et al., 2021; Zwier et al., 2012). In the cotton mealybug, researchers found a 30 fold increase in DNMT1 transcription among gravid females when compared to virgins (Omar et al., 2020). Furthermore, previous work in various insect species identified DNMT1 to play an essential function in oogenesis, while inhibition of DNMT1 resulted in abnormal ovary phenotypes (Bewick et al., 2019; Washington et al., 2020). We used fluorescence *in situ* hybridization to localize DNMT1 mRNA transcripts within the ant ovary. Furthermore, we used immunohistochemistry to visualize the DNMT1 protein in the same cells. Importantly, we observed large amounts of maternal DNMT1 transcript and protein, provisioned into oocytes from an early stage, potentially weeks before the completion of meiosis and initiation of mitosis.

5.1 *O. BIROI* OVARY ANATOMY

Female *O. biroi* reproductive anatomy is similar to that of other social insects, including *A. mellifera* (Dearden, 2006). Workers have two polytrophic meroistic ovaries, each composed of one to three ovarioles. Each ovariole is composed of the vitellarium, germarium and terminal filament (Figure 5.1). Unlike the reproductive castes observed in other social insects, with a highly fertile “queen” caste and a sterile “worker” caste, in this queenless species, all female workers are able to activate their ovaries and reproduce during the reproductive phase of their reproductive

cycle (Ravary et al., 2006; Ravary and Jaisson, 2002). In each ovariole, stem cells within the germarium enter meiosis and the young oocyte travels to the vitellarium. Here the developing follicle is surrounded by follicular cells and receives nourishment from an adjacent bundle of nurse cells (Figure 5.1). Unless reproduction is inhibited by brood signaling during the brood care phase of the reproductive cycle, (Ravary et al., 2006), the follicle will continue to grow until oviposition.

Often, multiple highly developed oocytes can be observed simultaneously in *O. biroi* ovaries (Figure 5.1), but it is not yet known how many eggs a single individual can lay per reproductive cycle, and how this number changes with variation in ovariole number. The mitosis to meiosis transition occurs in the *O. biroi* ovariole, and meiosis progresses through prophase I, the completion of which can be observed immediately post – partum. This is followed by reductional division and central fusion to create genetically clonal offspring (Oxley et al., 2014). Because DNMT1 is known to copy methylation patterns during replication, we expected to see increased signal in the germarium, where both the embryonic and somatic stem cells can be found (Kirilly and Xie, 2007).

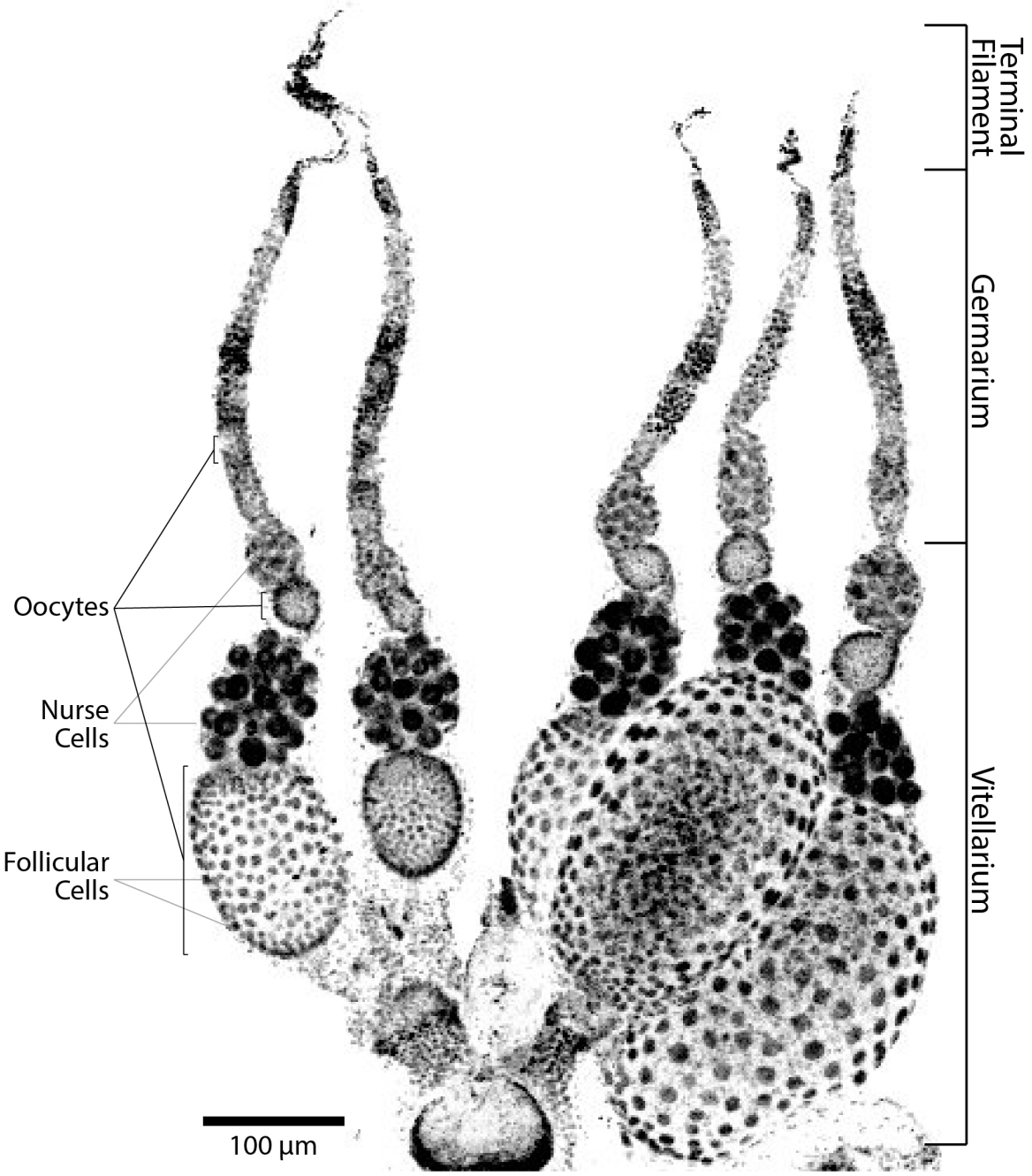

Figure 5.1. *O. biroi* Ovary Anatomy.

Fluorescent image showing two *O. biroi* ovaries, composed of five total ovarioles. DAPI used to visualize DNA (black). Each ovariole is made of the terminal filament, germarium and vitellarium. Ovaries appear very "active", with large oocytes (right bottom), as well as oocytes in various

earlier stages of development, observed in each of the ovarioles. The oocyte is surrounded by follicular cells and connected to an adjacent bundle of nurse cells which provide nutrients through early oogenesis.

5.2 DNMT1 mRNA AND PROTEIN IN THE *O. BIROI* OVARY

To visualize DNMT1 transcription in the *O. biroi* ovary, we used a previously established mRNA fluorescence *in situ* hybridization (FISH) protocol in the species (Fetter-Pruneda et al., 2021). We were able to observe fluorescence signal, representing DNMT1 transcription, in the cytoplasm of oocytes, nurse cells and some cells in the germarium (Figure 5.2). This signal is specific to DNMT1 transcripts, rather than autofluorescence, because we did not observe the same fluorescence pattern in the negative controls, which were processed in parallel, but without the DNMT1 mRNA detection probes (Figure 5.2).

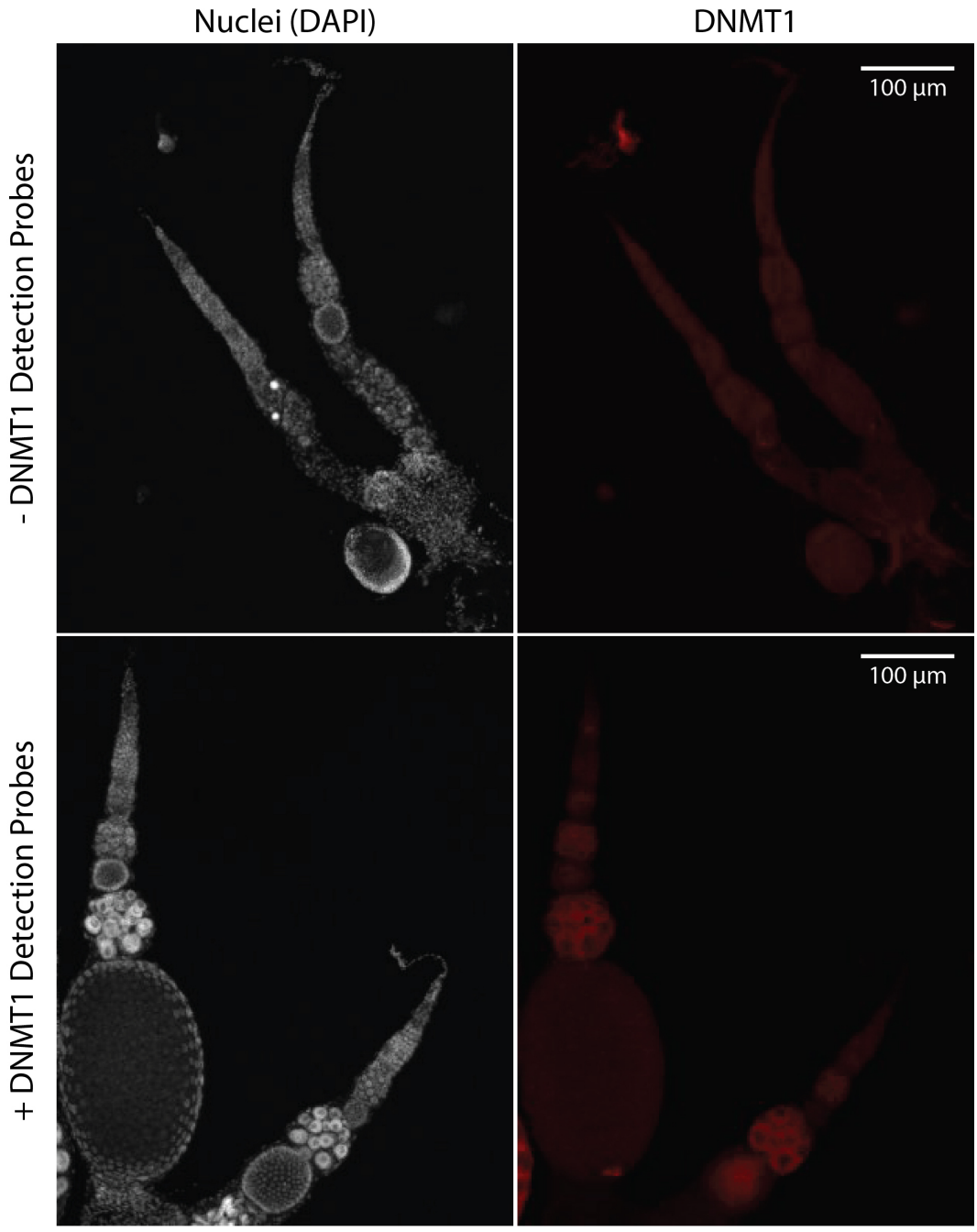

Figure 5.2. DNMT1 mRNA Fluorescence *in situ* Hybridization in Ovaries.

(Top) Negative control ovaries were incubated and processed using a previously established protocol for FISH in *O. biroi* (Fetter-Pruneda et al., 2021), in parallel, without the addition of probes targeting DNMT1 mRNA. Diffuse observed fluorescence seen throughout the ovary

corresponds to signal from autofluorescence (Right, Red Channel). DNA labeled with DAPI in grey. (Bottom) Addition of probes designed to target DNMT1 mRNA results in increased fluorescence specific to cells in the germarium, as well as cytoplasm of nurse cells and some oocytes within the vitellarium. Fluorescence signal corresponds to presence of active DNMT1 transcription in these cells. DNMT1 mRNA labeled in red, DNA labeled with DAPI in grey.

Next, we aimed to visualize the DNMT1 protein within the same tissue using protein immunohistochemistry. A commercial antibody, designed to target the conserved mammalian DNMT1 catalytic domain, was obtained. We observed protein signal in cells within the germarium, nurse cells, follicular cells. Additionally, DNMT1 protein appeared to be maternally provisioned into oocytes (Figure 5.3). Unlike the mRNA FISH, this signal was nuclear and co – localized with the DAPI stained DNA, consistent with the previous understanding of DNMT1's main function in methylating DNA within the nucleus.

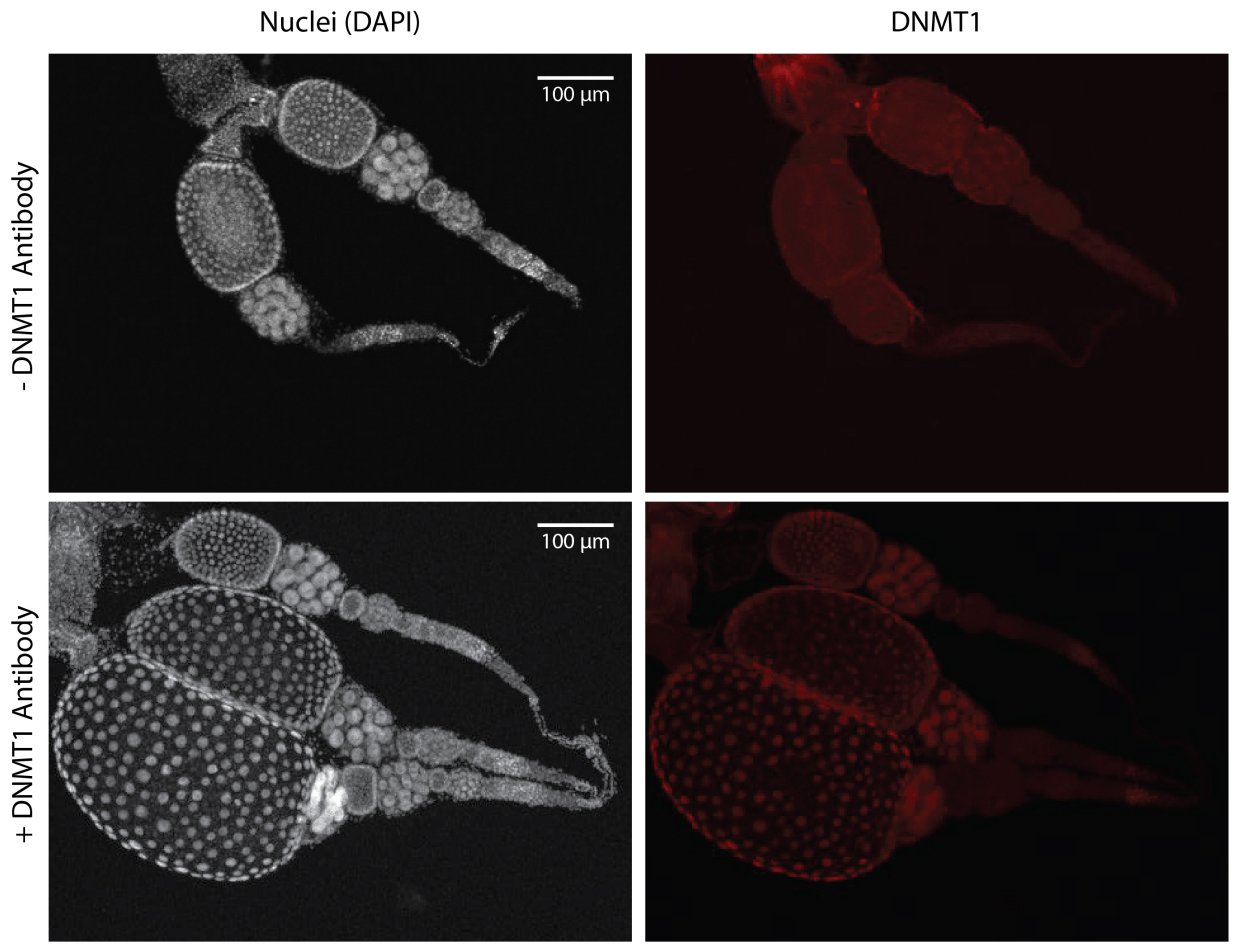

Figure 5.3. DNMT1 Protein Immunohistochemistry in Ovaries.

(Top) Ovary immunohistochemistry of *O. biroi* ovary, which was not incubated with primary antibody against DNMT1, but processed in parallel. DNA shown in grey labeled with DAPI. Diffuse signal seen in the DNMT1 channel represents autofluorescence or nonspecific secondary antibody binding, serving as a negative control. (Bottom) *O. biroi* ovary tissue incubated with DNMT1 antibody shows signal specific for DNMT1 protein. Increased signal observed in the germarium, nurse cells, follicular cells as well as within the oocyte. DNMT1 signal co – localizes with the DAPI stain, implying nuclear localization.

After observing DNMT1 protein and mRNA being maternally provisioned into oocytes, we wanted to further investigate this phenomenon, and how the pattern may change through the oocyte development. In *O. biroi*, developing oocytes can usually be observed in all ovarioles (Figure 5.1). Furthermore, within each ovariole, oocytes originate in the germarium and travel to the vitellarium as they mature and as a result, multiple oocytes, of various developmental stages can be observed in a single ovariole. This allowed us to visualize DNMT1 in the oocytes during early and late developmental stages using protein immunohistochemistry. In very young oocytes, which may be weeks from oviposition, we observed DNMT1 signal to overlap in its entirety with the DNA signal (visualized by DAPI), indicating that at this stage, the protein is confined to the nucleus (Figure 5.4). As the oocyte matures, this pattern changes to appear less smooth and extends beyond the nucleus, although still surrounding the nuclear material. Additionally, foci of DNMT1 signal appear around the perimeter of the oocyte (Figure 5.4).

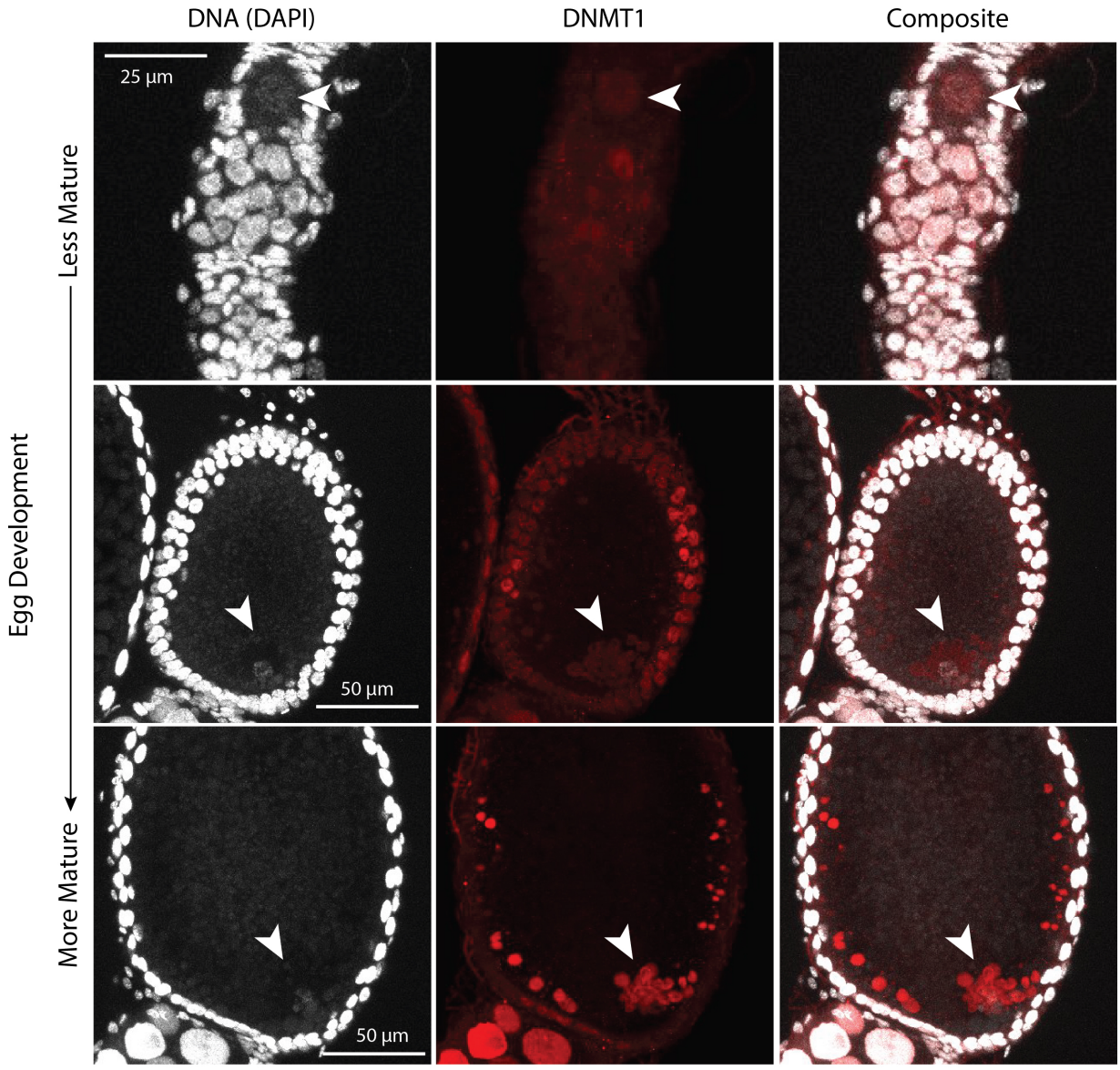

Figure 5.4. DNMT1 Protein Immunohistochemistry in Oocytes Pre – Oviposition.

(Top) DNMT1 (red) signal using immunohistochemistry co – localizes with DNA, as visualized by DAPI (grey), demonstrating confinement to the nucleus in young oocytes. (Middle) As the oocyte matures, the nuclear material moves toward one pole and DNMT1 appears to expand beyond the condensed nuclear material and change shape. (Bottom) In more mature oocytes, the DNMT1 pattern expands well beyond the localization of the nucleus and foci of increased intensity

can be observed around the edges of the oocyte as well. Arrowheads indicate location of nucleus and loci of increased DNMT1 protein in each oocyte.

Next, we wanted to learn more about this unique pattern of DNMT1 protein localization in developing oocytes as they near oviposition. To evaluate the timing of this phenomenon relative to other events during oogenesis, we used the formation of the Balbiani body as a landmark. Also called the mitochondrial cloud, or yolk nucleus, this structure has been identified in multiple species during oogenesis including *D. melanogaster* (Cox and Spradling, 2003; de Smedt et al., 2000). This structure is composed of various organelles including mitochondria and mRNA and its function remains unknown, although it may be involved in establishing oocyte asymmetry, or mitochondrial proliferation (de Smedt et al., 2000).

We used an antibody against the conserved mammalian mitochondrial ATP synthase alpha subunit (ATPS5A) to visualize mitochondria in *O. biroi* ovaries. It can be expected that transcriptionally active cells, such as the nurse cells, may require lots of energy and thereby have a high number of mitochondria. We observed increased fluorescence in the germarium, nurse cells and oocytes (Figure 5.5) as predicted. We did not observe this staining pattern in the negative control which only showed diffuse nonspecific signal from autofluorescence and possible secondary antibody binding (Figure 5.5). Finally, the mitochondrial staining signal observed was extra – nuclear as expected, compared to the nuclear DNMT1 staining.

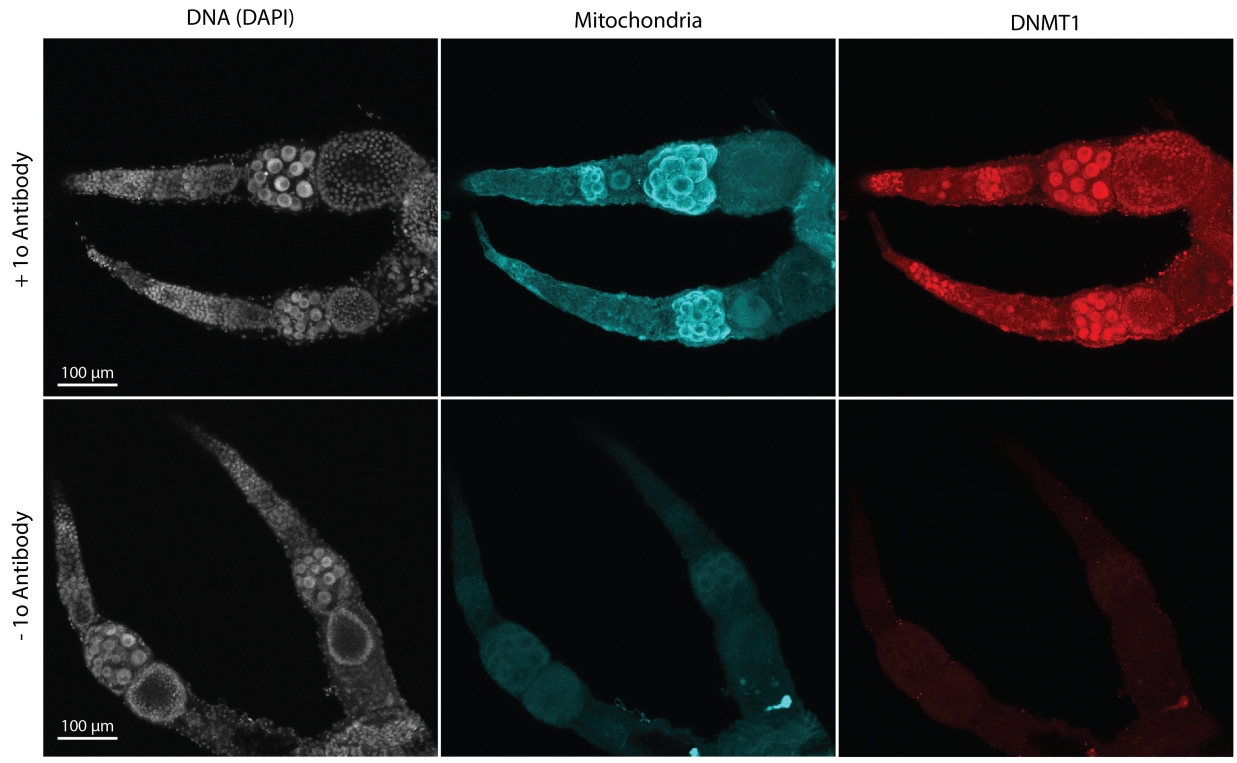

Figure 5.5. Protein Immunohistochemistry Detecting Mitochondria in *O. biroi* Ovaries.

(Top) Ovary fixed in paraformaldehyde and incubated with primary antibody (+ 1o Antibody) against mitochondrial ATPS5A (Middle) and antibody against DNMT1 (Right) compared with ovary which was only treated with DAPI and secondary antibody (-1o Antibody). (Left) DNA labeled with DAPI in both samples. (Middle, Top) Treatment with antibody against mitochondrial marker ATPS5A results in strong extra – nuclear signal in the nurse cells, cells in the germarium and oocytes. (Right, Top) DNMT1 protein immunohistochemistry consistent with previous experiments (Figure 5.3). (Bottom, Middle / Right). Diffuse brightness in ovaries not treated with primary antibody (-1o Antibody) shows signal due to nonspecific secondary antibody binding and autofluorescence, confirming the specificity of mitochondrial and DNMT1 antibody signal to the respective target.

When looking closer at oocytes nearing oviposition, we again observed a focus of DNMT1 density at the pole proximal to the nurse cells (Figure 5.6). Furthermore, we were able to capture a locus of increased mitochondrial density adjacent to this DNMT1 condensation (Figure 5.6). This condensation of mitochondria might be indicative of Balbiani body formation in these oocytes, which may be associated with the observed DNMT1 pattern.

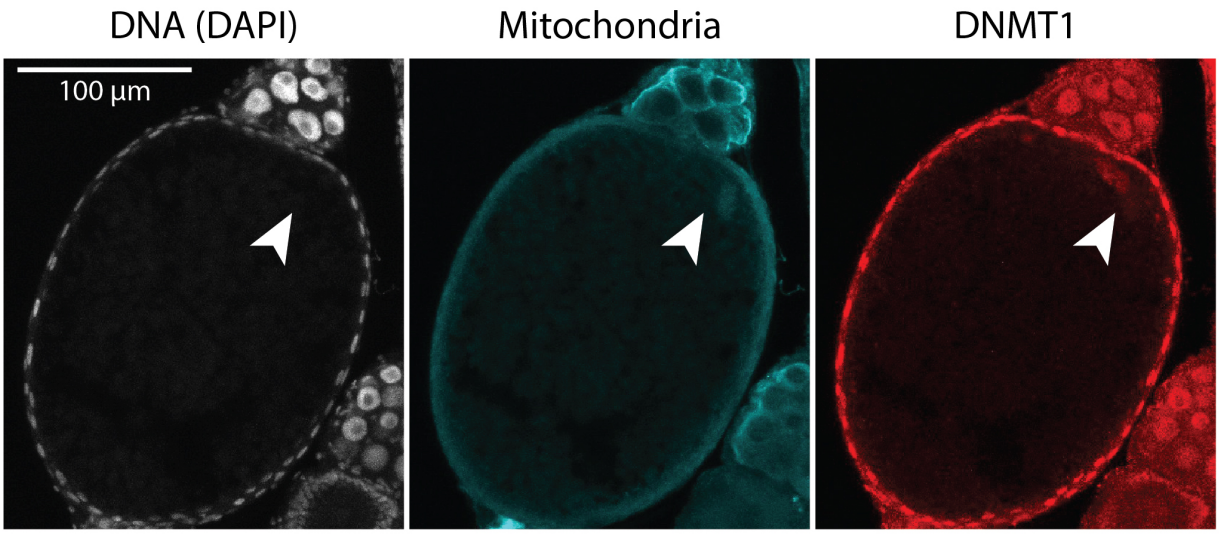

Figure 5.6. Mitochondria and DNMT1 in *O. biroi* Oocytes Pre – Oviposition.

Immunohistochemistry for mitochondrial marker ATPS5A and DNMT1 in large developing oocytes within the ovary. (Left) DAPI used to visualize DNA and structure of oocyte as well as surrounding follicular cells and adjacent nurse cell bundle. (Middle) Mitochondria visualized with antibody against ATPS5A shows increased signal by the oocyte pole adjacent to the nurse cells. (Right) Increased foci of DNMT1 intensity observed adjacent to the mitochondrial locus in a similar location within the oocyte. Signals of increased DNMT1 and mitochondrial densities appear adjacent but not overlapping.

5.3 DNMT1 BRAIN IMMUNOHISTOCHEMISTRY

Additionally, we wanted to evaluate the presence of DNMT1 protein in the *O. biroi* brain using protein immunofluorescence. However, previous studies in *Solenopsis invicta* have shown that DNMT1 expression is significantly lower in the heads of ants compared to their ovaries (Kay et al., 2018). While we observed some signal in the brain tissue including the mushroom body (Figure 5.7), this was likely due to tissue autofluorescence or nonspecific binding of the secondary antibody, because a similar pattern could be observed in the negative control tissue, which was not incubated with primary antibody against DNMT1. The mushroom body antibody staining is representative of what was observed in other brain regions.

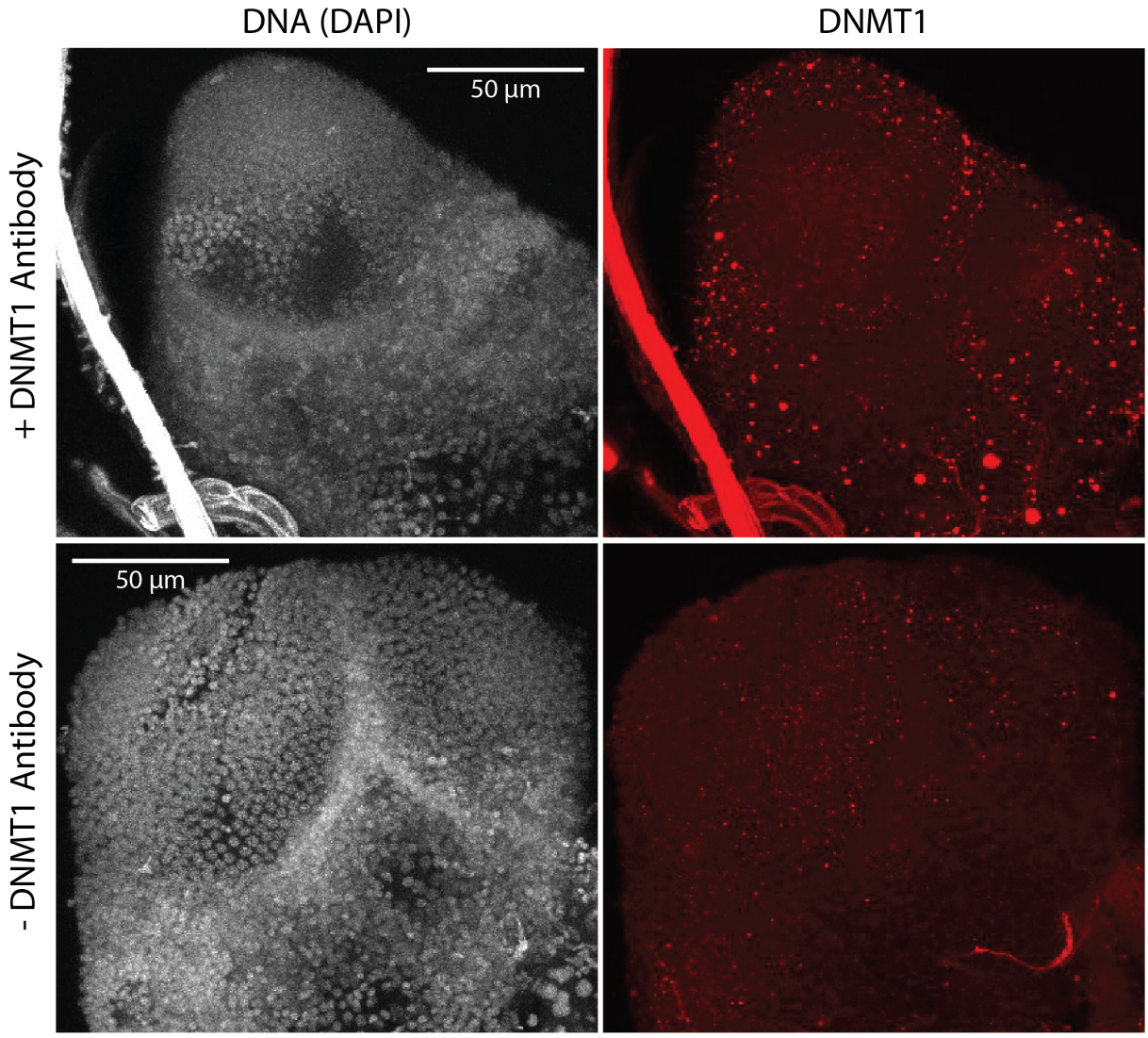

Figure 5.7. DNMT1 Protein Immunohistochemistry in the Brain.

(Top) *O. biroi* mushroom body, stained with DAPI, labelling DNA (grey) and antibody labeling DNMT1 (red). Diffuse signal and some punctate foci of increased fluorescence can be seen in the DNMT1 channel. (Bottom) *O. biroi* mushroom body, which was processed in parallel, but without DNMT1 antibody, shows a similar diffuse fluorescence pattern with speckled foci, likely corresponding to signal from nonspecific secondary antibody binding or autofluorescence.

5.4 DNMT1 PROTEIN IN DNMT1g1 AND DNMT1g2 MUTANTS USING IMMUNOHISTOCHEMISTRY

After localizing the DNMT1 protein using immunohistochemistry in the ovaries of *O. biroi* animals, we wanted to evaluate the effects of mutating DNMT1 using both DNMT1g1 and DNMT1g2 mutants. Because we did not observe any abnormal phenotypes or changes in methylation in the DNMT1g1 mutants, we did not expect to see any changes in protein immunohistochemistry. Additionally, because we saw a drastic decrease in genome wide DNA methylation, indicating DNMT1 inhibition, in the DNMT1g2 mutants, we expected to see a decrease or loss of DNMT1 in protein using immunofluorescence. Furthermore, after observing sterility in DNMT1g2 mutants, we aimed to evaluate the source of this phenotype including possible abnormal development of the ovarian somatic tissue, or deficits impacting oogenesis initiation.

Morphologically, ovaries of DNMT1g1 mutants appeared normal and active (with large oocytes nearing oviposition) at a similar level as wildtype samples. As predicted, we did not observe any differences in protein localization or quantity, in these mutants (Figure 5.8). Despite mutagenesis of the DNMT1 gene, we observed DNMT1 protein in the germarium, follicular cells, nurse cells and oocytes for both genotypes of DNMT1g1 mutants (-7bp / -7bp and -8bp / -7bp), a pattern resembling DNMT1 immunohistochemistry in wildtype animals. Additionally, the DNMT1 signal was nuclear as previously observed in wildtype animals, implying that the DNMT1 protein transport into the nucleus from the cytoplasm after translation of DNMT1 mRNA remained unaffected.

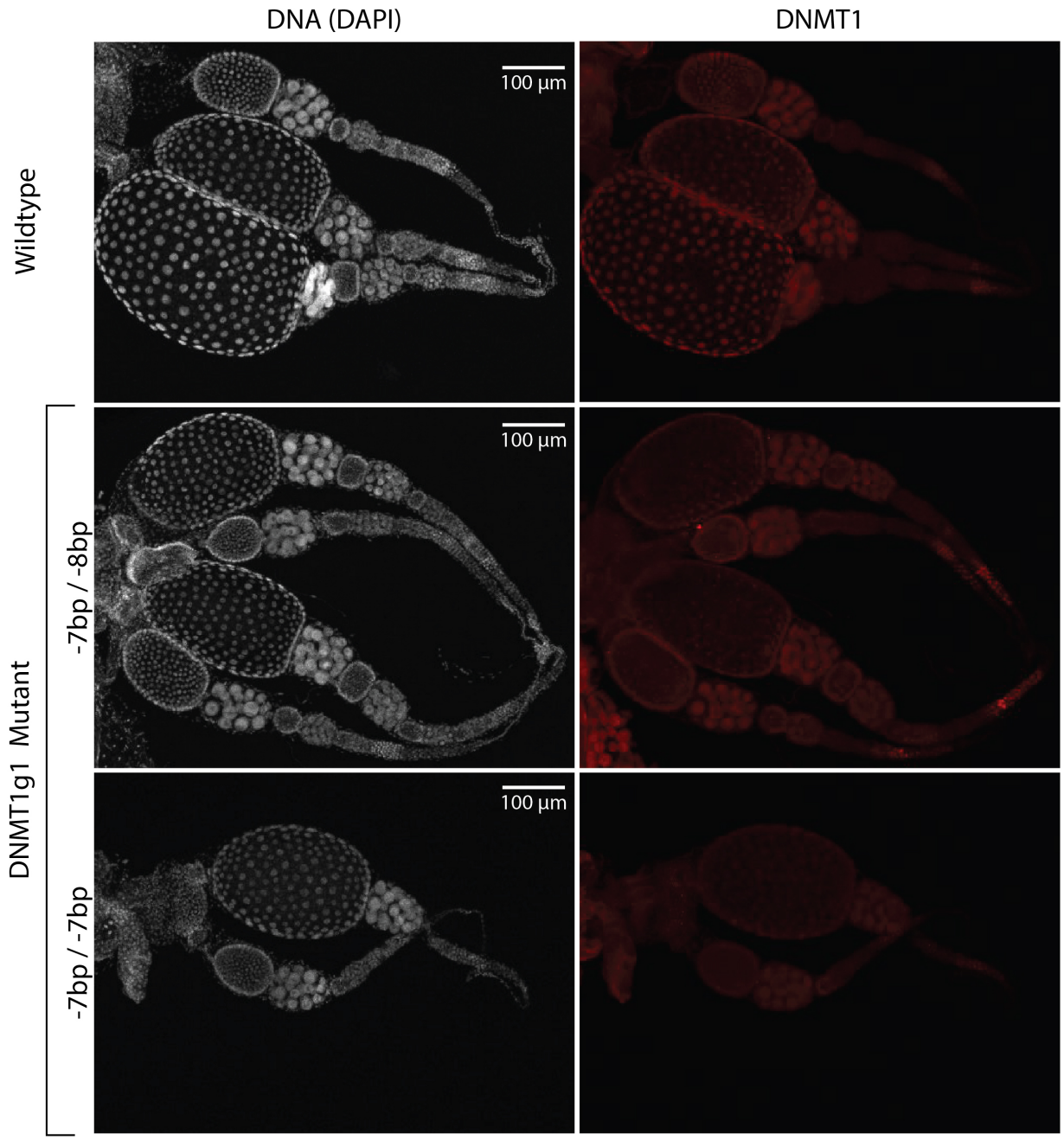

Figure 5.8. DNMT1 Protein Immunohistochemistry in DNMT1g1 Mutant Ovaries.

(Top) Reference image of DNMT1 protein immunohistochemistry in a wildtype animal (also shown in Figure 5.3) with three ovarioles. Increased signal intensity observed in the germarium, the nurse cells and follicular cells as previously described in Section 5.2. (Bottom) DNMT1g1

mutants with frameshift mutations in the second exon of the DNMT1gene. Similar to the wildtype, increased signal intensity seen in the germarium, nurse cells and follicular cells in mutant animals of both genotypes (-7bp / -8bp and -7bp/ -7bp). No discernable difference in DNMT1 protein localization or intensity noted using immunohistochemistry when compared to wildtype ovaries, or between the two genetic lines of DNMT1g1 mutants. Highly active, developed ovaries with large oocytes observed both in the wildtype and mutant samples. All samples were processed and imaged in parallel.

When looking more closely at the DNMT1g1 mutant oocytes (Figure 5.9), we again observed the same pattern of DNMT1 expression as previously observed in wildtypes (Figure 5.3). As previously observed in wildtype animals, this pattern of DNMT1 expression again appeared to co – stain with the nuclear DNA in young oocytes and changed as the oocyte matured in both DNMT1g1 mutant genotypes (-7bp / -8bp and -7bp / -7bp).

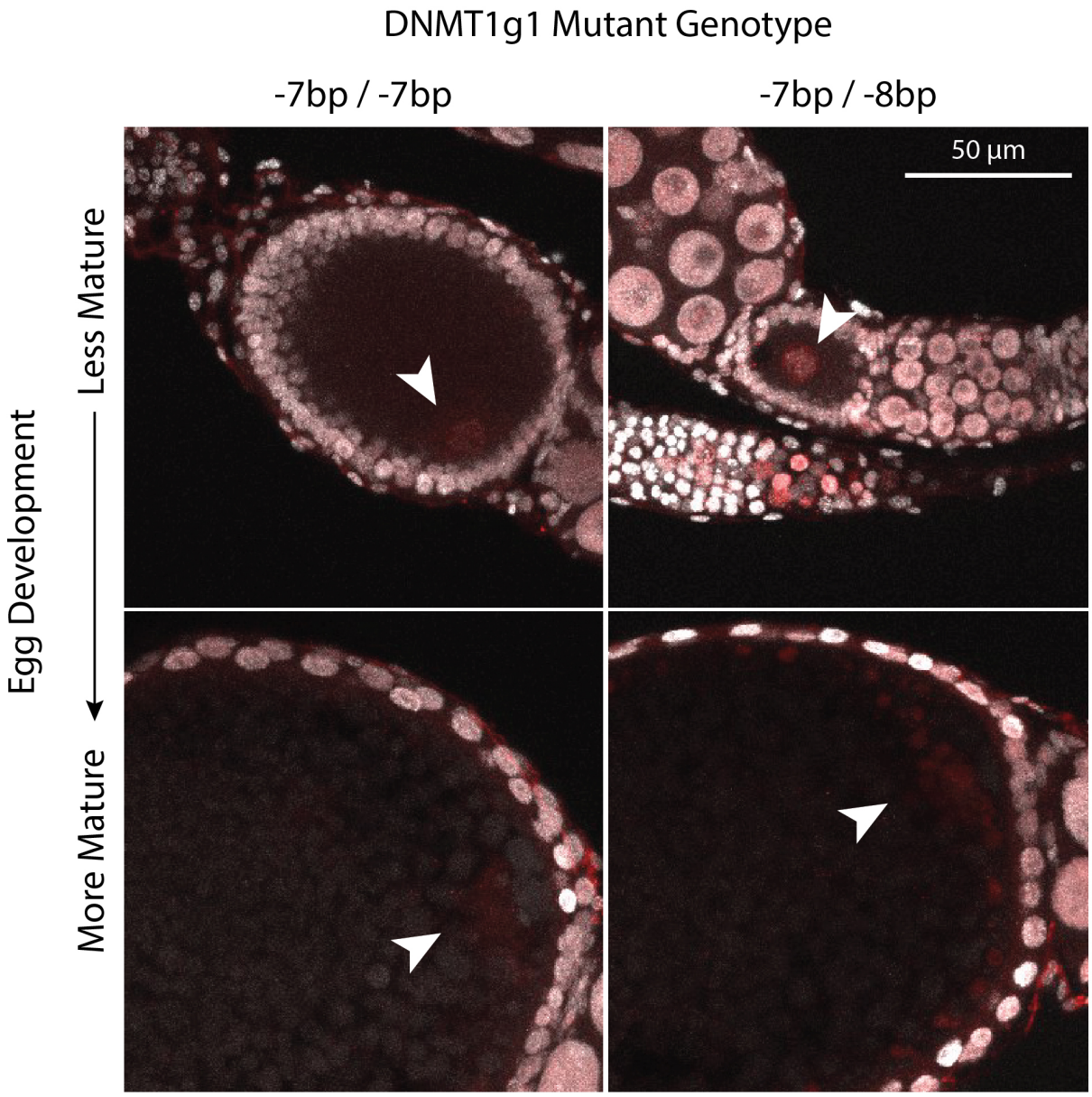

Figure 5.9. DNMT1 Protein Immunohistochemistry in DNMT1g1 Mutant Oocytes.

Images showing DNMT1 protein inside of oocytes of DNMT1g1 mutants, across both genotypes -7bp / -7bp and -7bp / -8bp, similar to signal observed in wildtype oocytes (Figure 5.4). DNMT1 appears more confined to the nucleus in younger, less developed, oocytes. This pattern changes to

a more diffuse locus around the base of the oocyte as it matures (arrowhead). DNA shown in gray and labeled with DAPI, DNMT1 shown in red.

Next, we aimed to evaluate the impact of the catalytic domain mutation (DNMT1g2) on ovarian morphology and DNMT1 protein localization. In these mutants we observed decreases in methylation levels, reproductive sterility and survival deficits. Because of the high mortality that resulted from the mutation, ants were dissected at ~1 week of age to evaluate ovary morphology and characterize the DNMT1 protein using immunohistochemistry. It is important to note that ants this young may not have fully activated their ovaries yet and can be expected to have significantly smaller oocytes which are not yet nearing oviposition. For comparison, we evaluated age matched control ants which were reared in parallel, as well as injected G0 wildtype ants, where mutagenesis was unsuccessful. We did not observe any obvious differences in ovary morphology or antibody staining pattern in G0 wildtype animals compared to uninjected, age matched wildtypes which were reared in parallel (not shown).

Three DNMT1g2 mutant ovaries were recovered. Of these, all ants had two ovarioles, and appeared grossly normal, containing a terminal filament, germarium and vitellarium (Figure 5.1, Figure 5.10). Furthermore, we observed developing oocytes in each of these mutant ovaries (Figure 5.10). However, the DNMT1 signal appeared diffuse and not localized to the regions observed in the wildtype ovaries. This indicates that the DNMT1 catalytic domain, which contains the antibody target site, is absent in the DNMT1g2 mutants. The remaining diffuse signal in this case likely is indicative of autofluorescence or nonspecific secondary antibody binding.

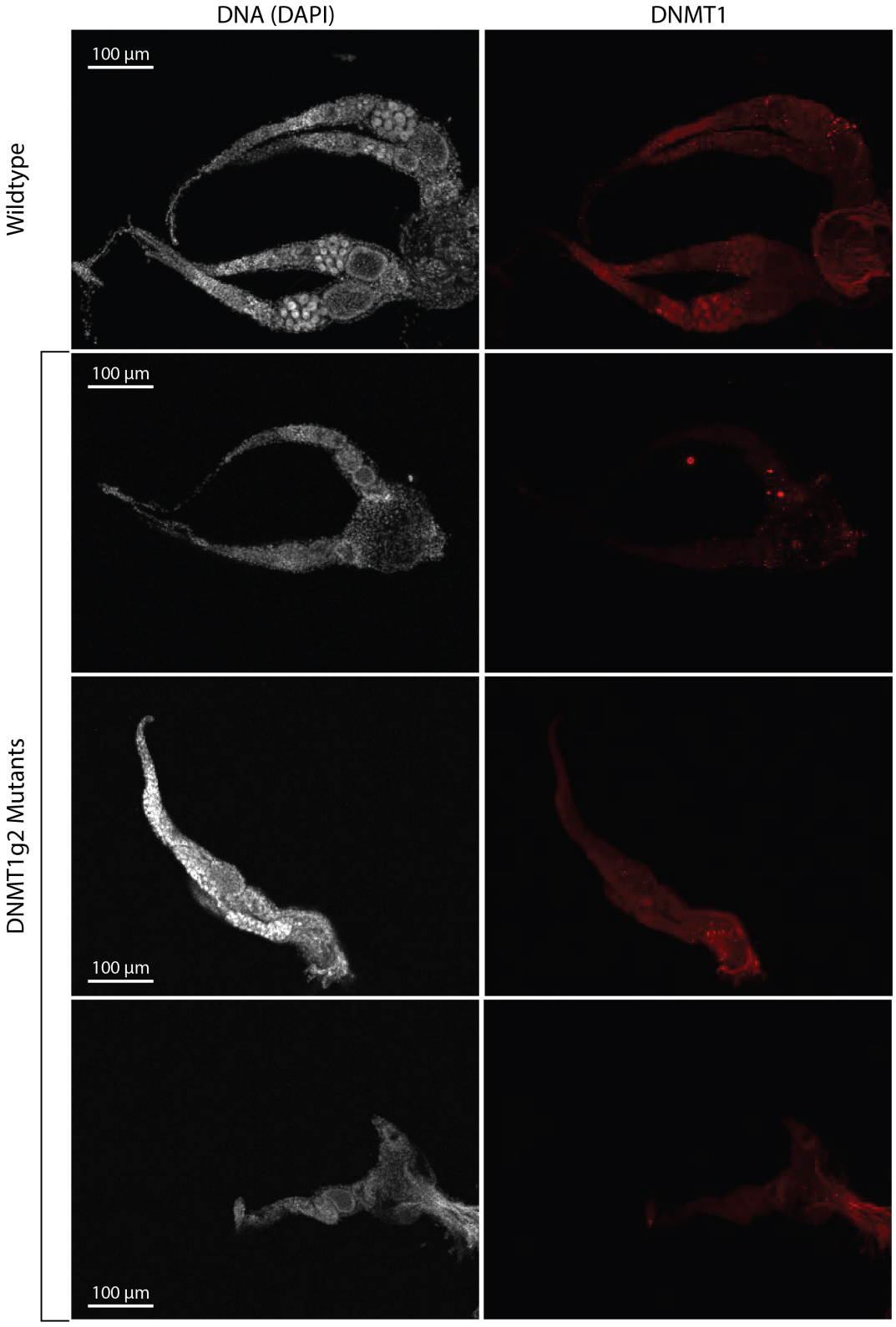

Figure 5.10. DNMT1 Protein Immunohistochemistry in DNMT1g2 Mutant Ovaries.

(Top) Protein immunohistochemistry shows DNMT1 in ovaries of a wildtype animal. Signal can be observed in cells within the germarium, nurse cells and oocytes (DNA labeled with DAPI in grey). (Bottom) DNMT1 protein immunohistochemistry in ovaries of three DNMT1g2 mutants, which carry mutations in the catalytic domain of DNMT1. Ovaries appear grossly normal and include developing oocytes. Nonspecific, diffuse signal is observed throughout the in the DNMT1 channel, likely due to nonspecific binding of the secondary antibody or autofluorescence. No relative increased in fluorescence signal is observed in the germarium, nurse cells, follicular cells or the oocytes.

Next we asked whether the DNMT1g2 mutation impaired fertility by limiting the number of ovarioles. In all three mutants, only one ovariole was observed in each ovary. We compared the number of ovarioles in DNMT1g2 G0 mutants (Inj. (Mut.)) to wildtype animals (Inj. (WT)) as well as controls which were uninjected but reared in parallel. We observed a significant difference in number of ovarioles (one – way ANOVA, $p = 0.0262$), but this difference was only significant when comparing the mutants to the uninjected controls (Tuckey's multiple comparisons test, $p = 0.0291$) and did not differ between the injected G0 mutants and wildtypes (Figure 5.11).

Furthermore, we wanted to evaluate whether oocytes were able to reach the same stage of development in DNMT1g2 mutants as in the wildtypes. This was measured by calculating the cross – sectional surface area of the largest oocyte and comparing across DNMT1g2 mutants, G0 wildtypes as well as uninjected controls. We did not observe any significant difference in the size of the largest oocyte as a result of DNMT1 inhibition in DNMT1g2 mutants (Figure 5.11).

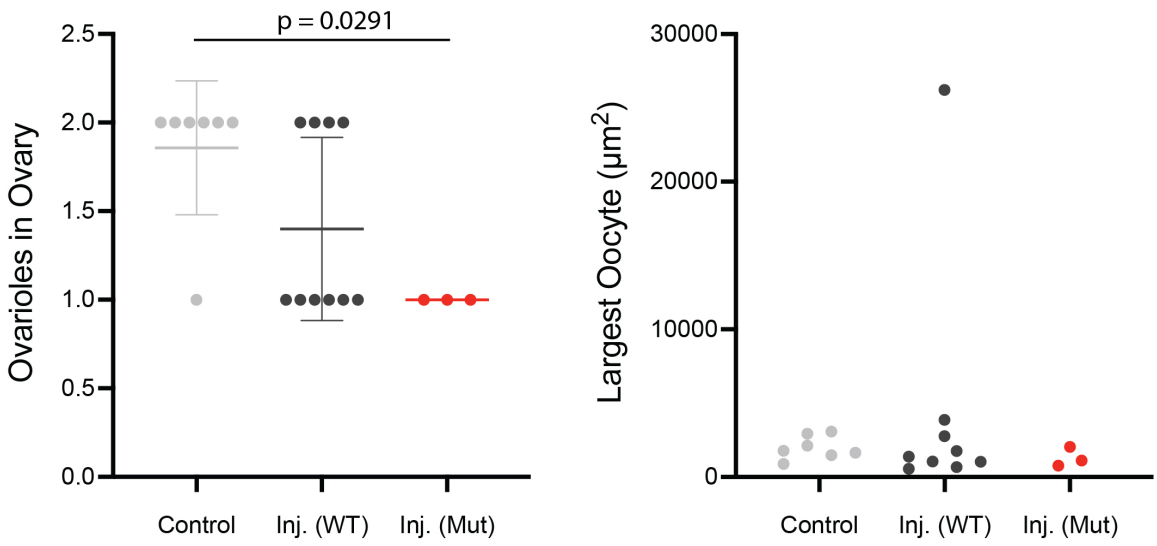

Figure 5.11. Ovariole Number and Oocyte Size in DNMT1g2 Mutants.

(Left) For each of the animals that were dissected, the minimum number of ovarioles was counted across the two ovaries. If there was an unequal number of ovarioles between the two ovaries, the lower number was used. For two out of seven control, two out of ten Inj. (WT) and one out of three Inj. (Mut), an accurate count of ovarioles could only be obtained for one of the ovaries. There was a statistically significant difference in ovariole number across the three groups (one – way ANOVA, $p = 0.0262$). Significant p – values Tukey's multiple comparisons test displayed on graph. (Right) Surface area of the largest oocyte observed for each animal shown on graph. No significant difference was observed across the three groups (one – way ANOVA, $p = 0.6316$). Of note, one animal in the Inj. (WT) group had a particularly large oocyte.

Finally, we were interested in evaluating brain development in the DNMT1g2 mutant animals, because abnormal neurological function has been associated with mutations in DNMT1 in mammals (Klein et al., 2011; Winkelmann et al., 2012, p. 1). By calculating the widest cross –

sectional area of the brain z projection on the axial plane, we estimated the size of the whole brain, mushroom body and antennal lobe for G0 mutants and uninjected controls. We did not observe any statistically significant differences in the size of the whole brain or either of these structures based on genotype (Figure 5.12).

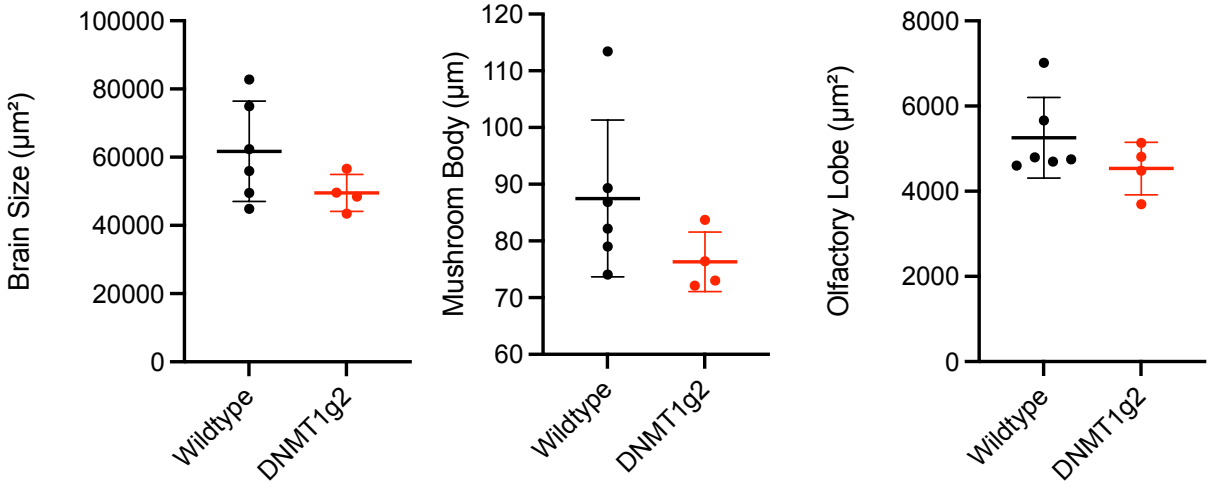

Figure 5.12. Brain Morphology in DNMT1g2 Mutants.

Mutant and wildtype brains were fixed, and nuclei visualized using DAPI. Brains were oriented similarly on a slide and cross – sectional area (brain size) was measured from a maximum z projection. No statistically significant difference was observed between mutant and wildtype brain size (unpaired t – test, $p = 0.1568$), the size of a mushroom body (unpaired t – test, $p = 0.1673$) or antennal lobe (unpaired t – test, $p = 0.2200$). In the event of tissue damage, the more intact mushroom body or antennal lobe was used for measurement. Otherwise, one was chosen at random for each animal.

5.5 DISCUSSION AND FUTURE DIRECTIONS

We were able to localize DNMT1 mRNA and protein successfully in the *O. biroi* ovary using fluorescence *in situ* hybridization and immunohistochemistry, respectively. DNMT1 mRNA is shuttled from the nucleus into the cytoplasm, where we observed it in cells within the germarium, nurse cells and follicular cells (Figure 5.2). After translation, the DNMT1 protein is shuttled back into the nucleus, where it can be detected via immunohistochemistry in these same cells (Figure 5.3). Additionally, both maternal DNMT1 mRNA and DNMT1 protein are provisioned into oocytes from an early stage, prior to oviposition.

In oocytes, we observed the DNMT1 protein pattern change from co – localizing with DNA, in young oocyte, to a cloud of protein surrounding the nuclear material in later stages of development (Figure 5.4). Furthermore, we discovered this to coincide with a mitochondrial condensation (Figure 5.6), likely a marker of Balbiani body formation. Further work to evaluate the role of DNMT1 in the later stages of oogenesis, prior to oviposition, is warranted to understand whether it plays a role in oocyte polarization along with the Balbiani body, or if it has an entirely different role during this stage of oocyte development.

In both DNMT1g1 and DNMT1g2 mutants, we observed grossly normal ovary development. While the DNMT1g1 mutants were indistinguishable from wildtypes using immunohistochemistry (Figure 5.8, Figure 5.9), the DNMT1g2 mutants appeared to lack the DNMT1 catalytic domain and no DNMT1 antibody binding was observed. These results simultaneously validate the specificity of the antibody to bind DNMT1, as well as the mutagenesis phenotypes. Because we did not observe any DNMT1 inhibition in DNMT1g1 mutants, we did not expect to observe

antibody changes. On the contrary, the DNMT1g2 mutants exhibited drastic decreases in DNA methylation and other phenotypes, and as expected, appeared to have a "knockout – like" phenotype using immunohistochemistry (Figure 5.10).

It is possible that DNMT1g2 mutants may develop fewer ovarioles (Figure 5.11), but these results are inconclusive and additional experiments, by either increasing the mutant sample size or, alternatively, using RNAi for DNMT1 inhibition, are warranted to evaluate this possibility. Although the DNMT1g2 mutants were sterile, developing oocytes could be observed in the ovaries of these animals, which were indistinguishable in size from those of age matched wildtype animals (Figure 5.11). These results indicate that DNMT1 is not essential for the initiation of meiosis or the early stages of oogenesis. Therefore, DNMT1 must be, in the very least, necessary for a portion of oogenesis after initiation, but before the end of prophase I, which occurs post – partum in this species.

Interestingly, the DNMT1g2 mutants were able to develop normally without a functioning DNMT1 protein. These animals were mutagenized as early zygotes, and because little evidence of mosaicism is observed, this mutagenesis likely took place when only one or two nuclei were present. This means that any DNMT1 protein in these animals likely stemmed from the maternal provisions, which were sufficient for completing normal development. Questions remain about how long these provisions last in the oocyte after oviposition, and how quickly they are diluted as cells inside the embryo begins dividing. Further work to evaluate the exact stages of oogenesis where DNMT1 plays an essential role, as well as the mechanism of this function can provide novel insight into the evolutionary role of this protein. Such future experiments may also shed light on

why this gene has been so widely conserved across eukaryotes, including species that do not methylate their DNA (Schulz et al., 2018).

CHAPTER 6. DNMT3

To further understand the role of DNA methylation and the DNA methyltransferases at the organismal level, we aimed to characterize and mutagenize DNMT3. DNMT3 is generally involved in *de novo* methylation and, unlike DNMT1, it does not have a preference for hemimethylated DNA over unmethylated DNA. Furthermore, mammalian DNMT3a appears to have non – CpG methylation activity (Gowher and Jeltsch, 2001). Unlike mammals, insects carry only a single copy of DNMT3 (Bewick et al., 2016). Additionally, DNMT3 is of particular interest, as DNA methylation studies in social insects have largely focused on inhibition of DNMT3 by RNAi or other pharmacological means (Kucharski et al., 2008; Li-Byarlay et al., 2013).

6.1 *O. BIROI* DNMT3 GENE STRUCTURE

The *O. biroi* DNMT3 gene resides on chromosome 4 (NCBI LOC105285577), and codes for a 1654 amino acid protein product (NCBI XP_011348142). This is substantially larger than the murine DNMT3a, which has two isoforms at 908 and 689 amino acids (Chen and Li, 2004). The eukaryotic DNMT3 gene contains multiple conserved domains including the PWWP domain, ADD domain and DNA methyltransferase catalytic domain (Chen and Li, 2004). The PWWP domain contains a conserved "proline – tryptophan – tryptophan – proline" motif, as well as a positively charged region, which has been predicted to bind DNA (Qiu et al., 2002). The ADD domain (also known as ATRX – DNMT3 – DNMT3L), is believed to play a function in DNMT3 recruitment to unmethylated DNA by recognizing the methylation state of lysine 4 on histone H3 (Otani et al., 2009).

These domains were identified in the *O. biroi* DNMT3 gene (Figure 6.1). Unlike DNMT1, only a single splice variant has been observed in *O. biroi* DNMT3. Therefore, we selected to target the first exon in an effort to disrupt the reading frame of the whole protein and ultimately inhibit DNMT3 function.

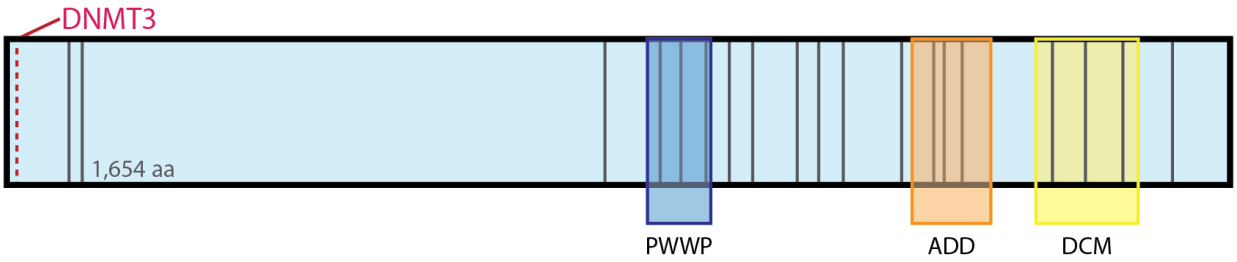

Figure 6.1. *O. biroi* DNMT3 Gene Diagram.

Structure of the conserved domains mapped to the *O. biroi* DNMT3 protein, including the PWWP domain (amino acids 1050 to 1106) in blue, ADD domain (amino acids 1220 to 1327) in orange and the Catalytic DNA Methyltransferase Domain (DCM, amino acids 1390 to 1529) in yellow. Custom antibody target site shown in purple (amino acids 1406 to 1425). CRISPR/Cas9 mutagenesis target site shown in red. Exon boundaries shown as vertical bars.

6.2 CRISPR/CAS9 DNMT3 MUTAGENESIS

We designed and tested three sets of primers (forward and reverse) as well as four guide RNAs to target the first exon of DNMT1. All four gRNAs showed *in vitro* cutting activity, when incubated with Cas9 enzyme and amplified PCR product of the target region (Figure 6.2). DNMT3 guide 4 was selected.

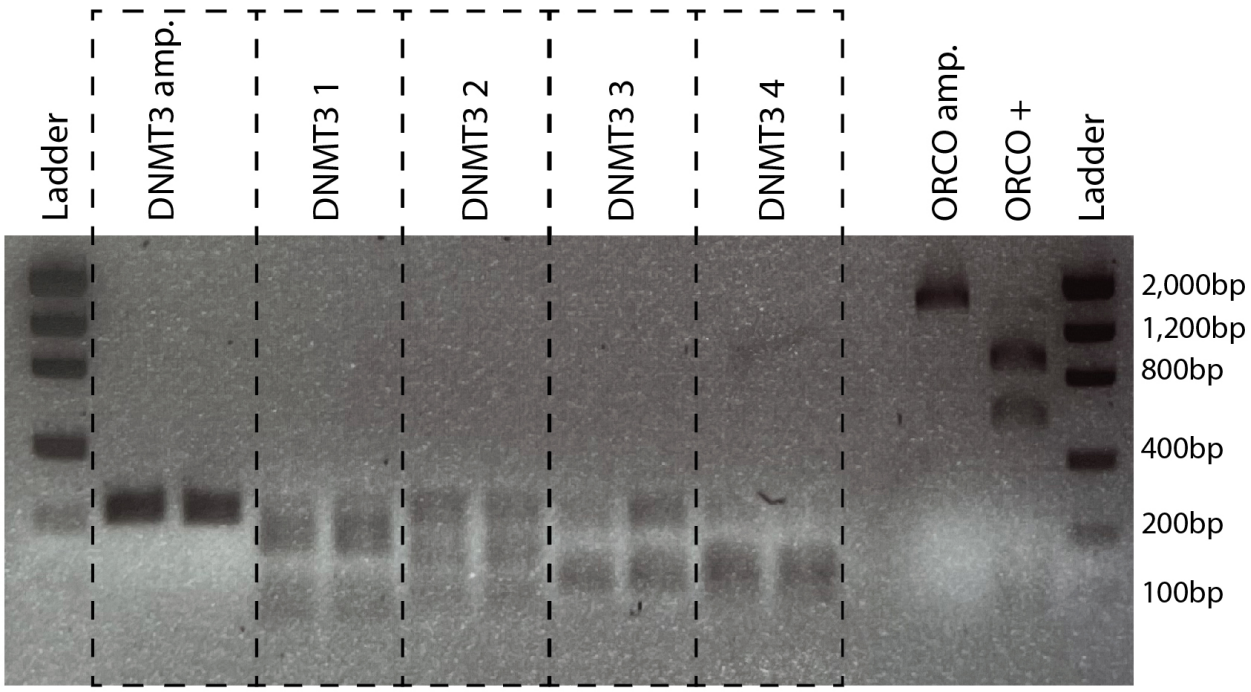

Figure 6.2. DNMT3 Guide RNA *in vitro* Verification.

The target region of the DNMT3 gene containing the target cut site is shown using gel electrophoresis after amplification. Degraded PCR product shown after incubation with Cas9 enzyme and four different gRNAs (DNMT3 1 – 4). Digested DNA in both replicates of each gRNA demonstrates cutting activity of all four potential gRNAs. Control Odorant Receptor Coreceptor (ORCO) amplified DNA (OCRO amp.) digestion using previously verified gRNA shown on right (ORCO+) under the same conditions. No bands of increased molecular weight observed.

Next, we injected the CRISPR/Cas9 mix containing DNMT3 guide RNA 4 (100 ng/ul) and Cas 9 enzyme (100 ng/ul) into 1,513 line B eggs of which 70 hatched (hatch rate 4.62%). 316 control eggs were reared in parallel of which 158 hatched (hatch rate 50%). Similar to mutagenesis experiments for DNMT1 (1.9% – 3.4%), an increased mortality was observed in injected eggs, but

in this instance, it appeared slightly less pronounced. However, variation is common between experiments and in this instance, hatch rate data for DNMT3 stems from a single experiment. Of the 70 hatched larvae which were injected, 44 were fostered.

The fostered larvae were reared to adulthood and generated 18 G0 adults. All eggs were collected and sequenced until the presence of a mutant egg verified germline penetration of the mutation. All subsequent eggs were fostered with line A chaperones to generate G1 adults. Among these adults, three unique mutant genotypes were observed, of which two included frameshift mutations in both alleles (-7bp / -4bp and -5bp / +5bp), and one included a single frameshifted allele and one allele with an in – frame deletion (-4bp / -3bp) (Figure 6.3).

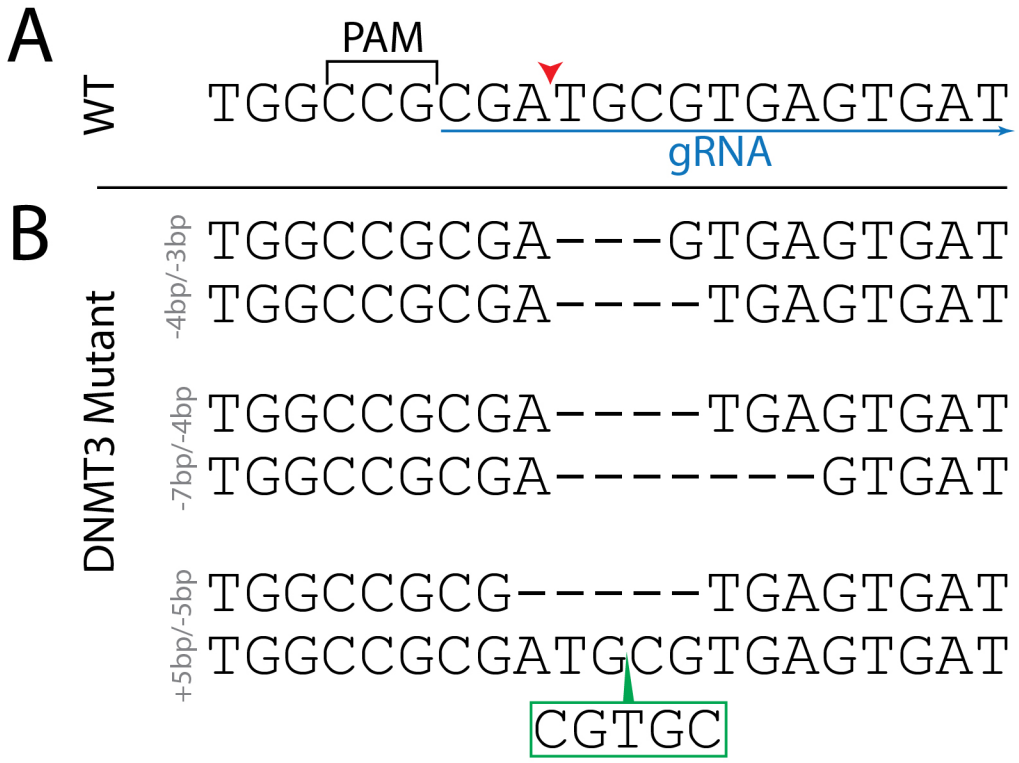

Figure 6.3. DNMT3 Mutant Genotypes.

(A) Wildtype DNMT3 genomic sequence shown at target site. gRNA target sequence shown in blue with protospacer adjacent motif (PAM) marked, as well as expected cut site (red arrowhead). (B) Multiple unique genetic lines of DNMT3 mutants established as a result of small insertions or deletions observed: -3bp/-4bp, -7bp/-4bp and -5bp/+5bp.

The DNMT3 mutants were propagated for generations, and ultimately sorted into pure colonies for each genotype. The next step was assessment of the impact of these mutations on the DNMT3 gene, DNA methylation and any other phenotypes. We evaluated whole genome DNA methylation levels using low coverage Whole Genome Bisulfite Sequencing (Figure 6.4) and did not see any difference in global methylation levels between mutant (of either the -7bp / -4bp or the -5bp / +5bp genotype) and wildtype animals (Dunnett's multiple comparisons test, $p = 0.9656$). Of note, this

experiment was run in parallel with the methylation analysis for DNMT1g1 with a single set of wildtype controls, therefore a one – way ANOVA with multiple comparisons is used for statistical analysis rather than a t – test.

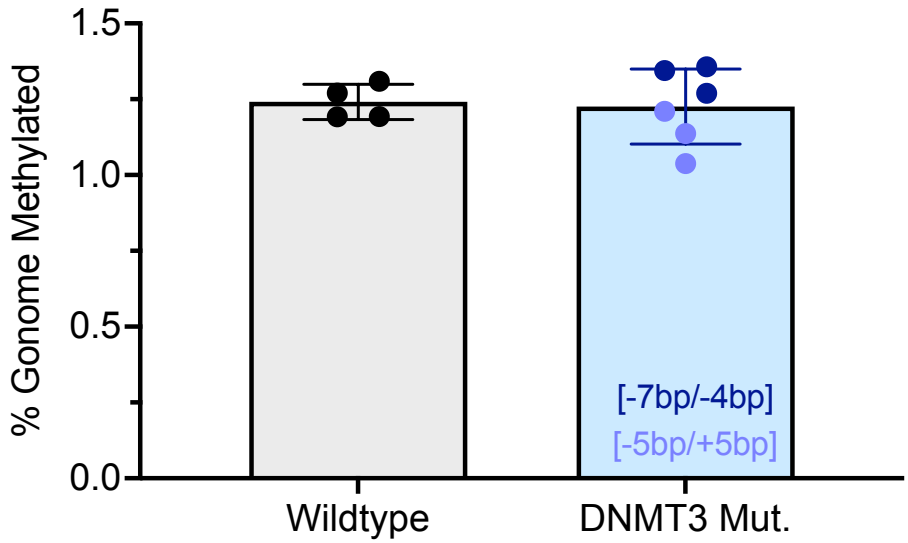

Figure 6.4. Genome – Wide DNA Methylation in DNMT3 Mutants.

Genome – wide methylation analysis using low coverage Whole Genome Bisulfite Sequencing. Data shown is corrected for bisulfite non – conversion estimates. Each data point represents DNA extracted from a single whole ant. Two genotypes, with frameshift mutations in both alleles, were tested out of the DNMT3 mutants (-7bp/-4bp and -5bp/+5bp) and marked on the graph. Whole genome bisulfite sequencing was done simultaneously on DNMT3 mutants, DNMT1g1mutants and wildtype controls. Therefore, ANOVA and Dunnett's multiple comparisons tests were used for statistical analysis instead of unpaired t – tests. No significant difference was observed between genome wide methylation levels of wildtype animals compared to DNMT3 mutants (Dunnett's multiple comparisons test, $p = 0.9656$).

Next, we set up egg laying units of 16 painted G1s. All eggs were removed weekly or bi – weekly, until the colonies stopped laying eggs. Eggs collected in the first 2 – 3 weeks were frozen for sequencing. All remaining eggs were fostered with line A chaperones and reared to adulthood for propagating the mutant lines. Carcasses of G1 adults were collected upon death, and a representative subset were successfully be sequenced. When comparing the frequency of mutants in the G1 adults to the G2 eggs that they laid, we did not see a significant difference in genotype frequency (Chi – square test, p = 0.3116) (Figure 6.5). Additionally, we did not observe a difference in survival between the mutants (of either -5bp / +5bp genotype or -7bp / -4bp genotype) and wildtypes (Log – rank test, p = 0.1132) (Figure 6.5).

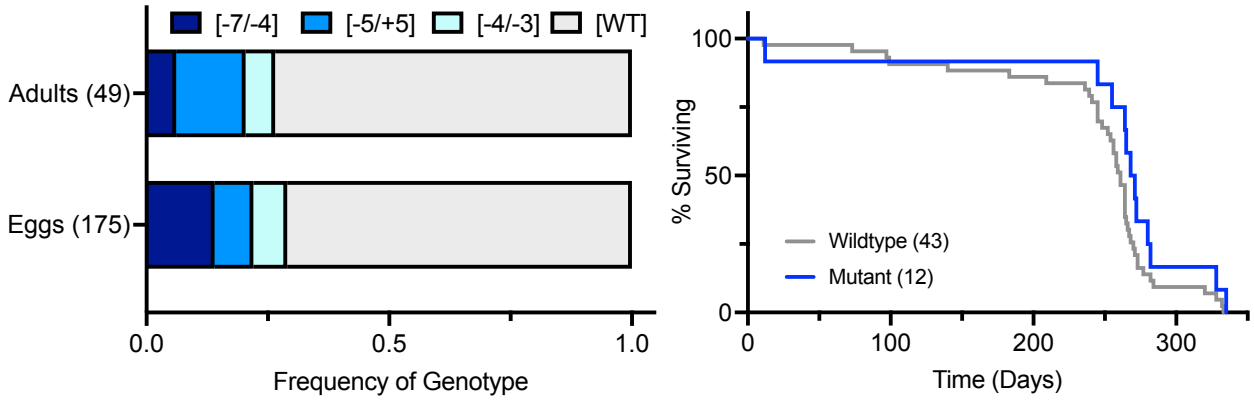

Figure 6.5. DNMT3 Reproduction and Survival.

(Left) Animals from the first generation (G1) were individually painted and placed in units of 16 ants (n = 5). All eggs were collected and frozen for the first 2-3 weeks of egg laying, the first 35 eggs were sequenced for each colony. All G1 ant carcasses were collected and sequenced, genotypes were collected from 49 out of 80 total ants. No difference was observed in the ratio genotype ratios between the G1 adults and eggs laid by them (G2 eggs) (Chi – square, p = 0.3116).

(Right) No significant difference was observed in survival between the DNMT3 frameshift mutants (either -7bp/-4bp or -5bp/+5bp genotype) and wildtypes (Log – rank test, $p = 0.1132$). A median survival of 269.5 days was observed for DNMT3 frameshift mutants (of either genotype) vs. 261 days for wildtypes.

6.3 DNMT3 MUTANT RNA SEQUENCING

To evaluate the impact of the DNMT3 mutation on transcription, we used bulk RNA sequencing to compare wildtype animals to frameshifted DNMT3 mutants (of the -7bp / -4bp genotype and -5bp / +5bp) (Figure 6.6). Prior to RNA sequencing, DNMT3 mutant genotypes were evaluated using Sanger sequencing using DNA extracted from a single leg. RNA was extracted and sequenced using the rest of the tissue for each animal. We were able to observe the predicted frameshift mutations in RNA reads aligned to the first exon of DNMT3. However, for replicates of the -7bp / -4bp genotype, we were only able to observe the -4bp allele. Additionally, only the "-5" allele was observed for one of the -5bp / +5bp replicates (Figure 6.6).

Figure 6.6. DNMT3 Mutation in mRNA Reads Aligned to the DNMT3 First Exon.

RNA reads aligned at DNMT3 mutation target site for four wildtype and four DNMT3 mutant replicates. The indicated DNMT3 genotype was determined from DNA extracted from a single leg, using Sanger sequencing. For -7bp / -4bp mutants, only mRNA reads of the -4bp allele were observed. For one of the -5bp / +5bp mutants, only -5bp reads were observed in one of the replicates.

Next, we visualized DNMT3 splicing using Sashimi plots. We did not observe any major splice variants in mutants of either genotype when compared to wildtypes (Figure 6.7).

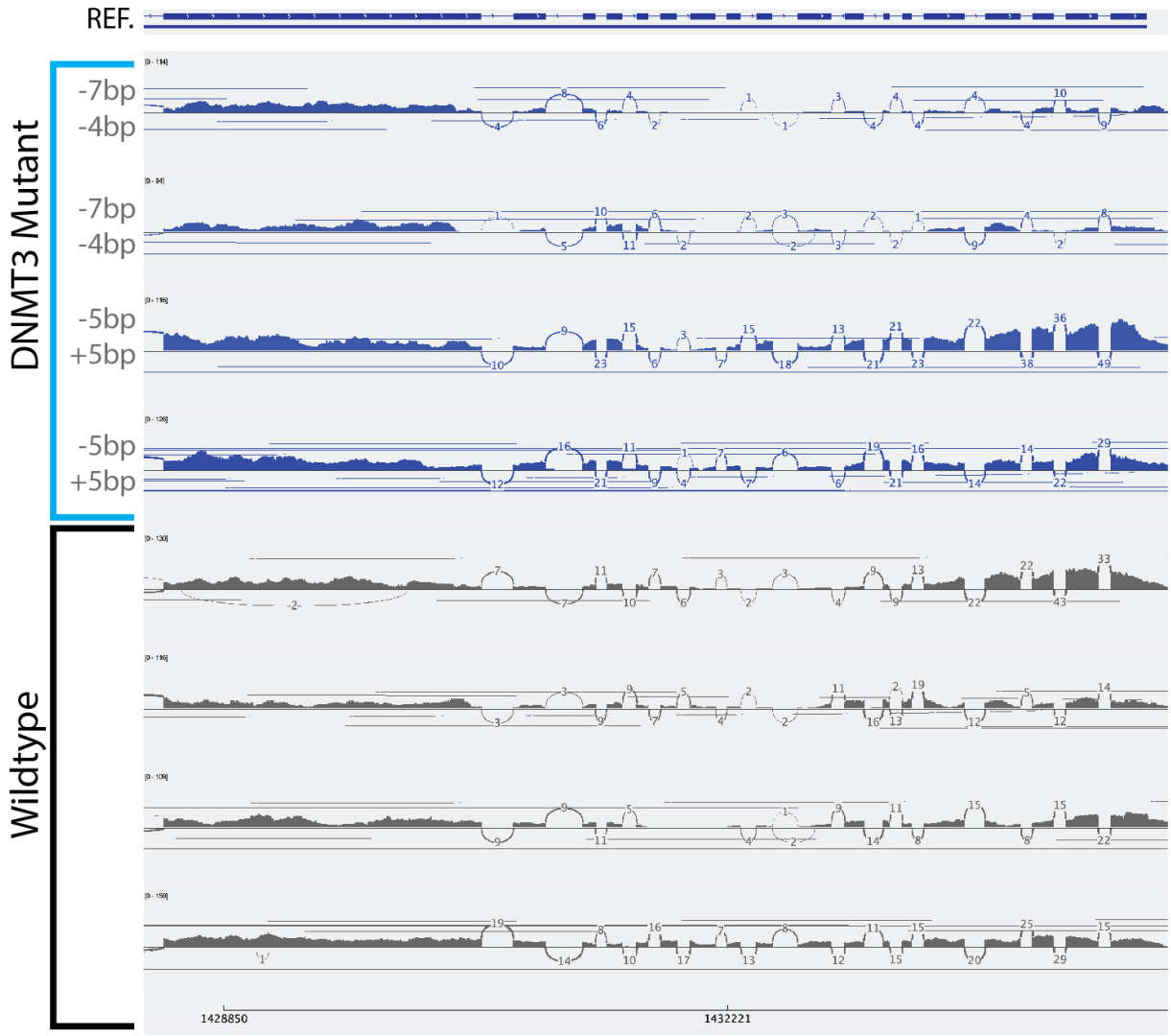

Figure 6.7. DNMT3 RNA Splicing in DNMT3 Mutants.

Reference (REF.) showing exons for DNMT3, starting at exon 2. Exon 1 is not shown due to the large distance in the genome between exons 1 and 2. Sashimi plots for four wildtype and four DNMT3 mutant replicates shown with mutant genotype indicated on graph. No major alternative splicing variants are observed in DNMT3 mutants.

When evaluating differentially expressed genes (DEGs), we did not find any genes to be differentially expressed in DNMT3 mutants, including DNMT3. The lowest recorded adjusted

p – value for any gene was 0.23 (Figure 6.8). While there is no statistically significant difference in DNMT3 expression, it is notable that reads could have been undercounted for the -7bp / -4bp genotype. This is due to the fact that the -7bp mutation might have caused reads from this allele to be discarded, without proper alignment, because they exceeded the mismatch threshold. Further analysis is necessary to assess this as a possibility. However, if we assume that the number of reads of the -7bp allele that were excluded is equal to those detected for the -4bp allele in these animals, this would only be a minor change and unlikely to change the results significantly.

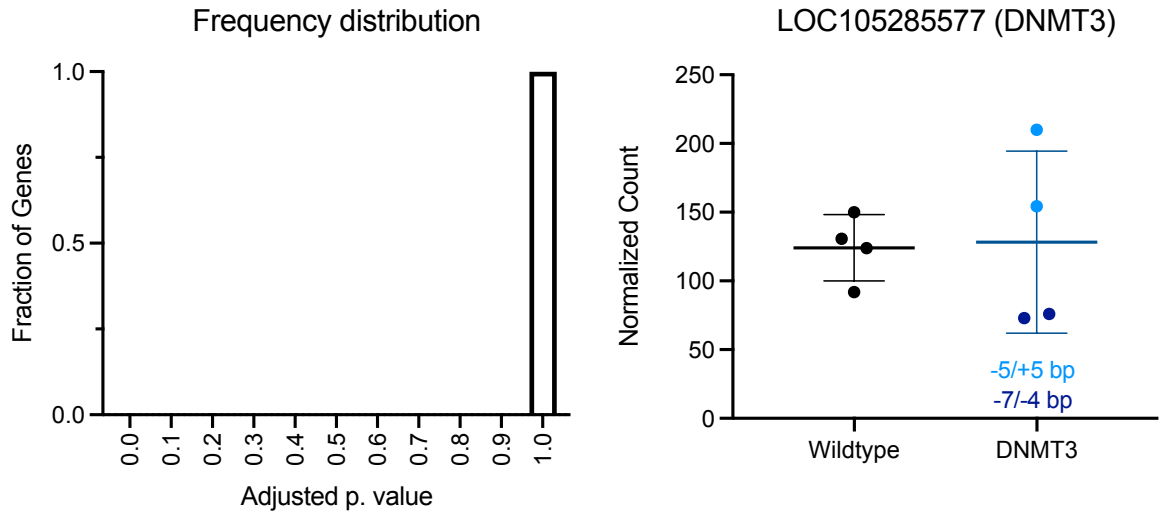

Figure 6.8. Analysis of Differential Gene Expression Resulting from DNMT3 Mutagenesis. (Left) Frequency distribution of adjusted p – values resulting from DEG analysis of DNMT3 mutants. Lowest p – value recorded was 0.23 (Right). LOC105285577 (*O. biroi* DNMT3 locus) is not differentially expressed in DNMT3 mutants. Each data point represents RNA extracted from a single ant, -7bp / -4bp and -5bp / +5bp genotypes are represented in DNMT3 mutant samples as noted.

6.4 DISCUSSION AND FUTURE DIRECTIONS

We were able to successfully generate frameshift mutations in the *O. biroi* DNMT3 gene, penetrate the germline, and propagate mutants for multiple generations. However, we did not observe any phenotype, including changes in reproduction, survival, or global DNA methylation levels. Furthermore, we observed transcription of the DNMT3 frameshift mutations using RNA sequencing but did not observe any major alternative splicing or differential gene expression as a result of these mutations. Questions remain about whether the frameshift mutation in the first exon of the DNMT3 gene resulted in any inhibition of DNMT3 function.

It is possible that DNMT3 is not essential for reproduction or survival in this species, as in previous studies of DNMT3 inhibition in social insects. However, previous work on DNMT3 inhibition in *A. mellifera* observed a ~21% decrease in genome wide methylation (Li-Byarlay et al., 2013). Based on this this data, we predicted that successful inhibition of DNMT3 function should result in detectable genome – wide methylation changes.

To further characterize the DNMT3 protein, and evaluate the effect of our mutations, we designed two custom antibodies. However, we did not see consistent results when using these antibodies to stain *O. biroi* ovaries or brains. It is possible that the immunohistochemistry conditions were not optimal for these specific antibodies or that the antibody binding site was not accessible on the mature protein. Alternatively, another explanation is that the DNMT3 gene is only expressed at high levels during a particular phase of development, and not easily detectable in ovaries or brains of mature adults. Indeed, studies of DNMT3 expression in *Solenopsis invicta,* have shown this

gene to be most highly expressed in the embryo when compared to various stages of larval development, pupae or adult heads (Kay et al., 2018).

Further attempts at characterizing DNMT3 in *O. biroi* should apply the established protocol for *in situ* hybridization to *O. biroi* eggs (Khila and Abouheif, 2009). This may allow for better visualization and localization of DNMT3 mRNA with fluorescence *in situ* hybridization, which could be followed by detecting DNMT3 protein with immunohistochemistry.

Thorough characterization of the DNMT3 protein localization is important for evaluating the impact of the DNMT3 frameshift mutations. It is possible that the DNMT3 mutants indeed have inhibited DNMT3 function, but this does not necessarily impact global methylation levels, which could be largely regulated by DNMT1 in this species. Furthermore, inhibition of DNMT3 has not previously been demonstrated to result in decreased reproductive fecundity or early mortality in other social insects and may appear normal in a knockout mutant. After this thorough characterization of DNMT3 in wildtype animals, it can be used to validate DNMT3 inhibition in mutants generated using CRISPR/Cas9. It is only after this validation of successful DNMT3 inactivation as a result of mutagenesis that such mutants can be used to assess the role of DNMT3 on an organismal level in social insects.

CHAPTER 7. DNMT1g1 AND DNMT3 DOUBLE MUTANT

To explore the relationship between the DNMT genes in *O. biroi*, DNMT1 and DNMT3, we modified the CRISPR/Cas9 protocol to simultaneously mutate both genes. As previously discussed, *O. biroi* is a queenless social insect, and all females are able to reproduce asexually through parthenogenesis. This allows for a mutation which penetrates the germline to be passed on to all offspring. While this unique reproductive system allows for genetic manipulation in this species, the lack of sexual reproduction also creates a unique challenge in establishing double mutant lines. In model organisms such as *D. melanogaster*, a double mutant would traditionally be generated by genetic crosses of two mutant lines, each of which carries one of the desired mutations. We tackled this challenge by multiplexing the CRISPR/Cas9 protocol to mutate both genes of interest simultaneously in a single egg. Specifically, we were able to make a double mutant, carrying both the DNMT1g1 and DNMT3 mutations, and penetrate the germline, demonstrating the versatility of this species in genomic engineering.

7.1 DNMT1g1/DNMT3 DOUBLE MUTANT GENERATION

To generate the double mutant, we made a new CRISPR injection mix, which contained the selected gRNAs for both genes, as well as Cas9 enzyme. For this experiment, we targeted the second exon of DNMT1, and the first exon of DNMT3. Each of the selected guide RNAs were successful in generating single mutants when injected at a concentration of 100 ng/ul. The guide RNA targeting the second exon of DNMT1 was used to generate the DNMT1g1 mutants described in Chapter 3, and the guide targeting the first exon of DNMT3 was previously used to generate the

DNMT3 mutants described in Chapter 6. The new CRISPR mix included Cas9 enzyme at 100 ng/ul as before in addition to both gRNAs at 100 ng/ul.

Across two batches of experiments, we injected 2,507 eggs, of which 48 transitioned and 36 hatched (hatch rate 1.44%). Additionally, 441 control eggs were reared in parallel, of which 225 hatched (hatch rate 51.02%). The increased mortality observed in injected eggs is comparable to what was observed when using each of the guides individually as described in Chapters 3 and 6, as well as in mutagenesis of the DNMT1 catalytic domain described in Chapter 4 (Figure 7.1). Because all DNMT3 mutants were generated as a result of a single experiment, all statistical analyses comparing hatch rates only included data for DNMT1g1, DNMT1g2 and the double mutant. Across these treatments, no statistically significant difference was observed (one – way ANOVA, $p = 0.1447$).

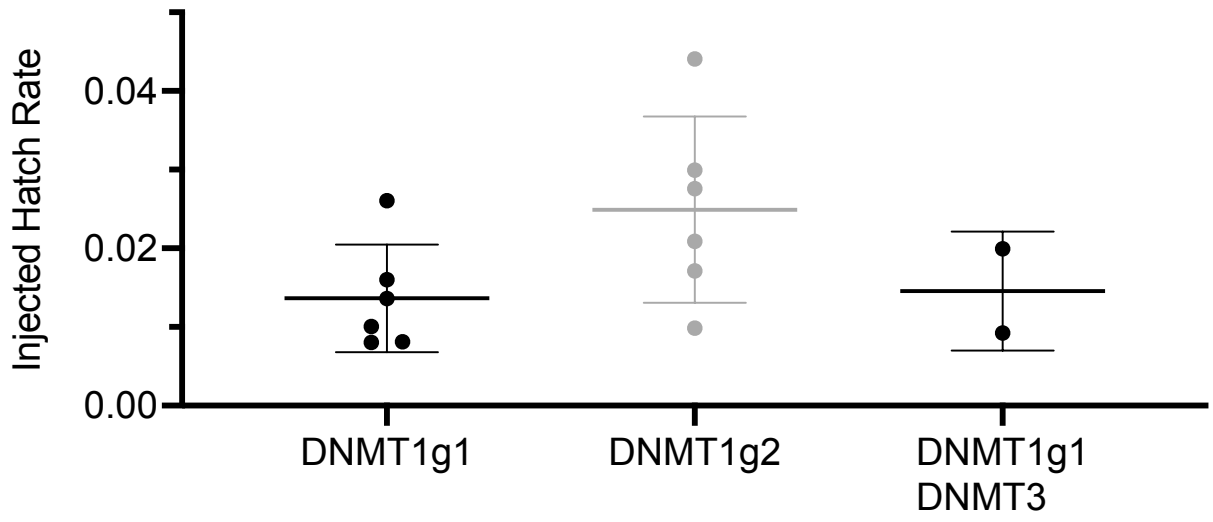

Figure 7.1. Comparing *O. biroi* Egg Hatch Rates Across Different CRISPR/Cas9 Experiments.

The mix for generating DNMT1g1 and DNMT1g2 mutants included Cas9 at 100 ng/ul, and each respective gRNA at 100 ng/ul. The mix for generating the DNMT1g1/DNMT3 double mutant included Cas9 at 100 ng/ul, DNMT1g1 gRNA at 100 ng/ul and DNMT3 gRNA at 100 ng/ul. Each data point represents hatch rate from a single experiment where > 600 eggs were injected. No statistically significant difference in hatch rate is observed across these treatments (one – way ANOVA, p value = 0.1447). DNMT3 data is excluded from analysis, because only a single experiment was conducted to generate all mutants. In this experiment, the hatch rate was 0.0463.

All G1 eggs were collected from the unit of pooled G0 adults, and sequenced until a mutant egg was observed. Of the 22 collected eggs, amplification and sequencing of both genes was successful for 16, of which one egg carried mutations only in the DNMT1 gene, and one had two mutant alleles in both genes (Figure 7.2).The remainder were wildtype. Additional independent rounds of amplification and sequencing confirmed the mutant egg genotype.

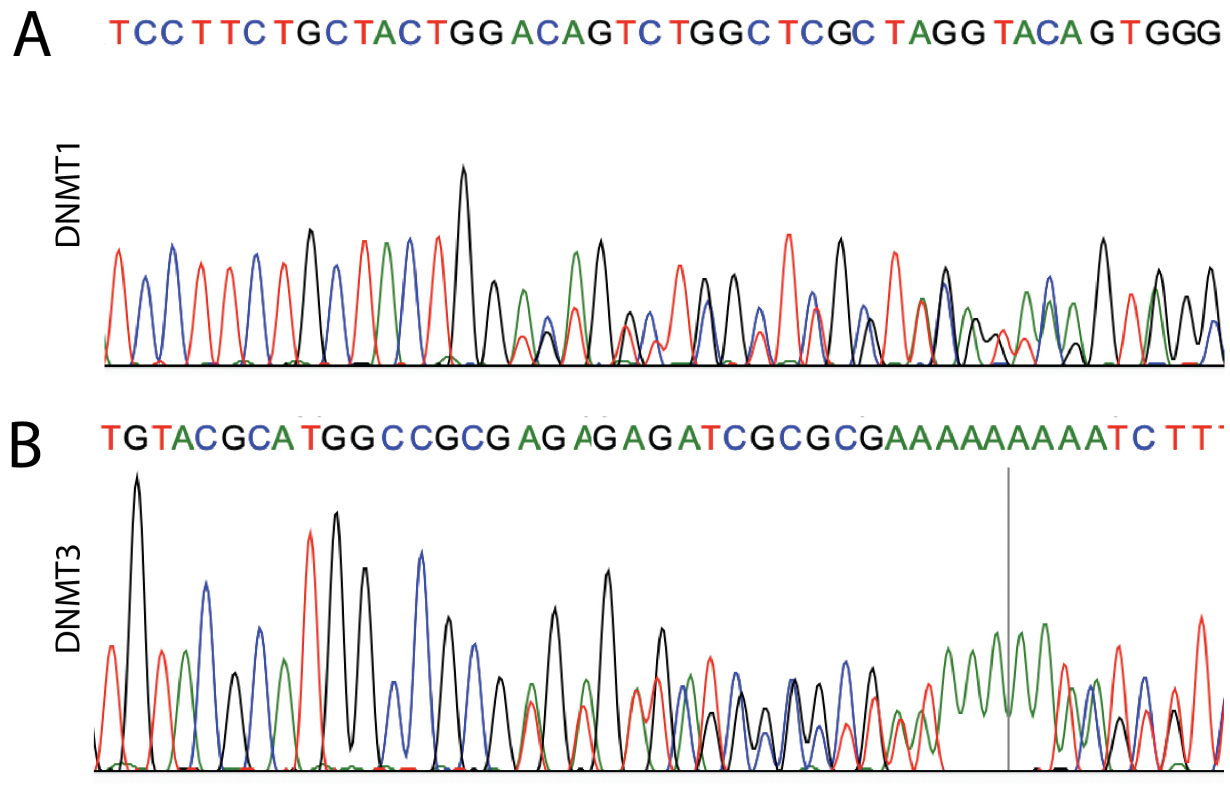

Figure 7.2. Sanger Sequences for DNMT1 and DNMT3 Genes Recovered from a Mutagenized G1 Egg.

Sanger sequences of a G1 egg for mutagenesis target regions of DNMT1 (in exon 2) and DNMT3 (in exon 1). Divergence in sequences observed is indicative of the different sizes of insertion/deletions in each of the two alleles at the mutagenesis site. The DNMT1 sequence here is the reverse of the same sequenced described in Chapter 3. The reverse primer was used for sequencing because it was further from the mutation and allowed for cleaner base resolution.

7.2 FUTURE DIRECTIONS

We successfully multiplexed the CRISPR/Cas9 protocol to introduce frameshift mutations into multiple genes, and successfully penetrate the germline, thereby creating a double mutant in this asexual species. We observed germline penetration of both mutations using Sanger sequencing of a single G1 egg, which was laid by one of the injected G0 adults. Immediately after this observation, all eggs ceased to be sequenced and were fostered with chaperones in an attempt to preserve and propagate the potential mutant genetic line.

For this experiment, we selected to target the second exon of DNMT1, and the first exon of DNMT3. The decision to target the second exon of DNMT1 (DNMT1g1, Chapter 3), as opposed to the catalytic domain (DNMT1g2, Chapter 4), was largely due to timing of these experiments relative to one another. Namely, the DNMT1g1 mutants were generated first and the double mutant protocol was prior to the DNMT1g2 mutants and phenotyping of DNMT1g1 and DNMT3 mutants. Future work will require repeating this multiplexing experiment with different target loci, targeting the catalytic domains of both genes. However, in this case, it should be expected that the sterility observed with the single DNMT1g2 mutant will also be observed. Moreover, it is possible that additional developmental defects will also result from mutating both genes.

Although, in this species, there is a high mortality in eggs associated with CRISPR/Cas9 mutagenesis, we did not observe any difference when targeting multiple genes compared to a single gene. Anecdotally, we have observed an association of increased mortality with increased mutagenesis efficiency. It is possible that the mortality observed is a direct result of the double stranded breaks introduced by the Cas9 enzyme, both on and off target, leading to DNA instability.

The hatch rate appeared slightly higher when generating the DNMT3 single mutants, than for the double mutant or individual DNMT1g1 or DNMT1g2 experiments. However, this hatch rate data is based on a single experiment, and variability in hatch rates should be expected across experiments.

For our CRISPR/Cas9 reagent mix in generating the double mutants, we maintained the same concentration for each guide RNA (DNMT1g1 and DNMT3) as well as Cas9, that was used when generating each single mutant. However, it is important to note, that the total gRNA concentration was, in essence, doubled at 200 ng/ul. Future experiments may benefit from testing changes in Cas9 concentration, and an increase of the Cas9 to 200 ng/ul may produce more desirable results in generating double mutants. On the other hand, this also could come at the cost of egg mortality. However, in order to successfully mutate multiple genes, high mutagenesis is necessary and may outweigh the cost of decreased survival.

Additionally, in the context of mutagenizing a single egg, we must ask whether mutagenesis of multiple genes can be treated independently. It is possible that the success of mutagenesis in target gene A is predictive of mutagenesis in target gene B within the same sample. For instance, since there is variation of egg age at the time of injection, some eggs may simply be more receptive to mutagenesis.

Finally, for future work in multiplexing CRISPR/Cas9, a few additional factors must be considered. First, the genes targeted should not be overlapping or near each other in the genome, and or be located on different chromosomes to avoid unexpected results. For instance, generating multiple double stranded close to one another in proximity may lead to unwanted deletions of

genes spanning the region. Additionally, the gRNA sequences for all genes targeted should not have complementary regions, as this could lead to possible dimerization.

Overall, despite their asexual nature, it is possible to simultaneously disrupt multiple genes in *O. biroi* by multiplexing the CRISPR/Cas9 protocol. However, the behavior of all reagents can be unpredictable, and it is important to test and optimize reagents for each planned multiplexed mutant carefully, including independent validation of each mutant.

CHAPTER 8. MATERIALS AND METHODS

8.1 SELECTION OF GENE TARGETS AND AMPLIFICATION

DNMT1 (LOC105286975) and DNMT3 (LOC105285577) gene loci were located in the published *O. biroi* genome (GenBank assembly accession: GCA_003672135.1) (Oxley et al., 2014). For DNMT1, two alternate splice variants (X1: XM_011352329 , X2: XM_011352333) were identified, and aligned with MAFFT (Katoh et al., 2019), verifying gRNA sequence presence in both splice variants. For DNMT3, the first exon was selected as a target.

For DNMT1, 6 sets of forward and reverse primers (custom DNA oligos from Integrated DNA Technologies) were tested, with three sets overlapping each gene region of interest (at DNMT1g1 and DNMT1g2) (Table 8.1). For DNMT3, five sets of primers were tested. All primers for both genes were selected to have similar melting points to allow for PCR multiplexing.

Table 8.1. Primers Targeting DNMT1g1, DNMT1g2 and DNMT3.

Forward (F) and Reverse (R) primer pairs used for amplifying each gene region of interest. DNMT1 primer sets 1 – 3 target the second exon, including the DNMT1g1 mutagenesis site, and sets 4 – 6 target the catalytic domain, including the DNMT1g2 cut site. All primer pairs were tested and those shown in bold selected for each respective target region.

DNMT1g1	F1	**CGTTCGCCTCGGTATTCATC**
	F2	TGTGTCCGCTGTTAGATCACC
	F3	CGGAGTTGTGTCCGCTGTTAG
	R1	**AATAAGAGACTGGTGGCACG**
	R2	AACGGACAGCGCATACGATC
	R3	TTTGATAACGGACAGCGCATAC
DNMT1g2	F4	**ATTAGGGTGATCGCACGGAC**
	F5	TCCATTAGGGTGATCGCACG
	F6	GGACGACAGTGGACAGAAAC
	R4	**ATCGCAGTAAGACAAACACGAG**
	R5	GGCCTGGACAATACCAAACG
	R6	ACGTACACTGGTAACCCATTC
DNMT3	F1	CGAAGGGGTCCACATAGCTT
	F2	GAAGGGGTCCACATAGCTTTC
	F3	**AGGGGTCCACATAGCTTTCG**
	F4	CCTTTAGGAACGAGTGCGGT
	R5	CGAGATTTACGAGACGAACAAG
	R1	ATTCTTTCCATCGCGACACT
	R2	TGTTAATCGCCATTCTTTCCA
	R3	**CCCGTAATCGTCTTCGTAGG**
	R4	GTCGCTCATCTCGGTAGGTG
	R5	CCCTGCCGAAAGCTATGTGG

8.2 gRNA DESIGN

All synthetic guide RNAs were designed using the Knockout Guide Design (Synthego) and for each gene target, four possible gRNAs were synthetized (Synthego) (Table 8.2).

Table 8.2 gRNAs Targeting DNMT1g1, DNMT1g2 and DNMT3 for CRISPR/Cas9 Mutagenesis.

For each target site, four guide RNAs were synthetized and tested *in vitro*. All guides led to DNA digestion of amplified PCR product, containing each respective target region, when incubated with the Cas9 enzyme. For each target, DNMT1g1, DNMT1g2 and DNMT3, a single gRNA was selected (bold) from the *in vitro* tests to be used for *in vivo* testing and eventual mutant generation.

DNMT1g1	1	UUCAACGGAUUCCUCCAUGC
	2	GCUGGCAUGCUUCCGACUAC
	3	**AUCCUUCUGCUACUGGAGUC**
	4	GGUUCGCUUGGUACAGUAGG
DNMT1g2	1	CCGCUAAAACCUUGACACGG
	2	**GGAGAAGUCGAGCUCCUGUG**
	3	AGCUCGACUUCUCCCUUCUG
	4	UGGACAGAAACUUCCCCAGA
DNMT3	1	UCGACCGCACUCGUUCCUAA
	2	CGAGUGCGGUCGAAUCAAGU
	3	**GCCAUGCGUACACUCGACGC**
	4	GGCCGAUCACUCACGCAUCG

8.3 CRISPR/CAS9 REAGENTS *IN VITRO* VALIDATION

To extract DNA for reagent validation and genotyping, the sample tissue (eggs, larvae, legs or whole adults) was incubated with Proteinase K in 1xPCR Buffer at 56 °C overnight, followed by a 15 minute incubation at 99 °C. For each anticipated mutant, the target region was amplified with the selected primer set (Table 8.1) and purified using the AMPure bead protocol (AMPure XP A63881). To test the guide RNAs, the purified PCR product (100ng/ul) was incubated with the respective gRNA (20 ng/ul, Synthego), Cas9 (0.1M, NE Biolabs, Catalog # M0386S) in NEB buffer 3 (1x) for 3 to 4 hours. Digestion success was evaluated using gel electrophoresis.

8.4 EGG INJECTIONS AND REARING

Egg harvesting, injections and rearing followed the previously established protocol for *O. biroi* (Trible et al., 2017). Briefly, an injection mix containing 100 ng/ul Cas9 enzyme and 100ng/ul respective gRNA was prepared. For the DNMT1/DNMT3 double mutant, 100ng/ul of each gRNA (DNMT1g1_3 and DNMT3_3) was used. Eggs were collected from egg laying units of line B ants in intervals of 3 to 4 hours, aligned on glass slides using double sided tape, and injected using a pulled capillary needle with the CRISPR mix using positive pressure.

Matched control eggs were simultaneously collected and aligned on the slides but not injected. All slides were placed inside a sealed container with a plaster of Paris floor, and maintained at 20% humidity at 25 °C or 30% humidity at 30 °C according to a previously published protocol (Trible et al., 2017). During a week of injection, eggs were collected and injected Monday to Wednesday. Those injected on Monday were reared at 25 °C for 9 to 11 days, eggs injected on Tuesday were

reared at 25 °C for 4 days and at 30 °C for 4 to 6 days, and eggs injected on Wednesday were reared at 30 °C for 7 to 9 days until hatching. Rearing the eggs using this method allowed for synchronization of egg hatching from different experimental days across each week.

8.5 CRISPR/CAS9 *IN VIVO* REAGENT TESTING AND MUTAGENESIS

Mutagenesis efficiency and embryonic lethality for each selected gRNA was evaluated with a pilot study. The slides were cleaned daily and monitored until some eggs transitioned from a uniform opaque color to appear more transparent and heterogeneous, and ultimately hatched. Once all larvae hatched, at 8 to 11 days, the larvae locations were noted and slides frozen at – 80 °C. Eggs arrested during development, as well as all larvae were collected, DNA extracted, amplified with PCR, and sequenced using Sanger sequencing. All Sanger sequences were manually scored against the wildtype genome.

Successful *in vivo* mutagenesis was confirmed in eggs, and additional injections were carried out to retrieve mutant larvae if necessary. The presence of mutant larvae provided evidence of embryonic viability for each attempted mutation. Finally, a large round of injections (~2,000 - 5,000 eggs) was carried out using line B eggs to generate each mutant. Most hatched larvae from this experiment were fostered in colonies of line A chaperones and reared to adulthood. When these G0 adults eclosed, they were separated and all eggs collected.

Where mutant lines could be propagated (DNMT1g1 and DNMT3), eggs continued to be collected from these G0 units and fostered with line A chaperones. Eclosing animals of the next generation (G1) were individually tagged and placed into colonies of 16 G1 ants. These animals were used to

assess reproductive output and survival for each respective mutant. Eggs from these units continued to be fostered with line A chaperones and used to propagate the genetic lines for each mutant genotype.

8.6 DNMT1g1 AND DNMT3 REPRODUCTION AND SURVIVAL

Sets if 16 G1 ants were individually painted and placed into hydrated plaster petri dishes, eggs were collected biweekly for 2.5 weeks and incubated for 48 hours on slides before freezing and genotyping. The remainder of the eggs produced by the units continued to be removed weekly and cross – fostered with chaperones to propagate the mutant genotype and produce G1 – G*n*. Eggs continued to be removed until the units stopped producing eggs, after which units continued to be fed until the last ant perished, in some cases at ~ 1 year. The carcasses of all ants which died were removed regularly and frozen for genotyping. Some carcasses could not be found or recovered, potentially as a result of dismemberment by nestmates. The ants for which carcasses were retrieved and successfully sequenced can be assumed to be representative of the G1 population.

DNA extraction from eggs, or adult carcasses, was done by overnight incubation with proteinase K in 1x PCR Buffer as described in Section 8.3. This was followed by PCR amplification, Sanger sequencing and manual genotype scoring.

8.7 DNMT1g2 REPRODUCTION, SURVIVAL AND MORPHOMETRICS

For DNMT1g2, mutants were generated across two experiments. All G0 animals in one experiment were used for studies of reproduction and survival. Meanwhile, G0s from the second experiment

were used for morphometrics, methylation analysis, ovarian morphology and immunohistochemistry.

8.7.1 DNMT1g2 REPRODUCTION AND SURVIVAL EXPERIMENT

Because these animals were sterile, reproductive experiments could not be conducted on G1 adults, and instead G0 animals were used. All DNMT1g2 G0 animals were placed in a single unit with painted line A chaperone ants to ensure colony stability. All eggs and corpses were removed from the colony 1 – 2x/week and frozen. The tissue was then genotyped using a mitochondrial CO1 digestion protocol (Trible et al., 2017) to distinguish the line B eggs, laid by G0 adults, from the line A eggs, which were laid by the line A chaperones. All line B eggs were then sequenced at the DNMT1g2 locus. Over the course of 2 months, 24 eggs were collected, of which 19 were line B, 4 were line A, and 1 did not amplify. Of the line B eggs, all were wildtype.

For evaluation of survival, the death date was recorded for each G0 corpse. At 61 days, two G0s remained in the colony and were sacrificed. Sanger sequencing of all corpses that were retrieved (four collected out of six ants) revealed only mutant reads, while sequencing of the two surviving ants revealed only wildtype reads.

8.7.2 DNMT1g2 MORPHOMETRICS AND SAMPLE COLLECTION FOR METHYLATION AND IMMUNOHISTOCHEMISTRY ANALYSIS

Eggs were injected and reared to adulthood as previously described. At ~1 week of age, all G0 adults (injected and uninjected) were photographed under a microscope for morphometrics

assessment. Animals were sacrificed, ovaries and brains were dissected and fixed for immunohistochemistry, a single leg was removed for genotyping and the remainder of the tissue frozen for WGBS. Morphometrics measurements were taken using the Fiji Image J package.

8.8 RNA SEQUENCING

8.8.1 RNA EXTRACTION, LIBRARY PREPARATION AND SEQUENCING

RNA was extracted from frozen whole ants using the RNeasy Mini Kit (QIAGEN Cat. No. 74104) and eluted in 30ul RNAse free water. 1 ng of total RNA was used to generate full length cDNA using Clontech's SMART – Seq v4 Ultra Low Input RNA Kit (Cat # 634888). 1 ng of cDNA was then used to prepare libraries using the Illumina Nextera XT DNA sample preparation kit (Cat # FC – 131 – 1024). Libraries with unique barcodes were pooled at equal molar ratios and sequenced on Illumina NextSeq 500 sequencer to generate 150 bp paired – end reads, following the manufacture's protocol (Cat# 15048776 Rev.E).

8.8.2 DATA PROCESSING AND ANALYSIS

Sequencing reads were trimmed using Trimmomatic (Bolger et al., 2014) with Nextera PE adapters and a minimum length of 40bp. About ~50% of reads were retained for each library. Trimmed read quality was verified using FastQC, and aligned using STAR (Dobin et al., 2013) to *O. biroi v5.4* genome. Aligned BAM files were converted to SAM files and sorted by gene name using Samtools (Li et al., 2009). BAM files were loaded into Integrative Genomics Viewer (Robinson et al., 2011) to visualized read alignments at the mutation site and alternative splicing of the

DNMT1 and DNMT3 genes, respectively. SAM files were used to determined gene counts via HTseq (Anders et al., 2015). Normalization, differential gene expression and visualizations were carried out in R using DEseq2 (Love et al., 2014).

8.9 WHOLE GENOME BISULFITE SEQUENCING

8.9.1 LIBRARY CONSTRUCTION

Genomic DNA was extracted from a single whole ant (DNMT1g1 and DNMT3) or the remaining tissue of a single ant after brain and ovary dissection (DNMT1g2) using the QIAamp DNA Micro Kit (QIAGEN). MethylC – seq libraries were constructed using the MethylC – seq protocol (Urich et al., 2015). Briefly, genomic DNA was sonicated to around 200 bp using a Covaris S – series focused ultrasonicator, and end – repaired with an End – It DNA end – repair kit (Epicentre). The end – repaired DNA was subjected to A – tailing using Klenow 3′ – 5′ exo− (NEB) and ligated to methylated adapters using T4 DNA ligase (NEB). The ligated DNA was treated with sodium bisulfite reagent using the EZ DNA methylation – Gold kit and amplified using KAPA HiFi uracil + Readymix Polymerase. Sequencing was performed on an Illumina NextSeq500 instrument.

8.9.2 METHYLOME MAPPING

The MethylC – seq data from GGBC were processed by “paired – end – pipeline” function of Methylpy (Schultz et al., 2015).The qualified reads were aligned to the *O. biroi v5.4* reference genome (McKenzie and Kronauer, 2018) using bowtie 2.2.4 (Langmead et al., 2009), and the

uniquely aligned and nonclonal reads were retained. The unmethylated lambda phage DNA was used as a control to calculate the sodium bisulfite conversion rate of unmethylated cytosines. A binomial test was used to determine the methylation status of cytosines with a minimum coverage of five reads.

8.10 FLUORESCENCE *IN SITU* HYBRIDIZATION

A set of 30 custom probes were designed for DNMT1 and purchased from Molecular Instruments Inc. The probes used a B2 HCR amplifier and were labeled with Alexa Fluor 546. Tissue was dissected in cold 1x PBS, fixed in 4% PFA, prepared and processed according to a previously established protocol for mRNA – FISH in *O. biroi* (Fetter-Pruneda et al., 2021). The probe detection stage was extended to 48 hours, and probe solution concentration increased to 2 pmol.

8.11 IMMUNOHISTOCHEMISTRY

Tissue was dissected in cold 1xPBS and fixed in 4%PFA for 2 hours. Following washes in 1xPBS, samples were blocked using 5% normal goat serum in PBSTx. The blocking solution was replaced with a primary antibody solution containing 1:100 DNMT1 (Abcam ab188453) and/or 1:100 the alpha 1 subunit for Mitochondrial ATP Synthase (ATP5A1, Thermo Fisher Scientific Cat# 43 – 9800) and incubated overnight at room temperature. Negative controls were incubated overnight at room temperature in the blocking solution. All samples were washed and incubated in the secondary antibody solution including 1:500 secondary antibody and 1:500 DAPI for 2 hours, after which they were washed and mounted on slides in DAKO fluorescence mounting medium. Slides

were imaged with an Inverted LSM 780 laser scanning confocal microscope (Zeiss). Images were processed in parallel using ImageJ and shown as maximum projection z – stacks.

REFERENCES

Alvarado, S., Rajakumar, R., Abouheif, E., Szyf, M., 2015. Epigenetic variation in the Egfr gene generates quantitative variation in a complex trait in ants. Nat Commun 6, 6513. https://doi.org/10.1038/ncomms7513

Amukamara, A.U., Washington, J.T., Sanchez, Z., McKinney, E.C., Moore, A.J., Schmitz, R.J., Moore, P.J., 2020. More Than DNA Methylation: Does Pleiotropy Drive the Complex Pattern of Evolution of Dnmt1? Front. Ecol. Evol. 8, 4. https://doi.org/10.3389/fevo.2020.00004

Anders, S., Pyl, P.T., Huber, W., 2015. HTSeq--a Python framework to work with high-throughput sequencing data. Bioinformatics 31, 166–169. https://doi.org/10.1093/bioinformatics/btu638

Arsala, D., Wu, X., Yi, S.V., Lynch, J.A., 2021. Knockdown of Dnmt1 links Gene body DNA methylation to regulation of gene expression and maternal-zygotic transition in the wasp *Nasonia* (preprint). Genomics. https://doi.org/10.1101/2021.02.02.429402

Bashtrykov, P., Jankevicius, G., Smarandache, A., Jurkowska, R.Z., Ragozin, S., Jeltsch, A., 2012. Specificity of Dnmt1 for Methylation of Hemimethylated CpG Sites Resides in Its Catalytic Domain. Chemistry & Biology 19, 572–578. https://doi.org/10.1016/j.chembiol.2012.03.010

Bewick, A.J., Sanchez, Z., Mckinney, E.C., Moore, A.J., Moore, P.J., Schmitz, R.J., 2019. Dnmt1 is essential for egg production and embryo viability in the large milkweed bug, Oncopeltus fasciatus. Epigenetics & Chromatin 12, 6. https://doi.org/10.1186/s13072-018-0246-5

Bewick, A.J., Vogel, K.J., Moore, A.J., Schmitz, R.J., 2016. Evolution of DNA Methylation across Insects. Mol Biol Evol msw264. https://doi.org/10.1093/molbev/msw264

Biergans, S.D., Claudianos, C., Reinhard, J., Galizia, C.G., 2017. DNA methylation mediates neural processing after odor learning in the honeybee. Sci Rep 7, 43635. https://doi.org/10.1038/srep43635

Biergans, S.D., Claudianos, C., Reinhard, J., Galizia, C.G., 2016. DNA Methylation Adjusts the Specificity of Memories Depending on the Learning Context and Promotes Relearning in Honeybees. Front. Mol. Neurosci. 9. https://doi.org/10.3389/fnmol.2016.00082

Bolger, A.M., Lohse, M., Usadel, B., 2014. Trimmomatic: a flexible trimmer for Illumina sequence data. Bioinformatics 30, 2114–2120. https://doi.org/10.1093/bioinformatics/btu170

Bonasio, R., Li, Q., Lian, J., Mutti, N.S., Jin, L., Zhao, H., Zhang, P., Wen, P., Xiang, H., Ding, Y., Jin, Z., Shen, S.S., Wang, Z., Wang, W., Wang, J., Berger, S.L., Liebig, J., Zhang, G., Reinberg, D., 2012. Genome-wide and Caste-Specific DNA Methylomes of the Ants Camponotus floridanus and Harpegnathos saltator. Current Biology 22, 1755–1764. https://doi.org/10.1016/j.cub.2012.07.042

Brown, K.D., Robertson, K.D., 2007. DNMT1 knockout delivers a strong blow to genome stability and cell viability. Nat Genet 39, 289–290. https://doi.org/10.1038/ng0307-289

Cardoso-Junior, C.A.M., Yagound, B., Ronai, I., Remnant, E.J., Hartfelder, K., Oldroyd, B.P., 2021. DNA methylation is not a driver of gene expression reprogramming in young honey bee workers. https://doi.org/10.1101/2021.03.12.435154

Chen, T., Li, E., 2004. Structure and Function of Eukaryotic DNA Methyltransferases, in: Current Topics in Developmental Biology. Elsevier, pp. 55–89. https://doi.org/10.1016/S0070-2153(04)60003-2
Colot, V., Rossignol, J.L., 1999. Eukaryotic DNA methylation as an evolutionary device. Bioessays 21, 402–411. https://doi.org/10.1002/(SICI)1521-1878(199905)21:5<402::AID-BIES7>3.0.CO;2-B
Cox, R.T., Spradling, A.C., 2003. A Balbiani body and the fusome mediate mitochondrial inheritance during *Drosophila* oogenesis. Development 130, 1579–1590. https://doi.org/10.1242/dev.00365
Damelin, M., Bestor, T.H., 2007. Biological Functions of DNA Methyltransferase 1 Require Its Methyltransferase Activity. MCB 27, 3891–3899. https://doi.org/10.1128/MCB.00036-07
de Smedt, V., Szöllösi, D., Kloc, M., 2000. The balbiani body: asymmetry in the mammalian oocyte. Genesis 26, 208–212. https://doi.org/10.1002/(sici)1526-968x(200003)26:3<208::aid-gene6>3.3.co;2-e
Dearden, P., 2006. Germ cell development in the Honeybee (Apis mellifera); Vasa and Nanos expression. BMC Dev Biol 6, 6. https://doi.org/10.1186/1471-213X-6-6
Dobin, A., Davis, C.A., Schlesinger, F., Drenkow, J., Zaleski, C., Jha, S., Batut, P., Chaisson, M., Gingeras, T.R., 2013. STAR: ultrafast universal RNA-seq aligner. Bioinformatics 29, 15–21. https://doi.org/10.1093/bioinformatics/bts635
Dunican, D.S., Ruzov, A., Hackett, J.A., Meehan, R.R., 2008. xDnmt1 regulates transcriptional silencing in pre-MBT *Xenopus* embryos independently of its catalytic function. Development 135, 1295–1302. https://doi.org/10.1242/dev.016402
Elango, N., Hunt, B.G., Goodisman, M.A.D., Yi, S.V., 2009. DNA methylation is widespread and associated with differential gene expression in castes of the honeybee, Apis mellifera. Proceedings of the National Academy of Sciences 106, 11206–11211. https://doi.org/10.1073/pnas.0900301106
Fatemi, M., Hermann, A., Pradhan, S., Jeltsch, A., 2001. The activity of the murine DNA methyltransferase Dnmt1 is controlled by interaction of the catalytic domain with the N-terminal part of the enzyme leading to an allosteric activation of the enzyme after binding to methylated DNA. Journal of Molecular Biology 309, 1189–1199. https://doi.org/10.1006/jmbi.2001.4709
Feng, S., Cokus, S.J., Zhang, X., Chen, P.-Y., Bostick, M., Goll, M.G., Hetzel, J., Jain, J., Strauss, S.H., Halpern, M.E., Ukomadu, C., Sadler, K.C., Pradhan, S., Pellegrini, M., Jacobsen, S.E., 2010. Conservation and divergence of methylation patterning in plants and animals. Proceedings of the National Academy of Sciences 107, 8689–8694. https://doi.org/10.1073/pnas.1002720107
Fetter-Pruneda, I., Hart, T., Ulrich, Y., Gal, A., Oxley, P.R., Olivos-Cisneros, L., Ebert, M.S., Kazmi, M.A., Garrison, J.L., Bargmann, C.I., Kronauer, D.J.C., 2021. An oxytocin/vasopressin-related neuropeptide modulates social foraging behavior in the clonal raider ant. PLoS Biol 19, e3001305. https://doi.org/10.1371/journal.pbio.3001305
Foret, S., Kucharski, R., Pellegrini, M., Feng, S., Jacobsen, S.E., Robinson, G.E., Maleszka, R., 2012. DNA methylation dynamics, metabolic fluxes, gene splicing, and alternative phenotypes in honey bees. Proceedings of the National Academy of Sciences 109, 4968–4973. https://doi.org/10.1073/pnas.1202392109
Gegner, J., Gegner, T., Vogel, H., Vilcinskas, A., 2020. Silencing of the *DNA methyltransferase 1 associated protein 1* (*DMAP1*) gene in the invasive ladybird *Harmonia axyridis*

implies a role of the DNA methyltransferase 1-DMAP1 complex in female fecundity. Insect Mol Biol 29, 148–159. https://doi.org/10.1111/imb.12616
Gowher, H., Jeltsch, A., 2001. Enzymatic properties of recombinant Dnmt3a DNA methyltransferase from mouse: the enzyme modifies DNA in a non-processive manner and also methylates non-CpA sites. Journal of Molecular Biology 309, 1201–1208. https://doi.org/10.1006/jmbi.2001.4710
Herb, B.R., Shook, M.S., Fields, C.J., Robinson, G.E., 2018. Defense against territorial intrusion is associated with DNA methylation changes in the honey bee brain. BMC Genomics 19, 216. https://doi.org/10.1186/s12864-018-4594-0
Herb, B.R., Wolschin, F., Hansen, K.D., Aryee, M.J., Langmead, B., Irizarry, R., Amdam, G.V., Feinberg, A.P., 2012. Reversible switching between epigenetic states in honeybee behavioral subcastes. Nat Neurosci 15, 1371–1373. https://doi.org/10.1038/nn.3218
Hsieh, C.-L., 1999. In Vivo Activity of Murine De Novo Methyltransferases, Dnmt3a and Dnmt3b. Mol Cell Biol 19, 8211–8218. https://doi.org/10.1128/MCB.19.12.8211
Jinek, M., Chylinski, K., Fonfara, I., Hauer, M., Doudna, J.A., Charpentier, E., 2012. A Programmable Dual-RNA-Guided DNA Endonuclease in Adaptive Bacterial Immunity. Science 337, 816–821. https://doi.org/10.1126/science.1225829
Katoh, K., Rozewicki, J., Yamada, K.D., 2019. MAFFT online service: multiple sequence alignment, interactive sequence choice and visualization. Briefings in Bioinformatics 20, 1160–1166. https://doi.org/10.1093/bib/bbx108
Kay, S., Skowronski, D., Hunt, B.G., 2018. Developmental DNA methyltransferase expression in the fire ant *Solenopsis invicta*: Fire ant developmental DNMT expression. Insect Science 25, 57–65. https://doi.org/10.1111/1744-7917.12413
Keller, L., 1998. Queen lifespan and colony characteristics in ants and termites. Insectes Sociaux 45, 235–246. https://doi.org/10.1007/s000400050084
Khila, A., Abouheif, E., 2009. In Situ Hybridization on Ant Ovaries and Embryos. Cold Spring Harbor Protocols 2009, pdb.prot5250-pdb.prot5250. https://doi.org/10.1101/pdb.prot5250
Kirilly, D., Xie, T., 2007. The Drosophila ovary: an active stem cell community. Cell Res 17, 15–25. https://doi.org/10.1038/sj.cr.7310123
Klein, C.J., Botuyan, M.-V., Wu, Y., Ward, C.J., Nicholson, G.A., Hammans, S., Hojo, K., Yamanishi, H., Karpf, A.R., Wallace, D.C., Simon, M., Lander, C., Boardman, L.A., Cunningham, J.M., Smith, G.E., Litchy, W.J., Boes, B., Atkinson, E.J., Middha, S., B Dyck, P.J., Parisi, J.E., Mer, G., Smith, D.I., Dyck, P.J., 2011. Mutations in DNMT1 cause hereditary sensory neuropathy with dementia and hearing loss. Nat Genet 43, 595–600. https://doi.org/10.1038/ng.830
Kronauer, D.J.C., Pierce, N.E., Keller, L., 2012. Asexual reproduction in introduced and native populations of the ant *Cerapachys biroi*. Mol Ecol 21, 5221–5235. https://doi.org/10.1111/mec.12041
Kronauer, D.J.C., Tsuji, K., Pierce, N.E., Keller, L., 2013. Non–nest mate discrimination and clonal colony structure in the parthenogenetic ant Cerapachys biroi. Behavioral Ecology 24, 617–622. https://doi.org/10.1093/beheco/ars227
Kucharski, R., Maleszka, J., Foret, S., Maleszka, R., 2008. Nutritional Control of Reproductive Status in Honeybees via DNA Methylation. Science 319, 1827–1830. https://doi.org/10.1126/science.1153069

Langmead, B., Trapnell, C., Pop, M., Salzberg, S.L., 2009. Ultrafast and memory-efficient alignment of short DNA sequences to the human genome. Genome Biol 10, R25. https://doi.org/10.1186/gb-2009-10-3-r25

Lev Maor, G., Yearim, A., Ast, G., 2015. The alternative role of DNA methylation in splicing regulation. Trends in Genetics 31, 274–280. https://doi.org/10.1016/j.tig.2015.03.002

Li, E., Beard, C., Jaenisch, R., 1993. Role for DNA methylation in genomic imprinting. Nature 366, 362–365. https://doi.org/10.1038/366362a0

Li, E., Bestor, T.H., Jaenisch, R., 1992. Targeted mutation of the DNA methyltransferase gene results in embryonic lethality. Cell 69, 915–926. https://doi.org/10.1016/0092-8674(92)90611-F

Li, E., Zhang, Y., 2014. DNA Methylation in Mammals. Cold Spring Harbor Perspectives in Biology 6, a019133–a019133. https://doi.org/10.1101/cshperspect.a019133

Li, H., Handsaker, B., Wysoker, A., Fennell, T., Ruan, J., Homer, N., Marth, G., Abecasis, G., Durbin, R., 1000 Genome Project Data Processing Subgroup, 2009. The Sequence Alignment/Map format and SAMtools. Bioinformatics 25, 2078–2079. https://doi.org/10.1093/bioinformatics/btp352

Li, Z., Dai, H., Martos, S.N., Xu, B., Gao, Y., Li, T., Zhu, G., Schones, D.E., Wang, Z., 2015. Distinct roles of DNMT1-dependent and DNMT1-independent methylation patterns in the genome of mouse embryonic stem cells. Genome Biol 16, 115. https://doi.org/10.1186/s13059-015-0685-2

Libbrecht, R., Oxley, P.R., Keller, L., Kronauer, D.J.C., 2016. Robust DNA Methylation in the Clonal Raider Ant Brain. Current Biology 26, 391–395. https://doi.org/10.1016/j.cub.2015.12.040

Li-Byarlay, H., Li, Y., Stroud, H., Feng, S., Newman, T.C., Kaneda, M., Hou, K.K., Worley, K.C., Elsik, C.G., Wickline, S.A., Jacobsen, S.E., Ma, J., Robinson, G.E., 2013. RNA interference knockdown of DNA methyl-transferase 3 affects gene alternative splicing in the honey bee. Proceedings of the National Academy of Sciences 110, 12750–12755. https://doi.org/10.1073/pnas.1310735110

Lorincz, M.C., Dickerson, D.R., Schmitt, M., Groudine, M., 2004. Intragenic DNA methylation alters chromatin structure and elongation efficiency in mammalian cells. Nat Struct Mol Biol 11, 1068–1075. https://doi.org/10.1038/nsmb840

Love, M.I., Huber, W., Anders, S., 2014. Moderated estimation of fold change and dispersion for RNA-seq data with DESeq2. Genome Biol 15, 550. https://doi.org/10.1186/s13059-014-0550-8

Lyko, F., Ramsahoye, B.H., Kashevsky, H., Tudor, M., Mastrangelo, M.A., Orr-Weaver, T.L., Jaenisch, R., 1999. Mammalian (cytosine-5) methyltransferases cause genomic DNA methylation and lethality in Drosophila. Nat Genet 23, 363–366. https://doi.org/10.1038/15551

Maleszka, R., 2008. Epigenetic integration of environmental and genomic signals in honey bees: the critical interplay of nutritional, brain and reproductive networks. Epigenetics 3, 188–192. https://doi.org/10.4161/epi.3.4.6697

Maunakea, A.K., Chepelev, I., Cui, K., Zhao, K., 2013. Intragenic DNA methylation modulates alternative splicing by recruiting MeCP2 to promote exon recognition. Cell Res 23, 1256–1269. https://doi.org/10.1038/cr.2013.110

McGraw, S., Oakes, C.C., Martel, J., Cirio, M.C., de Zeeuw, P., Mak, W., Plass, C., Bartolomei, M.S., Chaillet, J.R., Trasler, J.M., 2013. Loss of DNMT1o Disrupts Imprinted X

Chromosome Inactivation and Accentuates Placental Defects in Females. PLoS Genet 9, e1003873. https://doi.org/10.1371/journal.pgen.1003873
McKenzie, S.K., Kronauer, D.J.C., 2018. The genomic architecture and molecular evolution of ant odorant receptors. Genome Res. 28, 1757–1765. https://doi.org/10.1101/gr.237123.118
Mou, H., Smith, J.L., Peng, L., Yin, H., Moore, J., Zhang, X.-O., Song, C.-Q., Sheel, A., Wu, Q., Ozata, D.M., Li, Y., Anderson, D.G., Emerson, C.P., Sontheimer, E.J., Moore, M.J., Weng, Z., Xue, W., 2017. CRISPR/Cas9-mediated genome editing induces exon skipping by alternative splicing or exon deletion. Genome Biol 18, 108. https://doi.org/10.1186/s13059-017-1237-8
Mund, C., Musch, T., Strödicke, M., Assmann, B., Li, E., Lyko, F., 2004. Comparative analysis of DNA methylation patterns in transgenic Drosophila overexpressing mouse DNA methyltransferases. Biochemical Journal 378, 763–768. https://doi.org/10.1042/bj20031567
Norvil, A.B., Saha, D., Saleem Dar, M., Gowher, H., 2019. Effect of Disease-Associated Germline Mutations on Structure Function Relationship of DNA Methyltransferases. Genes 10, 369. https://doi.org/10.3390/genes10050369
Okano, M., Bell, D.W., Haber, D.A., Li, E., 1999. DNA Methyltransferases Dnmt3a and Dnmt3b Are Essential for De Novo Methylation and Mammalian Development. Cell 99, 247–257. https://doi.org/10.1016/S0092-8674(00)81656-6
Omar, M.A.A., Li, M., Liu, F., He, K., Qasim, M., Xiao, H., Jiang, M., Li, F., 2020. The Roles of DNA Methyltransferases 1 (DNMT1) in Regulating Sexual Dimorphism in the Cotton Mealybug, Phenacoccus solenopsis. Insects 11, 121. https://doi.org/10.3390/insects11020121
Otani, J., Nankumo, T., Arita, K., Inamoto, S., Ariyoshi, M., Shirakawa, M., 2009. Structural basis for recognition of H3K4 methylation status by the DNA methyltransferase 3A ATRX–DNMT3–DNMT3L domain. EMBO Rep 10, 1235–1241. https://doi.org/10.1038/embor.2009.218
Oxley, P.R., Ji, L., Fetter-Pruneda, I., McKenzie, S.K., Li, C., Hu, H., Zhang, G., Kronauer, D.J.C., 2014. The Genome of the Clonal Raider Ant Cerapachys biroi. Current Biology 24, 451–458. https://doi.org/10.1016/j.cub.2014.01.018
Patalano, S., Vlasova, A., Wyatt, C., Ewels, P., Camara, F., Ferreira, P.G., Asher, C.L., Jurkowski, T.P., Segonds-Pichon, A., Bachman, M., González-Navarrete, I., Minoche, A.E., Krueger, F., Lowy, E., Marcet-Houben, M., Rodriguez-Ales, J.L., Nascimento, F.S., Balasubramanian, S., Gabaldon, T., Tarver, J.E., Andrews, S., Himmelbauer, H., Hughes, W.O.H., Guigó, R., Reik, W., Sumner, S., 2015. Molecular signatures of plastic phenotypes in two eusocial insect species with simple societies. Proc Natl Acad Sci USA 112, 13970–13975. https://doi.org/10.1073/pnas.1515937112
Popp, M.W., Maquat, L.E., 2016. Leveraging Rules of Nonsense-Mediated mRNA Decay for Genome Engineering and Personalized Medicine. Cell 165, 1319–1322. https://doi.org/10.1016/j.cell.2016.05.053
Pósfai, J., Bhagwat, A.S., Pósfai, G., Roberts, R.J., 1989. Predictive motifs derived from cytosine methyltransferases. Nucl Acids Res 17, 2421–2435. https://doi.org/10.1093/nar/17.7.2421

Qiu, C., Sawada, K., Zhang, X., Cheng, X., 2002. The PWWP domain of mammalian DNA methyltransferase Dnmt3b defines a new family of DNA-binding folds. Nat. Struct Biol. https://doi.org/10.1038/nsb759

Ran, F.A., Cong, L., Yan, W.X., Scott, D.A., Gootenberg, J.S., Kriz, A.J., Zetsche, B., Shalem, O., Wu, X., Makarova, K.S., Koonin, E.V., Sharp, P.A., Zhang, F., 2015. In vivo genome editing using Staphylococcus aureus Cas9. Nature 520, 186–191. https://doi.org/10.1038/nature14299

Ran, F.A., Hsu, P.D., Wright, J., Agarwala, V., Scott, D.A., Zhang, F., 2013. Genome engineering using the CRISPR-Cas9 system. Nat Protoc 8, 2281–2308. https://doi.org/10.1038/nprot.2013.143

Ratnam, S., Mertineit, C., Ding, F., Howell, C.Y., Clarke, H.J., Bestor, T.H., Chaillet, J.R., Trasler, J.M., 2002. Dynamics of Dnmt1 Methyltransferase Expression and Intracellular Localization during Oogenesis and Preimplantation Development. Developmental Biology 245, 304–314. https://doi.org/10.1006/dbio.2002.0628

Ravary, F., Jahyny, B., Jaisson, P., 2006. Brood stimulation controls the phasic reproductive cycle of the parthenogenetic ant Cerapachys biroi. Insect. Soc. 53, 20–26. https://doi.org/10.1007/s00040-005-0828-7

Ravary, F., Jaisson, P., 2002. The reproductive cycle of thelytokous colonies of Cerapachys biroi Forel (Formicidae, Cerapachyinae). Insectes Sociaux 49, 114–119. https://doi.org/10.1007/s00040-002-8288-9

Robinson, J.T., Thorvaldsdóttir, H., Winckler, W., Guttman, M., Lander, E.S., Getz, G., Mesirov, J.P., 2011. Integrative genomics viewer. Nat Biotechnol 29, 24–26. https://doi.org/10.1038/nbt.1754

Rountree, M.R., Bachman, K.E., Baylin, S.B., 2000. DNMT1 binds HDAC2 and a new co-repressor, DMAP1, to form a complex at replication foci. Nat Genet 25, 269–277. https://doi.org/10.1038/77023

Rubio, A., Luoni, M., Giannelli, S.G., Radice, I., Iannielli, A., Cancellieri, C., Di Berardino, C., Regalia, G., Lazzari, G., Menegon, A., Taverna, S., Broccoli, V., 2016. Rapid and efficient CRISPR/Cas9 gene inactivation in human neurons during human pluripotent stem cell differentiation and direct reprogramming. Sci Rep 6, 37540. https://doi.org/10.1038/srep37540

Schultz, M.D., He, Y., Whitaker, J.W., Hariharan, M., Mukamel, E.A., Leung, D., Rajagopal, N., Nery, J.R., Urich, M.A., Chen, H., Lin, S., Lin, Y., Jung, I., Schmitt, A.D., Selvaraj, S., Ren, B., Sejnowski, T.J., Wang, W., Ecker, J.R., 2015. Human body epigenome maps reveal noncanonical DNA methylation variation. Nature 523, 212–216. https://doi.org/10.1038/nature14465

Schulz, N.K.E., Wagner, C.I., Ebeling, J., Raddatz, G., Diddens-de Buhr, M.F., Lyko, F., Kurtz, J., 2018. Dnmt1 has an essential function despite the absence of CpG DNA methylation in the red flour beetle Tribolium castaneum. Sci Rep 8, 16462. https://doi.org/10.1038/s41598-018-34701-3

Seong, H.J., Han, S.-W., Sul, W.J., 2021. Prokaryotic DNA methylation and its functional roles. J Microbiol. 59, 242–248. https://doi.org/10.1007/s12275-021-0674-y

Simpson, V.J., Johnson, T.E., Hammen, R.F., 1986. Caenorhabditis elegans DNA does not contain 5-methylcytosine at any time during development or aging. Nucl Acids Res 14, 6711–6719. https://doi.org/10.1093/nar/14.16.6711

Smith, Z.D., Meissner, A., 2013. DNA methylation: roles in mammalian development. Nat Rev Genet 14, 204–220. https://doi.org/10.1038/nrg3354

Smits, A.H., Ziebell, F., Joberty, G., Zinn, N., Mueller, W.F., Clauder-Münster, S., Eberhard, D., Fälth Savitski, M., Grandi, P., Jakob, P., Michon, A.-M., Sun, H., Tessmer, K., Bürckstümmer, T., Bantscheff, M., Steinmetz, L.M., Drewes, G., Huber, W., 2019. Biological plasticity rescues target activity in CRISPR knock outs. Nat Methods 16, 1087–1093. https://doi.org/10.1038/s41592-019-0614-5

Sui, T., Song, Y., Liu, Z., Chen, M., Deng, J., Xu, Y., Lai, L., Li, Z., 2018. CRISPR-induced exon skipping is dependent on premature termination codon mutations. Genome Biol 19, 164. https://doi.org/10.1186/s13059-018-1532-z

Svedružić, Ž.M., 2011. Chapter 6 - Dnmt1: Structure and Function, in: Progress in Molecular Biology and Translational Science. Elsevier, pp. 221–254. https://doi.org/10.1016/B978-0-12-387685-0.00006-8

Takada, Y., Yaman-Deveci, R., Shirakawa, T., Sharif, J., Tomizawa, S., Miura, F., Ito, T., Ono, M., Nakajima, K., Koseki, Y., Shiotani, F., Ishiguro, K., Ohbo, K., Koseki, H., 2021. Maintenance DNA methylation in pre-meiotic germ cells regulates meiotic prophase by facilitating homologous chromosome pairing. Development 148, dev194605. https://doi.org/10.1242/dev.194605

Takashima, S., Takehashi, M., Lee, J., Chuma, S., Okano, M., Hata, K., Suetake, I., Nakatsuji, N., Miyoshi, H., Tajima, S., Tanaka, Y., Toyokuni, S., Sasaki, H., Kanatsu-Shinohara, M., Shinohara, T., 2009. Abnormal DNA Methyltransferase Expression in Mouse Germline Stem Cells Results in Spermatogenic Defects1. Biology of Reproduction 81, 155–164. https://doi.org/10.1095/biolreprod.108.074708

Teseo, S., Kronauer, D.J.C., Jaisson, P., Châline, N., 2013. Enforcement of Reproductive Synchrony via Policing in a Clonal Ant. Current Biology 23, 328–332. https://doi.org/10.1016/j.cub.2013.01.011

Trible, W., Kronauer, D.J.C., 2021. Hourglass Model for Developmental Evolution of Ant Castes. Trends in Ecology & Evolution 36, 100–103. https://doi.org/10.1016/j.tree.2020.11.010

Trible, W., Olivos-Cisneros, L., McKenzie, S.K., Saragosti, J., Chang, N.-C., Matthews, B.J., Oxley, P.R., Kronauer, D.J.C., 2017. orco Mutagenesis Causes Loss of Antennal Lobe Glomeruli and Impaired Social Behavior in Ants. Cell 170, 727-735.e10. https://doi.org/10.1016/j.cell.2017.07.001

Tsuji, K., Yamauchi, K., 1995. Production of females by parthenogenesis in the ant,Cerapachys biroi. Ins. Soc 42, 333–336. https://doi.org/10.1007/BF01240430

Ulrich, Y., Burns, D., Libbrecht, R., Kronauer, D.J.C., 2016. Ant larvae regulate worker foraging behavior and ovarian activity in a dose-dependent manner. Behav Ecol Sociobiol 70, 1011–1018. https://doi.org/10.1007/s00265-015-2046-2

Unterberger, A., Andrews, S.D., Weaver, I.C.G., Szyf, M., 2006. DNA Methyltransferase 1 Knockdown Activates a Replication Stress Checkpoint. MCB 26, 7575–7586. https://doi.org/10.1128/MCB.01887-05

Urieli-Shoval, S., Gruenbaum, Y., Sedat, J., Razin, A., 1982. The absence of detectable methylated bases in *Drosophila melanogaster* DNA. FEBS Letters 146, 148–152. https://doi.org/10.1016/0014-5793(82)80723-0

Ventós-Alfonso, A., Ylla, G., Montañes, J.-C., Belles, X., 2020. DNMT1 Promotes Genome Methylation and Early Embryo Development in Cockroaches. iScience 23, 101778. https://doi.org/10.1016/j.isci.2020.101778

Wang, Y., Jorda, M., Jones, P.L., Maleszka, R., Ling, X., Robertson, H.M., Mizzen, C.A., Peinado, M.A., Robinson, G.E., 2006. Functional CpG Methylation System in a Social Insect. Science 314, 645–647. https://doi.org/10.1126/science.1135213

Washington, J.T., Cavender, K.R., Amukamara, A.U., McKinney, E.C., Schmitz, R.J., Moore, P.J., 2020. The essential role of *Dnmt1* in gametogenesis in the large milkweed bug *Oncopeltus fasciatus* (preprint). Evolutionary Biology. https://doi.org/10.1101/2020.07.23.218180

Winkelmann, J., Lin, L., Schormair, B., Kornum, B.R., Faraco, J., Plazzi, G., Melberg, A., Cornelio, F., Urban, A.E., Pizza, F., Poli, F., Grubert, F., Wieland, T., Graf, E., Hallmayer, J., Strom, T.M., Mignot, E., 2012. Mutations in DNMT1 cause autosomal dominant cerebellar ataxia, deafness and narcolepsy. Human Molecular Genetics 21, 2205–2210. https://doi.org/10.1093/hmg/dds035

Yarychkivska, O., Shahabuddin, Z., Comfort, N., Boulard, M., Bestor, T.H., 2018. BAH domains and a histone-like motif in DNA methyltransferase 1 (DNMT1) regulate de novo and maintenance methylation in vivo. Journal of Biological Chemistry 293, 19466–19475. https://doi.org/10.1074/jbc.RA118.004612

Yuan, J., Higuchi, Y., Nagado, T., Nozuma, S., Nakamura, T., Matsuura, E., Hashiguchi, A., Sakiyama, Y., Yoshimura, A., Takashima, H., 2013. Novel mutation in the replication focus targeting sequence domain of *DNMT1* causes hereditary sensory and autonomic neuropathy IE: Yuan. J Peripher Nerv Syst 18, 89–93. https://doi.org/10.1111/jns5.12012

Zhang, Q., Fu, Y., Thakur, C., Bi, Z., Wadgaonkar, P., Qiu, Y., Xu, L., Rice, M., Zhang, W., Almutairy, B., Chen, F., 2020. CRISPR-Cas9 gene editing causes alternative splicing of the targeting mRNA. Biochemical and Biophysical Research Communications 528, 54–61. https://doi.org/10.1016/j.bbrc.2020.04.145

Zhang, Z.-M., Liu, S., Lin, K., Luo, Y., Perry, J.J., Wang, Y., Song, J., 2015. Crystal Structure of Human DNA Methyltransferase 1. Journal of Molecular Biology 427, 2520–2531. https://doi.org/10.1016/j.jmb.2015.06.001

Zwier, M.V., Verhulst, E.C., Zwahlen, R.D., Beukeboom, L.W., van de Zande, L., 2012. DNA methylation plays a crucial role during early Nasonia development: DNA methylation is crucial for Nasonia development. Insect Molecular Biology 21, 129–138. https://doi.org/10.1111/j.1365-2583.2011.01121.x